

ABSTRACT

A STUDY OF THE DIELECTRIC CONSTANT

OF BOUND WATER.

by
J. Muir, B.Sc.

Thesis submitted for the degree of
Doctor of Philosophy in the
University of Edinburgh.

April, 1953.



CONTENTS.

PREFACE.

The work detailed in this thesis was carried out in the Physics Department, University College, Hull, during the period March 1950 to December 1952.

The research was conducted under the general supervision of Professor N. Feather. The work described, with the exception of that in section (6.10), is entirely the author's, and the apparatus required for the research, excluding that of section (4.9) and the commercial instruments, was built by him. The conclusions drawn from the results are his own.

The author wishes to thank Professor N. Feather for his supervision; Professor L.S. Palmer for suggesting and encouraging the research and providing laboratory facilities; Dr. J. Goodyear for his contribution in support of the work - section (6.10) and Dr. J. Goodyear and Mr. W.J. Duffin for helpful discussions.

CONTENTS.

<u>CHAPTER 1.</u>	- <u>INTRODUCTION.</u>	1.
<u>CHAPTER 2.</u>	- <u>AN OUTLINE OF THE WORK.</u>	55.
2.1	- The Mineral Halloysite.	14.
2.2	- A Summary of Dielectric Theory.	17.
2.3	- The Dielectric Constant of Halloysite.	20.
2.4	- The Dielectric Loss of Halloysite.	23.
2.5	- The Frequency of Relaxation Absorption.	24.
2.6	- The Variation of β with water content.	27.
2.7	- The Variation of $\epsilon_s - \epsilon_\infty$ with water content.	28.
2.8	- A Brief Indication of Experimental Results.	28.
2.9	- The Extension of the Investigation.	30.
2.10	- The Apparatus in Outline.	32.
2.11	- The Method in Outline.	37.
<u>CHAPTER 3.</u>	- <u>THE THEORY OF DIELECTRICS.</u>	73.
3.1	- The Static Dielectric Constant.	40.
3.2	- In Alternating Fields.	42.
3.3	- The Frequency Variation of $\epsilon_1(\omega)$ and $\epsilon_2(\omega)$.	44.
3.4	- The Debye Equations.	44.
3.5	- The Applicability of the Debye Equations.	46.
3.6	- The Generalised Debye Equations.	47.
3.7	- The Theoretical Calculation of $\epsilon_s - \epsilon_\infty$.	49.
3.8	- The Calculation of τ .	50.
5.6	- The Maintenance of Constant Humidity.	73.

<u>CHAPTER 4.</u>	<u>- APPARATUS.</u>	
4.1	- The Definition of Q.	51.
4.2	- The Measurement of ϵ_1 and ϵ_2 .	52.
4.3	- The Incremental Capacitance Method of Measuring Q.	55.
4.4	- The Direct Method of Measuring Q.	56.
4.5	- The Q Meter by Marconi Instruments.	57.
4.6	- The Additional Variable Standard Capacitor.	59.
4.7	- Lead Inductances.	60.
4.8	- The Coaxial Lead to the Test Capacitors.	62.
4.9	- The Test Capacitors.	62.
4.10	- The Constant Humidity Enclosures.	64.
4.11	- The External Oscillator.	64.
4.12	- The Negative Resistance Unit.	66.
4.13	- The Inductors.	69.
4.14	- Calibration of the Loss Measurements.	70.
4.15	- The Calibration of the normal range of the Q Meter.	73.
4.16	- The Calibration of the Extended Range.	74.

<u>CHAPTER 5.</u>	<u>- THE EXPERIMENTAL METHOD.</u>	
5.1	- The Preparation of the Minerals.	76.
5.2	- The Preparation of Halloysite.	76.
5.3	- The Preparation of the Intermediate States of Hydration.	77.
5.4	- The Preparation of Metahalloysite.	77.
5.5	- The Preparation of Capacitor Samples.	78.
5.6	- The Maintenance of Constant Humidity.	78.

5.7	- The Determination of the Interlayer Water Content of Halloysite.	79.
5.8	- The Determination of Adsorbed Water Content.	81.
5.9	- The Dielectric Measurements.	81.

CHAPTER 5. - CONCLUSIONS.

CHAPTER 6. - THE MINERALOGY OF HALLOYSITE AND RELATED MINERALS.

6.1	- Halloysite: Nomenclature.	85.
6.2	- The Structure of Halloysite.	86.
6.3	- The Layer of Oriented Water Molecules.	87.
6.4	- The Dehydration of Halloysite.	90.
6.5	- Surface Adsorbed Water on Silicate Clay Minerals.	92.
6.6	- The Determination of the Water Contents of Halloysite.	92.
6.7	- The Morphology of Halloysite.	95.
6.8	- Other Points about Halloysite.	97.
6.9	- The Related Minerals: Kaolinite, Talc and Gibbsite.	98.
6.10	- The X-Ray Examination of the Minerals.	99.

CHAPTER 7. - RESULTS.

7.1	- The Dehydration Rates.	102.
7.2	- The Form and Analysis of the $\epsilon_2(\omega)$ curves.	104.
7.3	- The Conductivity Loss.	106.
7.4	- Deductions from the Relaxation Absorption curves.	107.
7.5	- Results.	108.
7.6	- Metahalloysite.	109.
7.7	- Halloysite.	111.

7.8 - Talc. 111.

7.9 - Kaolinite. 112.

7.10 - Surface Layer Thickness. 113.

CHAPTER 8. - CONCLUSIONS.

8.1 - Metahalloysite. 115.

8.2 - Halloysite. 118.

8.3 - Talc. 121.

8.4 - Kaolinite. 122.

8.5 - Kaolinite, Halloysite and Metahalloysite. 123.

8.6 - Surface Shape Effects. 124.

8.7 - Concluding remarks. 127.

BIBLIOGRAPHY. 129.

good point from which to trace the history of this subject. Two definitions were proposed to distinguish 'bound' and 'free' water. One definition distinguished the two by their physical properties, viz., that bound water had different hydrodynamic properties from free water, both from the point of view of flow through fine-pored media and the passage of particles through the bulk fluid. The alternative definition was biological in origin and stated that bound water was not able to act as a solvent.

Based upon the latter definition, a method (23) was devised to estimate the bound water content of colloidal systems. It consisted of adding a known quantity of salt to the system and observing the resulting change in the vapour

CHAPTER 1.

INTRODUCTION.

It is the purpose of this thesis to show that a study of the dielectric loss properties of water adsorbed upon a mineral may yield information concerning the properties of 'bound' water, by which is meant adsorbed water bonded so strongly to a surface that it does not exhibit the normal properties of water in bulk.

For some twenty years 'bound' water has been postulated as existing in biological and colloidal systems. A paper by Gortner (23), and the resulting discussion, is a good point from which to trace the history of this subject. Two definitions were proposed to distinguish 'bound' and 'free' water. One definition distinguished the two by their physical properties, viz., that bound water had different hydrodynamic properties from free water, both from the point of view of flow through fine-pored media and the passage of particles through the bulk fluid. The alternative definition was biological in origin and stated that bound water was not able to act as a solvent.

Based upon the latter definition, a method (29) was devised to estimate the bound water content of colloidal systems. It consisted of adding a known quantity of salt to the system and observing the resulting change in the vapour

0.02 or 0.03 micron (200 to 300 Å). Secondly, the liquid pressure. From this change the amount of water in which the salt had dissolved could be calculated. The difference between this quantity and the total water content determined by drying methods gave the bound water content. In a similar way the depression of the freezing point could be employed.

On the basis of the physical definition, numerous attempts have been made to establish the existence of bound water with varying degrees of success. As far as the author knows, no approach has been made to the problem by considering the passage of particles through water as in normal sedimentation, but the passage of liquid through the solid has been widely employed.

Two alternative approaches have been used. Firstly, the water, or other liquid, (the same effect was expected with other liquids) was passed through very fine bore capillary tubes, its viscosity being calculated in the normal way. For this purpose capillaries with bores about 5 microns in diameter have been used, and numerous workers have quoted anomalous viscosities, especially with polar liquids. However, in one case, anomalous results have been shown to be due to impurities in the liquids (13). When the impurities were removed the results indicated that a number of liquids, including conductivity water, retained their bulk viscosity at least as close to the capillary surface as

0.02 or 0.03 micron (200 to 300 Å). Secondly, the liquid may be forced through a bed of fine-pored particles. The velocity of penetration of various liquids into porous materials such as kaolin and other clays was investigated by Wolkowa (42) who found that, although a consistent pore diameter could be calculated from the results with non-polar liquids, the pore diameter obtained with polar liquids was smaller and variable. To explain this he suggested the formation of oriented films on the surfaces of particles.

Other workers (41) measured the attractive forces binding liquids to particles of clay and sand by several different methods, and were led to the conclusion that, in fine-pored systems, part of the liquid exists under the constraining influence of the surface, but the range of action of the influence they left an open question.

Finally, Bowden and Bastow (8), who developed a method for measuring the viscosities of films as thin as ⁻⁵ 10 cm., showed that such thin films of water and other liquids behaved as normal fluids. They concluded that, if oriented films existed upon surfaces, they were certainly less than 1000 Å thick.

This mode of approach is one which might have given a measure of the thickness of the surface layer had not slight irregularities in the surfaces and impurities in the liquids set a lower limit of film thickness greatly in excess of the expected thickness of an oriented layer. It seems

likely (5) that surface inaccuracies and impurities in the liquids were the cause of the apparently positive effects obtained in some cases.

That adsorbed water films do exist has been shown conclusively by several independent methods, particularly by Neuhausen and Patrick (36), who found that silica gel retained 3.8% by weight of water after heating to 300 °C for six hours in a high vacuum. Thus there is a first layer adsorbed by materials which is held so tenaciously that the layer has no vapour pressure even at several hundred degrees centigrade.

In a recent discussion, the participants were more concerned to show the conditions under which bound layers existed than to establish their properties, their existence being no longer doubted. In this connection two sets of results by Bond, Griffith and Maggs (6) are particularly interesting. They showed that dilatometer experiments gave no evidence of the freezing of adsorbed water in pores in coal in a temperature range down to -72 °C. This temperature is much below the lowest possible freezing temperature of water which is -22 °C under a pressure of 2115 atmospheres (23). In the second experiment they measured the dielectric constant at 15 Kc/s of a sample of crushed coal containing adsorbed water and found it to decrease steadily as temperature decreased from 20 to -70 °C. They found no discontinuity in the curve which

could be attributed to the "freezing" of the adsorbed water. This latter result should be contrasted with the work of Alexander and Shaw (2) who made similar measurements on clays and did obtain a discontinuity which they said indicated the freezing point of the adsorbed water.

In their concluding remarks, Bond, Griffith and Maggs note that the adsorbed water on coal must be regarded as an altogether separate phase from bulk water, being a two dimensional phase with a high kinetic mobility, in accord with the results of Bangham and Razouk (3) for alcohol - charcoal systems.

Until recently, no clear distinction was drawn between liquid molecules bound to an ion, i.e., clustered about it, and molecules adsorbed on the external surfaces of particles. Now, however, the distinction is made and the effect of ions on the solvent in ionic solutions is being studied intensively by dielectric measurements (24).

As for the adsorbed film, efforts have been made to establish their specific properties. The techniques of infra-red absorption spectra have been used by Buswell and Dudenbostel (14) in the study of the condition of water in clays. Two peaks in the absorption spectrum were found to vary in height with hydration. The peak at the shorter wavelength was ascribed to "free OH" and the other to "hydrogen bonded OH". They assumed that the total water content in the clays was proportional to the total area

under the peaks but did not check this.

Marinesco (35) made an attempt to examine the thickness of the adsorbed water film in hydrophilic colloidal systems by measuring the dielectric constant of the colloids at various water contents. Unfortunately, he calculated his results using an approximation of the Clausius-Mossotti formula (7) for dielectric mixtures which is only valid for the case of non-polar gases at low pressures. However, he did show that the approach was useful in the study of adsorbed films.

Several others have employed measurements of dielectric constant to determine the moisture contents of materials, but this is not the best approach as the effective dielectric constant of a mixture is a complicated function of the volume fractions and dielectric constants of the constituents. In addition, several points have not been clearly appreciated by workers in this field. Firstly, the normal mixture formulae (7) cannot be used where one of the constituents is a film surrounding a second constituent. Secondly, the adsorbed film need not have dielectric properties resembling those of ice, as the film has probably a two-dimensional structure with different atomic spacings from ice. Further, the appearance of a rapid change of dielectric constant with changing temperature at a given frequency does not indicate the freezing of the liquid film but only indicates that the dipoles have not

sufficient thermal energy at the temperature to follow higher frequencies, and finally a large decrease in dielectric constant need not necessarily occur as the liquid freezes, as the dielectric constant of the solid phase depends greatly upon the frequency of measurement (38) and may even be greater than that of the liquid.

The dielectric property best suited to a study of the adsorbed water films is the dielectric loss, as the total loss of a mixture is the simple sum of the separate losses of the various components determined from their volume fraction in the mixture and their loss per unit volume in bulk. Where the adsorbed film is of polar molecules, as with water, the measurement of dielectric loss is particularly useful as polar dielectrics exhibit relaxation losses, i.e., there is a critical maximum value in the curve of loss against frequency at constant temperature, this maximum varying in height and frequency position with such factors as the strength of the bond to the surface, the degree of order in the film and its thickness.

Girard and Abadie (22) suggest that free and bound water can be distinguished on the basis that free water, owing to its conductivity, gives rise to a high dielectric loss at low frequencies while bound water does not. On the contrary, bound water causes an increased loss at higher frequencies, where conductivity losses are negligible, because its inclusion in the polar groups of the dielectric

causes increased polarisability. These workers illustrate their argument by contrasting results obtained with starch and gluten, each in a dry and a humid state. The two dielectric loss curves for starch coincide at higher frequencies and only differ at lower ones, which is taken to mean that all the water taken up by starch is free water. For gluten, on the other hand, the two curves differ widely at all frequencies, the losses for the greater water content being always the greater. This is taken to indicate that adsorbed water exists in both the free and the bound states in gluten.

Unfortunately, it is not necessarily true to say that bound water cannot give rise to conductivity losses, for it is likely that the films of bound water will not be perfect, and, consequently, rearrangement under the influence of an applied field will allow the migration of ions and so cause conductivity losses. This means that an estimate of the bound and free water contents cannot be made from the magnitude of the conductivity losses. The second distinction they draw is much more useful, though they do not make clear whether they believe the increased loss at higher frequencies to be due to the bound water directly or to some effect of the adsorbed water upon the samples used.

Dielectric relaxation losses as a means of distinguishing free and bound water were used by Freymann and Freymann (19) who point out that, at 3.10×10^4 Mc/s, bulk

water shows a maximum relaxation loss while ice shows no appreciable loss, so that the discovery of a high dielectric loss at this frequency may be taken as proof of the existence of free water in a system. They quote results to show that the water adsorbed on alumina and silica gel is free water and gives a loss at 10^4 Mc/s proportional to the water content. This application and a second of the same type (20) indicate that dielectric absorption measurements may be used in the study of bound water.

Freymann and Freymann have assumed, though they do not say so explicitly, that, since ice shows no loss at 10^4 Mc/s, bound water will not either. It is not a justifiable assumption as it is generally accepted that there can be no sharp distinction between bound water and free water, and that, in any system, all intermediate stages between the two will exist. The adsorbed water, owing to its various states of binding, may be expected to give rise to a number of loss curves with maxima at frequencies below 3.10^4 Mc/s, one peak arising from the water in each adsorbed molecular layer. The loss at 10^4 Mc/s will be the sum of the contributions from each absorption curve.

This objection is particularly applicable to the interpretation which these workers put upon the results in their second paper. There they show that the loss at 10^4 Mc/s, due to the water content of silica gel, decreases gradually to zero at -90° C as the temperature of measurement

is lowered. They interpret this as proving that adsorbed water freezes at -90° C. However, the loss decreases only gradually and the discontinuity in the loss/temperature curve, which is to be expected when water freezes, does not appear. It seems more likely that the various absorption peaks, which have just been proposed, shift gradually to lower frequencies as temperature decreases until the total loss at 10^4 Mc/s is zero. Since results are available for only a single frequency, the component losses cannot be separated to prove or disprove this point.

Buchanan et al. have also distinguished free from bound water on the assumption that all the absorption loss at 3.10^4 Mc/s is due to free water, and have calculated the bound water content of some protein solutions (12).

Roland and Bernard (37) have published interesting results obtained for silica gel. They measured the dielectric loss of the gel with adsorbed water, at frequencies around 10^4 Kc/s, in the temperature range 20° C to -130° C. At each frequency two absorption maxima were discovered. One maximum occurred at temperatures between 0° and -40° C, being at a temperature of -5° C at 10^4 Kc/s and at -35° C for 1^4 Kc/s. These figures were so like those obtained for pure ice that it was assumed that this loss maximum was due to the free water in the system. The second maximum occurred at -100° C for all frequencies and was assumed to be due to the bound water.

Carpeni (15), however, put a very different interpretation upon the results. Working from the one set of published curves he set up a few linear expressions and deduced from them that the two absorption maxima were due to the same water molecules differently associated at the higher and the lower temperatures. He deduced, too, that a truly bound layer, of one molecule thickness, was to be expected showing its maximum loss at 88^o C. This first layer takes no part in the dielectric absorption found experimentally. He remarked that the water adsorbed outside the first monolayer will be partly bound and partly free giving rise to dielectric absorptions at low frequencies and ultra high frequencies respectively.

In addition, it is of interest to note that in the results quoted the temperature of maximum loss decreases with increasing temperature which shows that, as water content increases, the layers causing the losses become less tightly bound.

To date, no fuller studies have been made of the dielectric properties of adsorbed films than these just quoted, which appear to have been no more than exploratory attempts. A much more promising base material than silica gel is provided by the silicate minerals whose particle shapes, surface areas and surface structures are known. There is a further advantage in their use, viz., that an acceptable model has been proposed by Hendricks and

Jefferson (28) for the actual structure of the adsorbed first and subsequent layers. The proposed structure is a hexagonal ring arrangement and is two dimensional only, which meets the condition proposed earlier (6). What is more, it has been remarked by Joly (30) that a value, in good agreement with experiment, may be calculated for the free energy of a monolayer of water molecules in contact with an organic monolayer if the water is assumed to be arranged in a hexagonal net as is proposed for the water on clays.

The silicate minerals have yet a further advantage in that certain of them have internal layers of water a known number of molecules thick and arranged with the same structure as external layers so that the properties of a single, double or triple layer are exposed for investigation.

To employ dielectric relaxation absorption measurements confers the advantage that the separate absorption losses due to the several layers have maximum values at frequencies depending upon the interaction of the molecules in each layer and the binding effect of the adsorbing surface. These absorption peaks are simply distinguishable as the total loss is the simple sum of the separate losses. By measuring the dielectric loss with varying frequency at a constant temperature, no possible ambiguity arises, as it did with Roland and Bernard, of the same water molecules being in two different states at two different temperatures.

CHAPTER 3
The work to be described follows these lines and is a study of the dielectric absorption properties of the adsorbed layers of water on the clay minerals Halloysite, Kaolinite and Talc. of the clay mineral Halloysite, a hydrous aluminum silicate. The variety used comes from Bedford, Indiana, U.S.A.

3.1 - The Mineral Halloysite.

From X-ray studies it is known that the crystallite of halloysite, which has a hollow cylindrical morphology, has a layer structure made up of monomolecular water layers alternating with Kaolin-type layers. In the latter the atoms in the unit cell are so arranged that one face of each layer consists wholly of oxygen atoms and the other wholly of hydroxyl groups. Thus, each monomolecular layer of water is bounded on one side by a plane of hydroxyl groups and on the other by a plane of oxygen atoms as shown in diagram (13a, b). A structure has been proposed by Hendricks and Jefferson (26) for this layer of water in which the water molecules are arranged in hexagonal rings as shown in diagram (13).

The water molecules in the interlayers are weakly bonded to the unit cell and may be removed readily either by heating the halloysite gently or by placing it in a lower relative humidity than is normal. To each value of relative humidity, in which the halloysite has settled, there

CHAPTER 2.

AN OUTLINE OF THE WORK.

In the work to be detailed, attention is concentrated upon the properties of the clay mineral Halloysite, a hydrous aluminium silicate. The variety used comes from Bedford, Indiana, U.S.A.

2.1 - The Mineral Halloysite.

From X-ray studies it is known that the crystallite of halloysite, which has a hollow cylindrical morphology, has a layer structure made up of monomolecular water layers alternating with Kaolin-type layers. In the latter the atoms in the unit cell are so arranged that one face of each layer consists wholly of oxygen atoms and the other wholly of hydroxyl groups. Thus, each monomolecular layer of water is bounded on one side by a plane of hydroxyl groups and on the other by a plane of oxygen atoms as shown in diagram (12a, b). A structure has been proposed by Hendricks and Jefferson (28) for this layer of water in which the water molecules are arranged in hexagonal rings as shown in diagram (13).

The water molecules in the interlayers are weakly bonded to the unit cell and may be removed readily either by heating the halloysite gently or by placing it in a lower relative humidity than is normal. To each value of relative humidity, in which the halloysite has settled, there

corresponds a definite water content.

When a water layer is removed the oxygen and hydroxyl surfaces of neighbouring kaolin-type layers move closer. They become so strongly bonded together by hydrogen bonds that water molecules cannot be returned to the places formerly occupied once they are removed. During dehydration, there is a progressive decrease in the average spacing between the oxygen and hydroxyl faces of neighbouring layers, although in any dehydration state the remaining water molecules must still cause a maximum spacing of the faces between which they lie.

X-ray evidence cannot distinguish between two possible modes of dehydration. In the first, dehydration proceeds by a complete layer of water molecules being removed at a time while others are untouched. In the second, the water molecules are removed randomly from the layers leaving isolated groups of molecules. It is likely that the remaining water molecules on either model are arranged according to the Hendricks' model of the undisturbed layer.

In the present work a study of the internal water layers was intended. It was expected to tell whether this layer had a random structure or an ordered one, and to distinguish between the modes of dehydration.

From the point of view of a study of the dielectric properties of the interlayers of water, halloysite has

certain advantages and disadvantages. Its advantages are:-

(1) - The structure of the basic mineral is known with certainty, and, with it, the probable structure of the water layer. In particular, the water layer is of one molecule thickness.

(2) - Samples with a definite interlayer water content may be prepared by dehydration to equilibrium in a known relative humidity and this water content may be preserved by storing the sample in a higher relative humidity.

(3) - Water molecules must be adsorbed on the outer surfaces of the crystallites and will cause spurious effects. The effects due to interlayer water may, however, be distinguished from those due to surface water because a material originally in equilibrium with a higher relative humidity, then brought to equilibrium with a lower one and finally brought back to equilibrium with the first will have precisely the same amount of water adsorbed on its external surfaces in the end as in the beginning. The interlayer water content will be, to begin with, that in equilibrium with the original atmosphere and, to end with, that in equilibrium with the lower relative humidity. The change in properties from beginning to end will be due to the loss of the interlayer water. Thus, experimental results may be obtained with a "difference" method.

There are two possible disadvantages with halloysite. Firstly, the mineral cannot be obtained in large crystals,

nor can the small crystallites be oriented by sedimentation. This prevents the measurement of the dielectric properties of the water layers for different directions of applied field. Secondly, because of the cylindrical form of the crystallites, no simple connection exists between their dielectric constant and the effective dielectric constant of a mass of them randomly oriented in air.

2.2 A Summary of Dielectric Theory.

It is possible to predict the nature of the dielectric properties which the water layers should possess. Water molecules are electrically dipolar and a material containing such dipoles shows the phenomenon known as 'relaxation absorption', the precise details of the absorption depending upon the various constraints acting on the dipoles.

If a dielectric contains dipoles, because of the lag of the dipolar polarisation upon the applied field, there is a power loss in the dielectric in alternating fields. This is taken into account by regarding the dielectric constant ϵ as a complex quantity $\epsilon_1 - j\epsilon_2$ where ϵ_1 is the normally accepted dielectric constant and ϵ_2 is the dielectric loss constant. The latter is proportional to the rate of loss of energy per unit time.

Both ϵ_1 and ϵ_2 vary with frequency, and at frequencies near a definite frequency f_m the dielectric shows 'relaxation absorption', i.e., $\epsilon(\omega)$ drops from a higher

value ϵ_s at lower frequencies to a lower value ϵ_∞ at higher frequencies, while $\epsilon_2(\omega)$ shows a maximum value at f_m . The curves are given by the Debye equations (3.3) and (3.4) and are plotted on graph (1).

To establish the Debye Equations it is assumed (a) that all dipoles in a material are in precisely the same environment, i.e. they are all constrained in exactly the same way and (b) that the dipoles do not interact with each other. If this is so, on the application of a steady field, the resulting dipolar polarisation reaches its final steady value exponentially with a relaxation time τ . This exponential approach to equilibrium is necessary if the Debye equations are to apply. The relaxation time τ is related to the frequency of maximum absorption by $\tau = \frac{1}{2\pi} f_m$.

According to the Debye equations the curves are characterised by two factors. The first, $\epsilon_s - \epsilon_\infty$, is the total change in $\epsilon_1(\omega)$ in passing through the absorption region, and is also equal to twice the maximum value of $\epsilon_2(\omega)$. The second factor is the relaxation time. In certain limited cases $\epsilon_s - \epsilon_\infty$ may be predicted. No theoretical prediction of τ is as yet possible.

In general, experimental curves are obtained which are flattened in comparison with the Debye curves, i.e., although the low and high frequency limits are still the same the change in $\epsilon_1(\omega)$ is less rapid and the peak in $\epsilon_2(\omega)$ is broader and less high. The general case differs from the Debye case

in the assumed environment of the dipolar molecules. Now it is assumed that the molecules are either each in slightly different states of binding to local non-polar molecules, as in the case of dipolar molecules in crystalline solids, or interacting with neighbouring dipoles. In either event, the

$\epsilon_1(\omega)$ and $\epsilon_2(\omega)$ curves are the resultants of a large number of separate curves of the Debye type, each caused by a group of dipoles having the same environment. The resulting curves are characterised by two relaxation times τ_0 and $\tau_1 = \beta^2 \tau_0$ which are in effect the limits of the range of possible τ values. Wider and less pronounced peaks occur in the $\epsilon_2(\omega)$ curves as the constant β increases, the Debye curve being the particular case, $\beta = 1$. The maximum value of $\epsilon_2(\omega)$ occurs at $\omega = 1/\beta \tau_0$.

Knowing this general theory of relaxation absorption, by fitting theoretical curves to sets of experimental results, it is possible to find $\epsilon_s - \epsilon_\infty$, τ_0 and β and so to tell several details of the dipolar molecules causing the relaxation absorption. Thus: -

(a) The value of $\epsilon_s - \epsilon_\infty$ may be used to calculate the effective dipole moment of the molecule if the dipoles are known to be in dilute solution, i.e., not interacting at all.

(b) The value of τ_0 gives some idea of the state of the molecule for it is known that τ_0 depends upon the state of binding of the dipolar molecule to other molecules

of the crystal of which it is part, and upon the degree of interaction between dipoles.

(c) The value of β gives an idea of the degree of irregularity of the environment of the dipolar molecules.

Since the two factors γ_0 and β yield the maximum information it is better to measure $\epsilon_2(\omega)$ than $\epsilon_1(\omega)$. The $\epsilon_2(\omega)$ curve shows a maximum value, from the frequency position of which γ_0 may be calculated. β may be found from the theoretical curve which best fits the experimental points. The $\epsilon_1(\omega)$ curve shows only a point of inflexion at f_m and the curve does not alter appreciably with varying β . It is important to note, too, that $\epsilon_1(\omega)$ for the whole material, because of its definition, will be a complicated function of the dielectric constants of the component materials, whereas $\epsilon_2(\omega)$ is simply the sum of the losses of the component materials.

2.3 - The Dielectric Constant of Halloysite.

The dielectric properties of halloysite may now be considered, the $\epsilon_1(\omega)$ properties being taken first. The kaolin-type layers should show no variation of ϵ_1 with frequency as the structure is strongly cross-bonded and contains no relatively free polar groups. The ϵ_1 for this layer should be about 8 - the general value obtained for dry material of this nature (25).

The water layers are completely different and are

composed of dipolar molecules in a definite arrangement, with the neighbouring molecules so close together that they must interact. The dielectric constant of such a layer may be expected to be about 80 at a sufficiently low frequency and about 3 at very much higher frequencies than the frequency of the relaxation absorption maximum.

Thus the halloysite crystal is a layer dielectric consisting of alternate layers of high and low dielectric constants. If the layers were entirely flat then the dielectric constant of the whole would have a different value in each of two different directions - one ϵ_{\parallel} which would apply for a field direction parallel to the layers and the other ϵ_{\perp} which would apply for a field direction perpendicular to the layers. Both can be calculated for this model by elementary theory. They involve not only the dielectric constants of the layers but also their thicknesses.

The model used above is too simple, however, for the crystallite is in fact a hollow cylinder. Even if it is assumed that the individual layers are isotropic in their dielectric properties, the crystal, because of its structure, will possess anisotropic properties, having an ϵ_{\parallel} for applied fields parallel to the axis of the crystal and ϵ_{\perp} for fields perpendicular to the axis. ϵ_{\parallel} will be a simple function of the dielectric constants of the layers but ϵ_{\perp} will be a complicated function because of the distribution of the field between the layers of high and low dielectric constant.

Further, halloysite crystallites cannot be oriented, and, as a result, the material upon which dielectric measurements must be made is an agglomerate of randomly oriented crystallites with all interspaces filled with air. Thus it would be extremely difficult mathematically to connect the dielectric constant of the material as a whole with that of the individual crystallites and then with those of the kaolin-type and water layers.

It is to be expected that the dielectric constant of the material, as a function of frequency, will show a drop approximately of the type predicted by the generalised Debye equation owing to the presence of the dipolar molecules, but that the change observed will be small as the water molecules are effectively finely dispersed among the kaolin-type layers and the air, both of which are of lower dielectric constant. The effective dielectric constant will depend more upon the dielectric constant of the layers of low dielectric constant and less upon that of the layers of high as the relative proportion of the latter decreases. Further, because of the formulae linking the effective dielectric constant with that of the water layer, the curve followed by the former will be a distorted form of the generalised Debye curve.

The change in dielectric constant of the water layer with changing states of hydration of the mineral is required. Because of the unknown intermediate formulae mentioned above, this cannot be done successfully by measuring the effective

dielectric constant.

2.4 - The Dielectric Loss of Halloysite.

Consider the layers of structure separately. The kaolin-type layers are expected to have a constant value of ϵ_1 at all frequencies and so $\epsilon_2(\omega)$ cannot show relaxation absorption since $\epsilon_1(\omega)$ and $\epsilon_2(\omega)$ are not independent. However, there will probably be a small loss in the dielectric because of internal frictions and thus a small value of $\epsilon_2(\omega)$ which will vary only slowly with frequency.

The water layers are composed of dipolar molecules in a definite order and certainly interacting. This must give rise to a relaxation absorption, probably of the general type.

The $\epsilon_2(\omega)$ curve for a crystallite is the sum of the two separate curves for the kaolin and water layers, i.e. a curve of the general relaxation absorption type superimposed on an almost constant background. The $\epsilon_2(\omega)$ curve for an aggregate of crystallites will be of the same form, for the loss introduced by the air filling the spaces between crystallites will be negligible.

At this stage account has to be taken of surface adsorbed water. This may give rise to two effects. Firstly, these water films have a conductivity σ and this gives rise to a loss constant $\epsilon_2 = \frac{4\pi\sigma}{\omega}$ which forms a background to the curves mentioned above. Secondly, one external surface of the halloysite crystal is a hydroxyl surface and another an oxygen surface. These surfaces are identical with those

facing the internal water layers, and it is, therefore, to be expected that adsorbed water will take up a hexagonal structure like that of internal layers. The binding of the external water is presumably looser than that of the internal, and thus the relaxation absorption maximum due to the external water is to be expected at a higher frequency than that due to the internal water layers.

2.5 - The Frequency of Relaxation Absorption.

It remains to discuss the likely values of the frequency at which $\epsilon_2(\omega)$ will show maximum values. This can only be done by comparing the arrangement of the internal and adsorbed water layers with the short term arrangement of the water molecules in water and the crystalline state in ice.

Water and ice have the same local structure, i.e. each water molecule has four nearest neighbours which occupy the four corners of a tetrahedron with the first molecule at the centre (40). In water this arrangement does not persist far beyond first neighbours and the molecules of a group are always changing. In ice this order persists through the crystal, each corner molecules of one tetrahedron being also a corner molecule of a second. The frequency of maximum absorption for water is 3.10^4 Mc/s at 20° C, while that for ice is 35 Kc/s at -5° C (16), (31), the vast difference in the corresponding frequency values being due to the greater

order in ice.

(a) Internal Water Layers.

The structure of the internal water layer is a two dimensional structure. In it each water molecule is surrounded by three others occupying the corners of a triangle having the molecule as centre, the spacing of the molecules being almost the same as that in the tetrahedra in water and ice. Further, there is a high degree of order in the layer. From this it is expected that the water layer will behave like ice and show an absorption maximum at a frequency of the same order as that for ice.

In addition, the layer is affected by the mineral layers between which it is confined. The effect of the 'crystalline field' is to decrease further the frequency at which maximum absorption occurs.

This frequency might increase or remain constant as the layers are dehydrated, depending upon the way the arrangement of the water molecules varies. If dehydration proceeds with the removal of a complete layer at a time, ν_m will remain constant. If, as suggested by Brindley and Robinson (10a), dehydration proceeds with molecules leaving all layers at the same time, remaining molecules being left in groups each with the internal arrangement of a complete layer, ν_m will remain constant with perhaps a slight increase as the groups become smaller and the effect of long range order less. If the molecules rearrange in the groups, a

large increase in f_m is to be expected, for any rearrangement will probably be less compact and so dipolar interactions will be less.

(b) External Water Layers.

The frequency of maximum absorption due to the external layers can be estimated in the same way. The first layer adsorbed upon the surface will probably have the same arrangement as an internal layer as it is adsorbed upon the same type of surface. This external layer is bonded only to one surface and consequently will have a much higher value of f_m than the internal layer.

If it is assumed that, after the first few molecules are adsorbed in the first layer, the others form groups round them, then the value of f_m for the incomplete layer will become that for a full layer before the groups are large enough to join, perhaps even before the loss due to them becomes appreciable.

It is possible for more than one layer of water to be adsorbed on the external surfaces. The second layer will not have the crystal surface to build upon but will build upon the somewhat mobile first water layer. It will be less regular in its arrangement of molecules and will be less constrained by the surface and is to be expected to give rise to an absorption maximum at a higher frequency than that of the first layer.

The situation will degenerate rapidly with the number

of water layers adsorbed. Perhaps in even a fourth layer the molecules will be as free as in water with the absorption maximum due to it occurring at a frequency approaching 10^4 Mc/s.

Further, the second, and to a lesser extent the third and subsequent layers, will react on the first. Since the second layer is less ordered than the first, the reaction will take the form of a weakening of the bonding of molecules of the first layer causing f_m for this layer to increase.

2.6 - The Variation of β with Water Content.

(a) Internal Water Layers.

In the case of the internal layers, even at full hydration, it is not expected that $\beta=1$, for the crystal will not be perfect, and also the environment of water molecules at the edges of layers will be different from those in the centre. β will vary as the layers are dehydrated in a way depending on the manner in which dehydration proceeds. It will remain constant if the water molecules are removed one complete layer at a time. It will increase with dehydration if the Brindley and Robinson model applies because of the increased edge effects as the group size decreases. It may decrease if the molecules in the groups rearrange in a less compact form.

(b) External Water Layers.

The first adsorbed layer should have a greater value

of β than an internal layer as the external layer is not expected to be quite as well ordered. The addition of a second layer is expected partly to disarrange the first layer further increasing β .

Second and subsequent layers will be less ordered than the first but it is doubtful whether β will be larger or smaller, for these layers are tending towards the arrangement of normal water for which $\beta = 1$.

2.7 - The variation of $\epsilon_s - \epsilon_o$ with water content.

$\epsilon_s - \epsilon_o$ will be proportional to the number of absorbing water molecules. In the case of interlayer water it will decrease proportionally with the interlayer water content, and for adsorbed layers it will increase with the number of molecules added in the water layer becoming constant once the layer is complete.

2.8 - A brief indication of Experimental Results.

Because of its lack of usefulness, the $\epsilon_1(\omega)$ curve is seldom taken. Attention is concentrated upon $\epsilon_2(\omega)$.

The various intermediate hydration states of halloysite are prepared by dehydrating the powdered, natural mineral in known relative humidities. The completely dehydrated halloysite, or metahalloysite, is prepared by heating powdered, natural halloysite to 360° C for three hours. This treatment ensures complete dehydration without breaking down the structure of the mineral.

Experimental results on these two types of sample, the partly and the totally dehydrated halloysite, taken when they have settled in the same atmosphere give almost the same curve for both.

These curves show the constant background due to the kaolin layers, the $\epsilon_2 = \frac{4\pi\sigma}{\omega}$ background due to the conductivity of the external water layers and one absorption peak. With increasing humidity the conductivity background increases and the absorption peak moves to higher frequencies. Graphs (7) and (10) are typical of the results.

Since a similar absorption peak is obtained for both the hydrated and dehydrated halloysites, and the maximum value moves to higher frequencies with increasing humidity, the absorption must be attributed to the external water layers.

The frequency range of measurement possible with the apparatus used is 2.5 Kc/s to 25 Mc/s. The frequency position of the maximum absorption obtained with metahalloysite varies from about 10 Mc/s in a 100% relative humidity to 2 Kc/s in a 20% relative humidity. At lower relative humidities the absorption maximum occurs at frequencies below the lower frequency limit of the apparatus.

Throughout the frequency range no evidence is found of any other absorption maximum. The maximum due to the internal water layers must therefore occur at a frequency below 2.5 Kc/s, i.e. at a much lower frequency than for ice.

Weighing measurements and a knowledge of the surface area of the sample shows that the external water is at least one layer thick even at 20% relative humidity. However, no evidence is found of an absorption maximum due to even the second external layer. This must occur at some frequency well above 25 Mc/s.

2.9 - The Extension of the Investigation.

When it was found that the results were to be attributed to the externally adsorbed layers of water on the halloysite, it was thought that the work could usefully be extended by examining the dielectric absorption curves of the externally adsorbed layers on minerals related to halloysite. By a suitable choice of minerals it was thought possible to establish the effect of crystal size and shape, and whether the water layers bonded more firmly to the oxygen or hydroxyl faces.

The minerals chosen were KAOLINITE, TALC and GIBBSITE.

Kaolinite is built up of the same kaolin layers as halloysite but there are no internal water layers. The crystal is a large, flat, thin plate having a diameter up to 3000 microns. The two large-area surfaces are composed of oxygen atoms and hydroxyl groups, exactly like those of halloysite, so that the effect of crystal size and shape may be examined by comparing the $\epsilon_2(\omega)$ curves for kaolinite and halloysite.

Talc is again a flat, plate-like crystal but having both large faces built of oxygen atoms in the same arrangement as in the oxygen face of halloysite.

Gibbsite has both main faces composed of hydroxyl groups similarly arranged to the hydroxyl faces of halloysite.

By a comparison of the curves due to the surface adsorbed layers on talc, gibbsite and halloysite, it is possible to tell whether the water layers are bonded to the oxygen or the hydroxyl surface in halloysite.

Nil results are obtained with the gibbsite, possibly because the material is not a natural mineral but has been chemically treated, section (6.10).

The results obtained with talc show an absorption maximum at about 10 Kc/s, the maximum increasing as humidity increases but staying in the same frequency position. Judging from these results, the first external layer of water on a large oxygen surface is still building up at 100% relative humidity and has an absorption maximum at about 10 Kc/s. This indicates that the bonding of water to an oxygen surface is weak as only one layer is adsorbed, but that a high degree of order obtains since the frequency of maximum is as low as 10 Kc/s.

The results obtained with kaolinite are extremely interesting as two maxima are noted. One maximum is constant in frequency position at about 10 Kc/s, and is to be compared

with that obtained with talc. This maximum must be attributed to the water layer adsorbed upon the oxygen face of the kaolinite. The other maximum moves to higher frequencies as the humidity is increased, and is to be compared with the maximum observed with halloysite. The maxima obtained with kaolinite and halloysite are therefore due to the layer of water adsorbed on the hydroxyl surfaces of the crystals. As these maxima move to higher frequencies with higher relative humidities, more than one layer is adsorbed and the hydroxyl groups are to be regarded as the stronger bonding centres.

A complete discussion of the results and conclusions is deferred to chapters 7 and 8.

2.10 - The Apparatus in Outline.

The dielectric properties are calculated from the change in natural resonant frequency and Q value of a series resonant inductance-capacitance circuit when the capacitor of the circuit is shunted by a test capacitor containing the powder being examined.

Let such a circuit have a total tuning capacitance C and a Q value Q_0 when in resonance. Let a capacitor of capacitance C_0 , filled with a lossy dielectric of complex dielectric constant $\epsilon_1 - j \epsilon_2$, be placed in parallel with the tuning capacitance. The circuit is detuned by the addition of the test capacitance, but resonance may be re-established

by reducing the original capacitance of the circuit to C_1 . This change in capacitance will give ϵ_1 for

$$\epsilon_1 = \frac{C - C_1}{C_0} \quad (4.6)$$

When resonance is re-established the Q value Q_1 will be lower than Q_0 . It may be shown that

$$\epsilon_2 = \frac{C}{C_0} \left(\frac{1}{Q_1} - \frac{1}{Q_0} \right) \quad (4.5)$$

(a) The Q Meter.

The apparatus used to measure the dielectric properties (diagram 1) is designed round a Q meter by Marconi Instruments Ltd. This instrument reads Q values directly.

A block diagram of the instrument is shown in diagram (4). It contains an oscillator, with a working range from 50 Kc/s to 50 Mc/s, which supplies power via the "set power" unit to a series resonant circuit consisting of an interchangeable inductor and a variable standard capacitor. When the circuit is in resonance the "read Q" meter indicates the Q value of the circuit. The dial of the standard capacitance gives C. A capacitor, filled with the powder whose complex dielectric constant is to be measured, is connected across the "capacitor test" terminals. Resonance is re-established and C_1 and Q_1 are found. From these readings ϵ_1 and ϵ_2 may be calculated.

(b) Additional Apparatus.

Several additions were made to the Q meter including an inductor for each frequency of measurement, an additional variable standard capacitor and a unit containing the test

capacitors. capacitance of the test capacitor is chosen by

Reference to equation (4.5) shows that the greatest sensitivity of measurement of ϵ_2 is obtained when the total tuning capacitance is a maximum. The value chosen is 400 picofarads. An inductance for each frequency of measurement is then required to resonate with this capacitance.

Measurements are required at only three frequencies in each decade, but still thirteen inductors are required to cover the total range of frequency.

External to the Q meter there are the test capacitor units. The material in the test capacitor has to be brought to equilibrium with a definite relative humidity, and measurements have to be made without disturbing this equilibrium. To achieve this, units are used of four capacitors suspended beneath Pye-type sockets passing through a strong brass plate, which forms the lid of a six-inch dessicator, the capacitors being inside. For test purposes connection is made to the capacitors via the sockets in the brass plates.

A set of four small glass tubes is kept in each enclosure. Small samples of the minerals in the test capacitors are kept in these tubes, and, by weighing them, the percentage weights of adsorbed and interlayer water are found.

The humidity within these enclosures is maintained by known concentrations of Sulphuric Acid.

The capacitance of the test capacitor is chosen by experiment to be 3.3 picofarads, i.e., as large as possible within the limit that the total error in measuring a maximum value of ϵ_2 must not exceed three percent. The test capacitors are built as cylindrical capacitors.

The value of C_0 is very small so that $(\epsilon_s - \epsilon_0) C_0$, the change in test capacitance over an absorption range, is also very small, perhaps 10 to 20 picofarads.

As the dial of the main variable capacitor cannot be read to better than 1 picofarad, the variation of total capacitance of samples cannot be followed by readings on this dial, and a further variable capacitor has to be added. The capacitor used has a total range of 50 picofarads and is driven via a slow motion dial with a reading limit of 0.025 picofarads, which is beyond the detection sensitivity of the apparatus. This additional capacitor is mounted directly upon the capacitance test terminals.

A short length of best quality coaxial cable, terminating in a Pye-type plug, connects the test capacitance to the test terminals.

(c) The extended Frequency Range.

Experiment showed that the range of the Q meter, 50 Kc/s - 25 Mc/s, was not sufficient and that an extension of the range to lower frequencies was necessary.

The major problem involved was the provision of inductors of sufficiently high Q value, as initial Q values

less than 100 do not allow an accurate measurement of ϵ_2 . The problem was made more difficult by the fact that the maximum tuning capacitance was only 400 picofarads requiring a tuning inductance of 0.6 henrys at 10 Kc/s and about 8 henrys at 2.5 Kc/s. It was possible to make inductors of these inductances, but the highest Q values which could be produced were about 20 and 2 respectively, the first inductor having an iron dust core and the latter a laminated iron core. The latter inductor was the largest which could readily be made, and thus 2.5 Kc/s was the lowest frequency which could be reached.

The low Q values of these inductors are due partly to the resistance of the windings and partly to the core losses. These losses may be overcome if power is supplied to the inductor by some circuit external to the Q meter. The total effect of an inductor with such a circuit in parallel is that of an inductor with lower losses, i.e. higher Q value.

Such an external circuit was constructed as detailed in section (4.12). The 2.5 Kc/s inductor was the most lossy of all and the negative resistance unit was designed to give a maximum effective Q value of 250 with this inductor. The power feedback may be varied so that Q values of about 200 can be produced with any inductor. The unit was made to plug into the inductor terminals in parallel with the inductor.

To reach the low frequencies an audio frequency oscillator was used in place of the internal oscillator of

of the Q meter. is prepared by heating halloysite to 360 C

(d) Overall Calibration.

An overall calibration of the apparatus was necessary. This was achieved at all frequencies using a simple series resistance-capacitance network which exhibited the properties of the Debye absorption curves. The ϵ_2 values could be calculated readily for this circuit, and so, by making measurements upon it and comparing the calculated and experimental results, the apparatus could be calibrated.

2.11 - The Method in Outline.

From the natural Halloysite a total stock of about 200 gms. was accumulated after the mineral had been freed from impurity and had been crushed to pass a 100 mesh sieve. A sample of this proved to be about 98% halloysite. The other minerals were already in a finely powdered state when received and required no further treatment. The kaolinite was known to be English China Clay and so practically pure kaolinite. On X-ray examination, the talc proved to be a good specimen of the mineral but there was some doubt about the quality of the gibbsite.

(a) Preparation of partially dehydrated halloysite.

The partially dehydrated states of halloysite are prepared by dehydration in appropriate constant relative humidities. Three weeks are required for the dehydration to be completed. Fully dehydrated halloysite, or weighing samples are always subjected to the same humidity

metahalloysite. is prepared by heating halloysite to 360° C for three hours.

(b) The Measurements.

There are two separate sets of measurements to be made - one set to determine the dielectric properties and the second set to determine the percentage weights of the interlayer and the surface water.

The dielectric properties are found for a sample in a test capacitor by means of equations (4.5) and (4.6), the necessary unknown quantities being determined using the Q meter. The total tuning capacitance, C , and initial Q value, Q_0 , of a circuit are noted for a tuned circuit resonating at the frequency of measurement. The test capacitance is then shunted across the tuning capacitance. The decrease in this capacitance, $C - C_1$, required to bring the circuit back to resonance, and the new Q value Q_1 are noted. The air capacitance, C_0 , of the test capacitor is known, by calculation, from the capacitor dimensions, hence ϵ_1 and ϵ_2 may be determined at each frequency.

A complete set of measurements at spot frequencies between 2.5 Kc/s and 25 Mc/s gives the $\epsilon_1(\omega)$ and $\epsilon_2(\omega)$ curves for the sample.

To avoid excessive handling of the capacitors the weighing measurements are made upon small samples of about 0.5 gm. of each mineral contained in weighing tubes. These weighing samples are always subjected to the same humidity

as the capacitor samples. Their weights are taken after the dielectric measurements are complete, and, from them, the interlayer and adsorbed water contents are calculated.

The dielectric properties of substances are usually described in terms of the dielectric constant. For most materials this quantity is independent of the strength of the electric field over a wide range, but is dependent upon the frequency if the field is alternating. The dielectric constant also depends upon temperature.

3.1 - The Static Dielectric Constant.

If a capacitor is taken, consisting of two parallel plates whose distance apart, d , is small compared with their linear dimensions, and one plate is charged with a surface density of charge $+\sigma$ and the other with a surface density $-\sigma$ then, in vacuo, there exists between the plates an electrostatic field, E_0 , where $E_0 = 4\pi\sigma$. Now let the capacitor be filled with a dielectric without disturbing the charges on the capacitor plates. Although it is electrically neutral, the dielectric consists of equal amounts of positive and negative charge which are displaced relative to each other under the action of the charges on the capacitor plates. The total amount of displaced charge passing across unit area parallel to the plates is constant and is called the dielectric polarization, P .

A negative surface charge of surface density, P .

CHAPTER 3.

THE THEORY OF DIELECTRICS.

The dielectric properties of substances are usually described in terms of the dielectric constant. For most materials this quantity is independent of the strength of the electric field over a wide range, but is dependent upon the frequency if the field is alternating. The dielectric constant also depends upon temperature.

3.1 - The Static Dielectric Constant.

If a capacitor is taken, consisting of two parallel plates whose distance apart, d , is small compared with their linear dimensions, and one plate is charged with a surface density of charge $+\sigma$ and the other with a surface density $-\sigma$ then, in vacuo, there exists between the plates an electrostatic field, E_v , where $E_v = 4\pi\sigma$. Now let the capacitor be filled with a dielectric without disturbing the charges on the capacitor plates. Although it is electrically neutral, the dielectric consists of equal amounts of positive and negative charge which are displaced relative to each other under the action of the charges on the capacitor plates. The total amount of displaced charge passing across unit area parallel to the plates is constant and is called the dielectric polarisation, P .

A negative surface charge of surface density, P ,

appears on the face of the dielectric close to the positively charged plate and vice versa. These two surface charges give rise to a field $E_p = 4\pi P$ in the opposite direction to the applied field so causing the effective field, E , acting in the dielectric to be -

$$E = E_v - 4\pi P = 4\pi\sigma - 4\pi P. \quad (3.1)$$

Now, the dielectric constant ϵ_s of the dielectric is defined as the ratio of the field in vacuo to that in the dielectric in the situation above, i.e. $\epsilon_s = E_v/E$.

Introduce a quantity D , the electric displacement, defined by

$$D = 4\pi P$$

Then

$$D = E_v = \epsilon_s E.$$

From equation (3.1) above

$$D = E + 4\pi P.$$

and so

$$\epsilon_s = 1 + 4\pi \frac{P}{E}.$$

hence

$$\epsilon_s - 1 = 4\pi \frac{P}{E}.$$

Further, surface densities of charge $+P$ and $-P$ have appeared on opposite faces of the dielectric which are of area, A , and distance apart, d , and so an effective dipole moment $PA d$ has been generated in a volume Ad .

Therefore, P may be replaced by m , the effective dipole moment generated per unit volume of the dielectric.

That is $\epsilon_s - 1 = 4\pi \frac{m}{E}$.

In dielectrics, the acquired dipole moment may arise in two ways. Firstly, an atomic polarisation arises because

the positively charged nucleus and the negatively charged electron cloud are displaced relative to each other by the action of the field. This generates a small dipole moment per molecule which depends directly upon the applied field. Secondly, a dipolar polarisation arises when the molecules of the dielectric have permanent dipole moments. Normally these dipoles are randomly arranged so that the material as a whole does not possess a dipole moment, but, when a field is applied, the dipoles attempt to orient with their axis in the direction of the field. Orientation is opposed by thermal agitation so that complete alignment is not possible. However, an effective dipole moment, proportional to the applied field, is generated throughout the volume of the material, its magnitude depending upon the temperature, the moment and concentration of the dipoles and the extent of their interactions.

3.2 - In Alternating Fields.

Because of the extremely low inertia of the electron cloud, atomic polarisation is able to follow precisely the variation of an alternating applied field of the highest frequency which can be produced. Molecular dipoles, on the other hand, owing to their appreciable inertia, are not able to follow all frequencies of field, and, in general, the component of polarisation due to dipole orientation lags behind the applied field.

If a periodic field $\vec{E} = E_0 e^{j\omega t}$ is applied to a dipolar dielectric, the resultant displacement \mathcal{D} will lag behind the applied field and so

$$\mathcal{D} = D_0 e^{j(\omega t - \phi)}$$

The dielectric constant ϵ is defined by $\mathcal{D} = \epsilon E$ hence $D_0 e^{j(\omega t - \phi)} = \epsilon E_0 e^{j\omega t}$

This requires ϵ to be complex, i.e. $\epsilon = \epsilon_1 - j\epsilon_2$ in which

$$D_{in} = D_0 \cos \phi = \epsilon_1 E_0$$

and $D_{out} = D_0 \sin \phi = \epsilon_2 E_0$

where the effective dielectric constant consists of two components ϵ_1 and ϵ_2 which relate the applied field to the 'in phase' and 'out of phase' components of the polarisation. ϵ_1 and ϵ_2 are both dependent on frequency.

ϵ_1 is precisely the dielectric constant as defined for static fields and will be the result of the atomic polarisation and the effective dipole polarisation. It has a larger value ϵ_s at zero frequency where dipole polarisation is fully effective and a smaller value ϵ_∞ at a very high frequency where dipole polarisation is negligible.

ϵ_2 , termed the dielectric loss constant, depends entirely upon the out of phase component of polarisation and may be shown (21) to be proportional to the rate of energy loss in the dielectric, this being given by

$$L = \frac{\epsilon_2 E_0^2 \omega}{8\pi}$$

If \mathcal{D} and ϵ are linearly related, as is true normally, ϵ_1 and ϵ_2 are not independent but are connected by the

equation

$$\epsilon_s - \epsilon_\infty = \frac{2}{\pi} \int_0^\infty \epsilon_2(\omega) \frac{d\omega}{\omega} \quad (3.2)$$

3.3 - The Frequency Variation of $\epsilon_1(\omega)$ and $\epsilon_2(\omega)$.

Before deriving the two equations which give the frequency dependence of $\epsilon_1(\omega)$ and $\epsilon_2(\omega)$ it is necessary to consider some further points about the two sources of polarisation. Atomic polarisation arises almost immediately upon the application of the field. The resulting steady value of polarisation is reached by a very rapid approach to the final value followed by a damped oscillation about it. Dipolar polarisation occurs when the probabilities of a dipole occupying any one of a number of initially equally probable orientations are altered by the action of the applied field, the orientation nearest in direction to that of the field being preferred. This chance process leads to equilibrium polarisation being established exponentially if a steady field is suddenly applied. Because of this exponential approach to equilibrium relaxation absorption occurs.

3.4 - The Debye Equations.

In a dielectric, owing to the lag of the polarisation, at any time, t , after a field $E(u)$ has been applied there is a resulting displacement $D(t)$ such that

$$D(t) = E(u) \chi(t-u)$$

where α is a decay function expressing the fact that the polarisation decays exponentially, i.e.

$$\alpha(t) \propto e^{-t/\tau}$$

where τ is a constant called the relaxation time.

There is also a contribution to \mathcal{D} due to atomic polarisation given by

$$\mathcal{D}(t) = \epsilon_0 E(t)$$

The total displacement due to a long established varying field is

$$\mathcal{D}(t) = \epsilon_0 E(t) + \int_{-\infty}^t E(u) \alpha(t-u) du.$$

If this equation is differentiated and the substitution used: -

$$\frac{d\alpha(t)}{dt} = -\frac{1}{\tau} \alpha(t)$$

then $\tau \frac{d\mathcal{D}(t)}{dt} = \epsilon_0 \tau \frac{dE(t)}{dt} + \tau \alpha(0) E(t) - \int_{-\infty}^t E(u) \alpha(t-u) du.$

adding this equation and the last gives

$$\tau \frac{d}{dt} (\mathcal{D} - \epsilon_0 E) + (\mathcal{D} - \epsilon_0 E) = \tau \alpha(0) E.$$

Now when a constant field is applied

$$\frac{d}{dt} (\mathcal{D} - \epsilon_0 E) = 0 \quad \mathcal{D} = \epsilon_s E$$

and so

$$\tau \alpha(0) = \epsilon_s - \epsilon_0$$

therefore $\tau \frac{d}{dt} (\mathcal{D} - \epsilon_0 E) + (\mathcal{D} - \epsilon_0 E) = (\epsilon_s - \epsilon_0) E$

This is the differential equation connecting $\mathcal{D}(t)$ with $E(t)$

provided $\alpha(t) = \frac{\epsilon_s - \epsilon_0}{\tau} e^{-t/\tau}$

If now a periodic field is applied,

$$E = E_0 e^{-j\omega t}$$

and $\frac{dE}{dt} = -j\omega E$, $D = \epsilon(\omega)E$, $\frac{dD}{dt} = -j\omega \epsilon(\omega)E$,

which when substituted in the differential equation give

$$\epsilon(\omega) - \epsilon_\infty = \frac{\epsilon_s - \epsilon_\infty}{1 - j\omega\tau}$$

Separating the real and imaginary parts of

$$\epsilon_1(\omega) - \epsilon_\infty = \frac{\epsilon_s - \epsilon_\infty}{1 + \omega^2\tau^2} \quad (3.3)$$

$$\epsilon_2(\omega) = \frac{(\epsilon_s - \epsilon_\infty)\omega\tau}{1 + \omega^2\tau^2} \quad (3.4)$$

which are the Debye Equations.

Graph (1) shows the variation with frequency of

$\epsilon_1(\omega)$ and $\epsilon_2(\omega)$ as expressed by these equations.

The maximum value of $\epsilon_2(\omega)$ occurs when

$$\frac{d\epsilon_2}{d\omega} = 0 \quad \text{ie} \quad \omega\tau = 1$$

at which frequency

$$\epsilon_1 = \frac{1}{2}(\epsilon_s + \epsilon_\infty) \quad \epsilon_2 = \frac{1}{2}(\epsilon_s - \epsilon_\infty)$$

from which it is seen that the frequency at which $\epsilon_2(\omega)$

has its maximum may be used to find the value of τ and the

magnitude of $\epsilon_2(\omega)$ may be used to give $(\epsilon_s - \epsilon_\infty)$, which, in

turn, may be used to give the dipole moment per unit volume

and so the dipole moment per dipole.

3.5 - The Applicability of the Debye Equations.

Provided three conditions are fulfilled by a dipolar dielectric an exponential approach to equilibrium is to be expected and the Debye equations are applicable. The

conditions are that -

1. there is no interaction between dipoles.
2. equilibrium is approached by only one process such as transition over a potential barrier.
3. all dipole positions are exactly alike.

Thus the equations are only applicable to gases and dilute solutions of dipolar substances in non-polar liquids. Exceptions exist particularly in the case of crystalline solids.

3.6 - The Generalised Debye Equations.

As has been noted, the Debye equations are specialised in their applicability. In practice, it is not usual for there to be a complete absence of dipolar interaction. When interaction does occur the energy of a dipole depends upon the arrangement of its neighbours. This arrangement varies from point to point throughout the dielectric so that all dipole positions are not equivalent and one relaxation time cannot characterise the assemblage.

However, it is possible to choose a distribution of relaxation times to represent the assemblage. Each set of dipoles represented by a small range $d\tau$ of relaxation times near τ will give rise to a contribution $E(\tau)$ to the static dielectric constant and so the total static dielectric constant will be given by

$$\epsilon_s - \epsilon_\infty = \int_0^\infty E(\tau) d\tau \quad (3.5)$$

on the basis of which it may be shown (21) that

$$\begin{aligned}\epsilon_1(\omega) - \epsilon_\infty &= \int_0^\infty \frac{\epsilon(\tau) d\tau}{1 + \omega^2 \tau^2} \\ \epsilon_2(\omega) &= \int_0^\infty \frac{\epsilon(\tau) \omega \tau d\tau}{1 + \omega^2 \tau^2}\end{aligned}$$

If the variation of $\epsilon_2(\omega)$ with frequency is considered, each group of dipoles represented by relaxation times in the range $d\tau$ about τ will contribute an $\epsilon_2(\omega)$ curve of the simple Debye type centred at $\omega = \frac{1}{\tau}$ and of a height depending upon the number of dipoles represented.

In the practical case, the majority of dipoles fall into an average grouping such that they can be represented by relaxation times lying continuously between two extreme values τ_0 and τ_1 . It may be assumed that all dipoles are represented by this distribution, i.e. that no dipoles have relaxation times outside the range τ_0 to τ_1 where $\tau_1 = \beta^2 \tau_0$. On this assumption the following equations for $\epsilon_1(\omega)$ and $\epsilon_2(\omega)$ may be derived from equation (3.5): -

$$\begin{aligned}\epsilon_1(\omega) - \epsilon_\infty &= (\epsilon_s - \epsilon_\infty) \left[1 - \frac{1}{2 \log \beta} \cdot \log \frac{1 + \left(\frac{\omega}{\omega_m} \beta\right)^2}{1 + \frac{\omega}{\omega_m} \beta} \right] \\ \epsilon_2(\omega) &= (\epsilon_s - \epsilon_\infty) \frac{1}{\log \beta^2} \left[\tan^{-1} \frac{\omega}{\omega_m} \beta - \tan^{-1} \frac{\omega}{\omega_m} - \frac{1}{\beta} \right] \quad (3.6)\end{aligned}$$

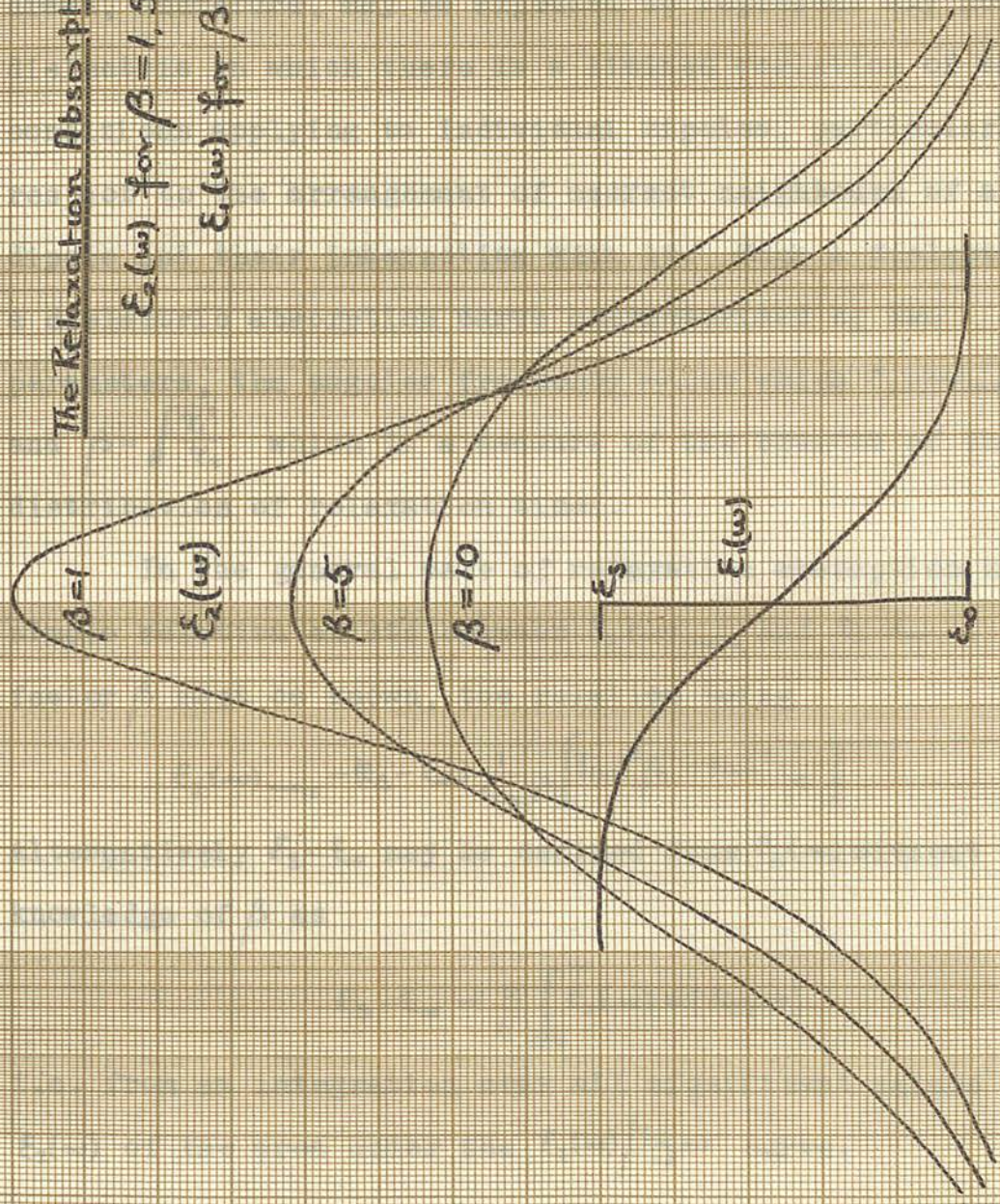
Graph (1) shows $\epsilon_2(\omega)$ for various values of the parameter β viz. $\beta = 1, 5$ and 10 . The curve $\beta = 1$ is the normal Debye curve as, at $\beta = 1$, τ_0 and τ_1 are coincident. Increasing β has the effect of making the curves less high and broader than the Debye curve. The maximum of $\epsilon_2(\omega)$ occurs at $\omega_m = \frac{1}{\beta \tau_0}$.

The Relaxation Absorption Curves

$\epsilon_2(\omega)$ for $\beta = 1, 5, 10$

$\epsilon_1(\omega)$ for $\beta = 1$

Graph 1



10⁻² 1 2 3 4 5 6 7 8 9 10⁰ 1 2 3 4 5 6 7 8 9 10¹ 1 2 3 4 5 6 7 8 9 10² frequency →

It may be shown that any smooth distribution of relaxation times which is large between τ_0 and $\beta\tau_0$ and small outside this range gives substantially the same shape of curve near the absorption maximum. The curves drawn, therefore, may be expected to represent any normal dielectric in which there is a limited variation of the conditions applying to individual dipoles, particularly with respect to the arrangement of nearest neighbours of a dipole and their interaction with it. Such a dielectric has a dielectric absorption curve characterised by two parameters, the angular frequency ω_m at which $\epsilon_2(\omega)_{max}$ occurs, and $\beta = \sqrt{\frac{\tau_1}{\tau_0}}$ which is a measure of the breadth of the distribution of relaxation times.

In the general case of relaxation absorption no simple relation exists between $\epsilon_2(\omega)_{max}$ and $\epsilon_s - \epsilon_\infty$. The factor β must be known, the relation being

$$\epsilon_2(\omega)_{max} = (\epsilon_s - \epsilon_\infty) \frac{1}{\log \beta^2} \left[\tan^{-1} \beta - \tan^{-1} \frac{1}{\beta} \right] \quad (3.7)$$

Alternatively $\epsilon_s - \epsilon_\infty$ may be derived from $\epsilon_2(\omega)$ without a knowledge of β as

$$\epsilon_s - \epsilon_\infty = \frac{2}{\pi} \int_0^\infty \epsilon_2(\omega) d(\log \omega) \quad (3.8)$$

i.e. from an integration over all significant values of $\epsilon_2(\omega)$ of the area under the $\epsilon_2(\omega)/\log \omega$ curve.

3.7 - The Theoretical Calculation of $\epsilon_s - \epsilon_\infty$.

The magnitude of $\epsilon_s - \epsilon_\infty$ can only be predicted in

certain specific cases, using the formulae of Onsager and Kirkwood (21), where such complete details of the dielectric are known as the number of dipoles per unit volume, the dipole moment per molecule and the relation of each dipole to its neighbours.

3.8 - The Calculation of τ .

No general formula exists for the calculation of τ but the factors influencing its value may be shown by an example. Consider a dipolar dielectric in which each dipole has two equilibrium positions, equally probable in the absence of a field, and separated by an energy barrier of height H . On a field being applied, the dielectric polarises exponentially with a relaxation time τ , which may be shown (21) to be

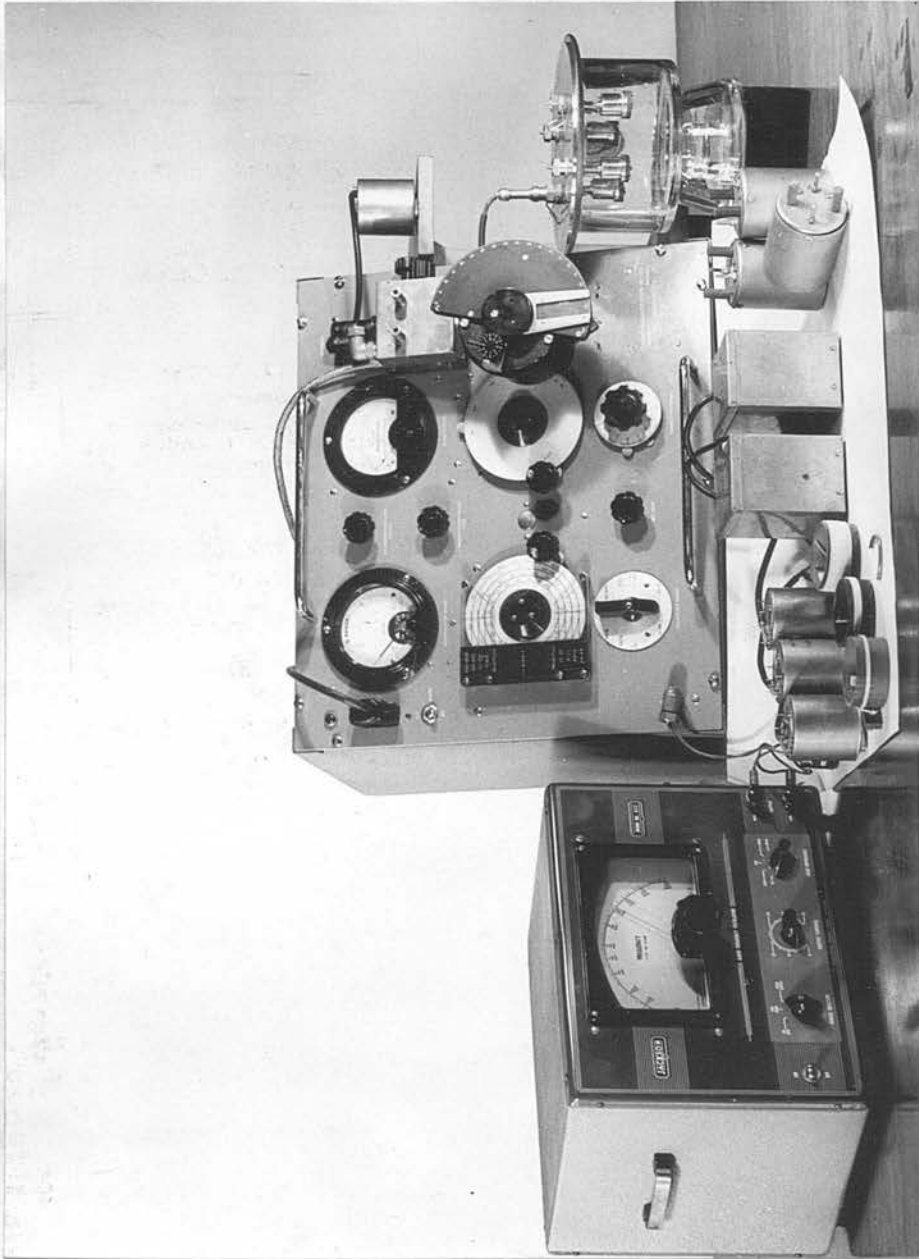
$$\tau = A e^{H/kT}$$

where A is a constant depending upon temperature.

Thus τ depends upon H the height of the potential barrier between equilibrium positions. The height of this barrier will depend upon the crystalline field.

In a general case H will depend upon the crystalline field, i.e. upon the strength of bonding of the dipolar molecules to surfaces or ions, and upon the extent of the interaction between dipoles. An increase in the strength of bonding or in the degree of interaction will increase τ .

Diagram 1.



THE APPARATUS.

CHAPTER 4.

APPARATUS.

In this chapter details are given of the design and mode of action of the apparatus which is shown in Diagram (1).

4.1 - The Definition of Q.

Consider a series circuit of inductance L and capacitance C . Such a circuit has energy losses associated with it. These occur mainly in the inductor and are represented by the addition of a resistance r in series with the inductance.

Now let an alternating voltage e of angular frequency ω be applied across the circuit. At this frequency the impedance of the circuit is

$$Z = r + j\omega L \left(1 - \frac{1}{\omega^2 LC}\right)$$

which is a minimum when $\omega = 1/\sqrt{LC}$

In this condition the circuit is said to be in resonance.

A voltage V appears across the capacitance where

$$\begin{aligned} V &= e \frac{Z_C}{Z} = e \frac{1/j\omega C}{r + j\omega L - 1/j\omega C} \\ &= e \cdot \frac{1}{j\omega C r - (\omega^2 LC - 1)} \end{aligned}$$

Taking the modulus

$$V = e \frac{1}{\sqrt{(\omega C r)^2 + (\omega^2 LC - 1)^2}} \quad (4.1)$$

V is a maximum when the denominator of the right-hand side is a minimum. To a good approximation, this happens when the second term in the denominator is zero, i.e. when

$$\omega^2 = 1/LC.$$



giving

$$V_m = e \cdot \frac{1}{\omega C r} = e \frac{\omega L}{r}$$

If a quantity Q is defined as the ratio of the maximum voltage generated across the capacitance to that applied across the circuit then

$$Q = \frac{V_m}{e} = \frac{\omega L}{r}$$

i.e. Q is equal to the ratio of the inductive impedance and the effective series resistance at the frequency considered.

If the full expression for the denominator of equation (4.1) is differentiated for a minimum, the true angular frequency of resonance and the true Q value are found to differ by a negligible factor from the approximate values quoted. Thus for all practical purposes the resonant frequency and Q value of a series resonant circuit are given by

$$\omega^2 LC = 1$$

$$Q = \frac{\omega L}{r}$$

4.2 - The Measurement of ϵ_1 and ϵ_2 .

Consider first of all the equivalence, as in diagram (2), between (a) a lossy capacitance $C_0(\epsilon_1 - j\epsilon_2)$ in parallel with a pure capacitance C_1 , and (b) a pure capacitance C_e with a series resistance r .

The admittance of circuit (a) must equal that of circuit (b).

$$\text{Thus } j\omega C_1 + j\omega C_0(\epsilon_1 - j\epsilon_2) = \frac{1}{r + 1/j\omega C_e}$$

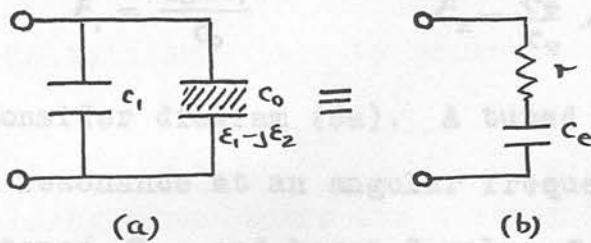
$$\text{or } j\omega(C_1 + \epsilon_1 C_0) + \omega C_0 \epsilon_2 = \omega^2 C_e^2 r + j\omega C_e \quad (r^2 \ll \frac{1}{\omega^2 C_e^2}).$$

Diagrams 2 & 3.

Equating real and imaginary parts

$$C_1 + \epsilon_1 C_0 = C_e \quad \epsilon_2 C_0 = \omega C_e r \quad (4.2)$$

or $f = \frac{C_0 - C_1}{C_0} \quad \epsilon_2 C_0 = \omega C_e r \quad (4.3)$



Now assume the circuit is initially in resonance at an angular frequency ω with a total capacitance C , and has a Q value Q_0 .

A lossy capacitor $C_0 (\epsilon_1 - j\epsilon_2)$ is placed in parallel with the first (3b). The circuit is again brought to resonance by changing the capacitance C to a new value C_1 , and now the Q value is Q_1 .

Diagram 2.

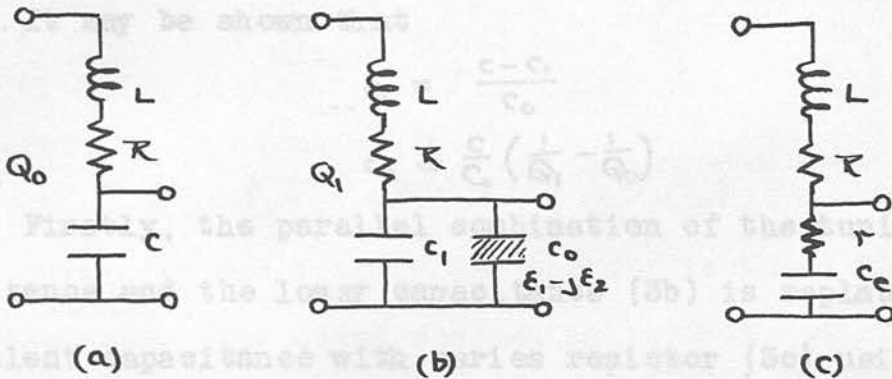


Figure 3 shows the parallel combination of the lossy capacitor and the lossy capacitor (3b) is replaced by an equivalent capacitance with series resistor (3c) using the equivalence derived above.

Diagram 3.

The Q value for this circuit is given by the ratio of the applied voltage and the voltage developed across the points A.A.. This voltage is given by

$$V = e \frac{r + \sqrt{j\omega C_e r}}{r + \sqrt{j\omega C_e r} + k + j\omega L}$$

$$= e \frac{1 + j\omega C_e r}{j\omega C_e (r + k) - (\omega^2 L C_e - 1)}$$

Equating real and imaginary parts

$$C_1 + \epsilon_1 C_0 = C_e \quad \epsilon_2 C_0 = \omega C_e^2 r \quad (4.2)$$

$$\text{or} \quad \epsilon_1 = \frac{C_0 - C_1}{C_0} \quad \epsilon_2 = \frac{C_e}{C_0} \omega C_e r \quad (4.3)$$

Now consider diagram (3a). A tuned circuit is initially in resonance at an angular frequency ω with a total capacitance C , and has a Q value Q_0 .

A lossy capacitance $C_0(\epsilon_1 - j\epsilon_2)$ is placed in parallel with the first (3b). The circuit is again brought to resonance by changing the capacitance C to a new value C_1 , and now the Q value is Q_1 .

It may be shown that

$$\epsilon_1 = \frac{C - C_1}{C_0}$$

$$\epsilon_2 = \frac{C}{C_0} \left(\frac{1}{Q_1} - \frac{1}{Q_0} \right)$$

Firstly, the parallel combination of the tuning capacitance and the lossy capacitance (3b) is replaced by an equivalent capacitance with series resistor (3c) using the equivalence derived above.

The Q value measured for this circuit is given by the ratio of the applied voltage and the voltage developed across the points $A.A.$. This voltage is given by

$$V = e \frac{r + 1/j\omega C_e}{r + 1/j\omega C_e + R + j\omega L}$$

$$= e \frac{1 + j\omega C_e r}{j\omega C_e (r + R) - (\omega^2 L C_e - 1)}$$

If, as before, $r \ll \frac{1}{\omega C_e}$ then $\omega C_e r$ may be ignored compared with 1, and the modulus of V becomes

$$V = e \frac{1}{\sqrt{[\omega C_e(r+R)]^2 + (\omega^2 LC - 1)^2}}$$

The Q value follows from this by comparison with equation (4.1) and is

$$Q_1 = \frac{\omega L}{r+R}$$

Without the lossy capacitance the circuit has an initial Q value,

$$Q_0 = \frac{\omega L}{R}$$

Obviously

$$\frac{r}{\omega L} = \frac{1}{Q_1} - \frac{1}{Q_0}$$

Now, it has been assumed that $\omega C_e r \ll 1$. For this condition the circuit will resonate when $\omega^2 LC_e = 1$ and hence

$$\omega C_e r = \frac{r}{\omega L} = \frac{1}{Q_1} - \frac{1}{Q_0} \quad (4.4)$$

and referring to equation (4.3)

$$\epsilon_2 = \frac{C_e}{C_0} \omega C_e r = \frac{C_e}{C_0} \left(\frac{1}{Q_1} - \frac{1}{Q_0} \right)$$

Since initially and finally the circuit is tuned to the same frequency, the total resonating capacitance is the same in both cases. Thus the initial tuning capacitance

C must equal the final tuning capacitance which is the equivalent capacitance C_e hence

$$\epsilon_2 = \frac{C_e}{C_0} \left(\frac{1}{Q_1} - \frac{1}{Q_1} \right) \quad (4.5)$$

and from equation (4.3)

$$\epsilon_1 = \frac{C - C_1}{C_0} \quad (4.6)$$

The assumption used throughout the derivation has still to be justified viz. - $\omega C_e r \ll 1$

From equation (4.4)

$$\omega C r = \left[\frac{1}{Q_1} - \frac{1}{Q_0} \right]$$

In practice, likely values of Q_0 and Q_1 are 200 and 60.

Therefore

$$\omega C r = \frac{1}{60} - \frac{1}{200} = \frac{1}{100}$$

and

$$\omega C r \ll 1$$

4.3 - The Incremental Capacitance Method of Measuring Q.

In this method the applied and output voltages need not be known absolutely though the applied voltage must be constant. The Q value is given by two measurements of capacity.

The circuit is brought to resonance at the required frequency, the resonant capacitance being C and the voltage developed across it $\sqrt{V_m}$ a maximum value. The capacitance is altered by an amount ΔC and a new, lower voltage $\sqrt{V_1} = \sqrt{V_m}/n$ is developed.

The voltage across the capacitance is, by equation

$$(4.1) \quad \sqrt{V} = e / \sqrt{r^2 \omega^2 C^2 + (\omega^2 L C - 1)^2}$$

Hence $\sqrt{V_m} = e / \omega C r$

and $\sqrt{V_1} = e / \sqrt{r^2 \omega^2 (C + \Delta C)^2 + [\omega^2 L (C + \Delta C) - 1]^2}$

which may be reduced to

$$\sqrt{V_1} = e / \sqrt{1 + \frac{\Delta C^2}{C^2} Q^2}$$

Rearranging

$$1 + \frac{\Delta C^2}{C^2} Q^2 = \frac{V_m^2}{V_1^2} = n^2$$

therefore

$$Q^2 = \frac{C^2}{\Delta C^2} (n^2 - 1) \quad , \quad Q = \frac{C}{\Delta C} (n^2 - 1)^{1/2}$$

In normal procedure the capacitance is altered until

$V_1 = \sqrt{2} V_m$ a voltage of this
in which case $Q = \frac{C}{\Delta C}$

This method is useful in cases where the injection voltage is unknown although it is constant and is of particular advantage when low losses have to be measured.

4.4 - The Direct Method of Measuring Q.

In this method Q is obtained from the definition

$Q = \frac{V_m}{e}$ and the magnitudes of the applied voltage e and the voltage V_m across the capacitance when the circuit is in resonance.

In the application of the method there are several practical points to be noted. If a true value of the Q of the circuit is to be obtained, the voltmeter placed across the capacitance must not shunt it with any appreciable admittance, for any conductance losses introduced by the voltmeter lower the Q value, and any shunt capacitance introduced alters the apparent value of the tuning capacitance.

The source impedance of the generator supplying e must be very low, otherwise the magnitude of e will depend upon the input impedance of the series resonant circuit.

This impedance changes very rapidly in modulus as the circuit is tuned through resonance, the change being more rapid as the Q value of the circuit increases.

Usually the voltage V_m is chosen to be about one volt,

as this is a convenient value for measurement, and so $e = \frac{V}{Q}$ is about one hundredth of a volt. A voltage of this order having a very low source impedance is best produced by passing an alternating current of about one ampere through a known resistance of about one hundredth of an ohm. The voltage e is directly proportional to the current flowing, which is of a magnitude readily measured by a thermocouple ammeter. If e is a fixed voltage, the voltmeter measuring V_m may be calibrated directly in Q values.

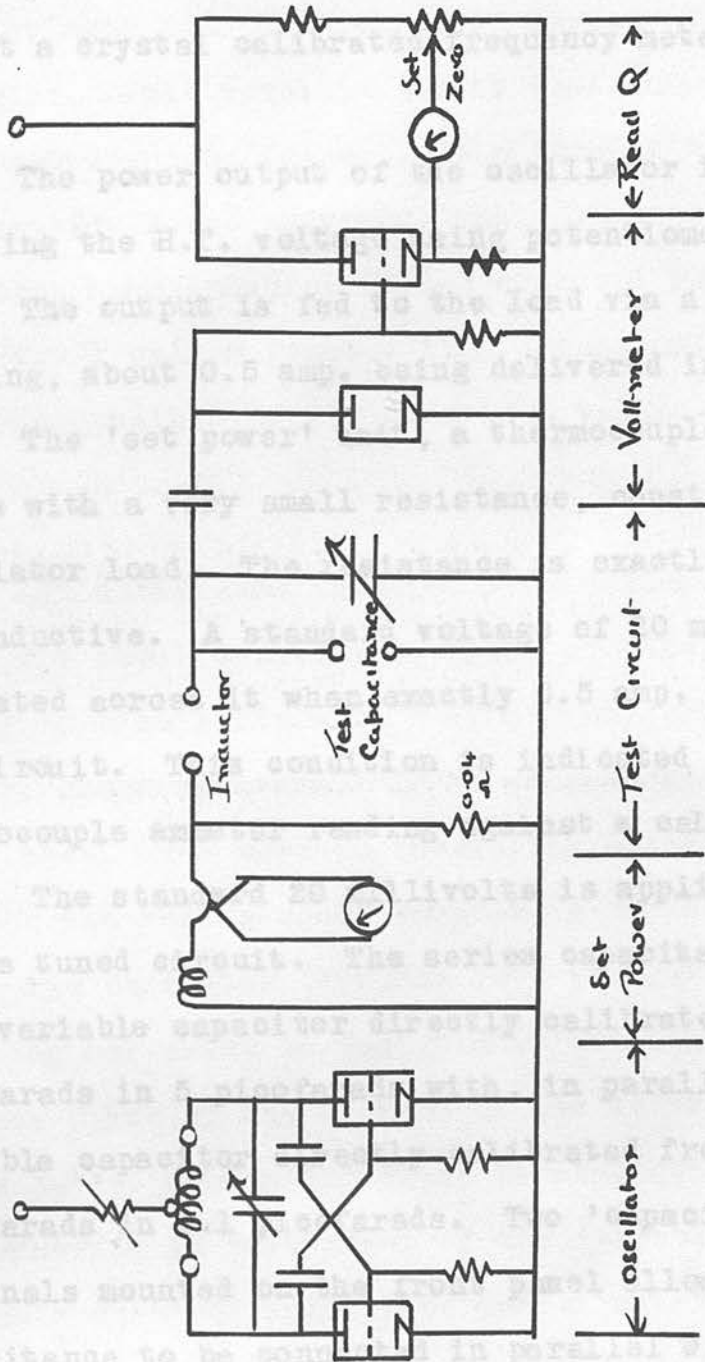
An instrument designed to measure Q by this method can also be used to give Q values by the incremental capacitance method, as the input voltage is constant and the voltmeter may be used to indicate the condition $V_1 = V_m/n$.

4.5 - The Q Meter by Marconi Instruments.

This basic part of the apparatus is designed to read Q values directly by the method detailed in the preceding section. A block diagram and a functional circuit are shown in diagram (4).

The oscillator is of the Hartley type, using two triode valves in push-pull for extra power output at higher frequencies. Within a range the frequency is altered by varying the value of the tuning capacitance, the dial of the capacitor being calibrated directly in frequency. The range of frequency covered is altered by interchanging the tuning inductors which are mounted in a turret behind a rotary

Diagram 4.



FUNCTIONAL CIRCUIT OF THE Q METER.

Diagram 4.

switch. Seven ranges cover all frequencies from 50 Kc/s to 50 Mc/s. The calibration of the oscillator, checked against a crystal calibrated frequency meter, is correct to 1%.

The power output of the oscillator is varied by adjusting the H.T. voltage using potentiometers in the H.T. lead. The output is fed to the load via a loose transformer coupling, about 0.5 amp. being delivered into 1 ohm.

The 'set power' unit, a thermocouple ammeter in series with a very small resistance, constitutes the oscillator load. The resistance is exactly 0.04 ohm and is non-inductive. A standard voltage of 20 millivolts is generated across it when exactly 0.5 amp. is passed round the circuit. This condition is indicated by the thermocouple ammeter reading against a calibration mark.

The standard 20 millivolts is applied across the series tuned circuit. The series capacitance is provided by a variable capacitor directly calibrated from 40 to 475 picofarads in 5 picofarads with, in parallel, a small variable capacitor directly calibrated from -3 to +3 picofarads in 0.1 picofarads. Two 'capacitor test' terminals mounted on the front panel allow a test capacitance to be connected in parallel with the main capacitance. The tuning inductor completing the circuit plugs into two similar 'inductor' terminals.

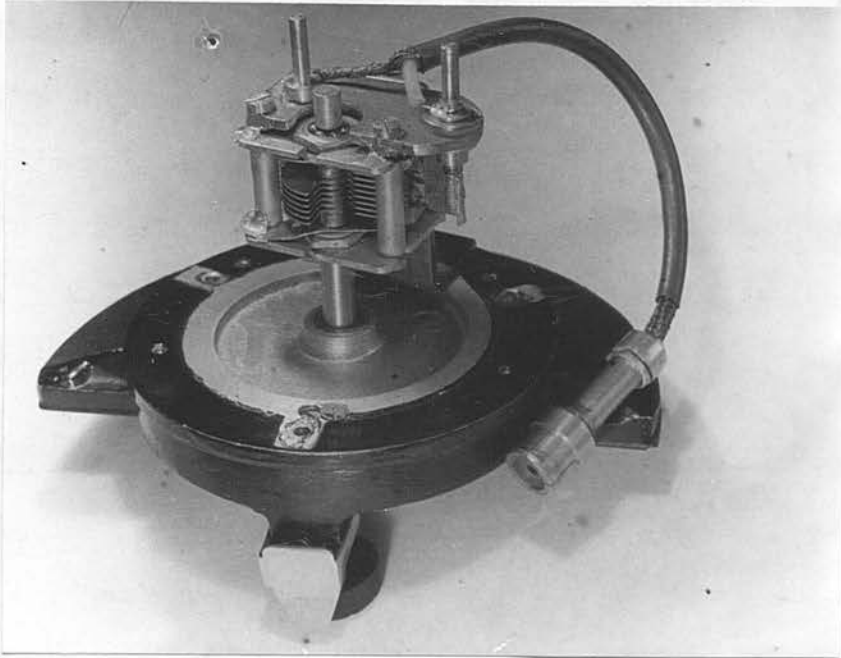
The voltage developed across the capacitance is

measured by the valve voltmeter which consists essentially of a diode rectifier followed by a directly coupled triode amplifier with a bridge-connected ammeter to read voltage or Q value. This meter is set to read zero for zero input to the voltmeter by adjusting the bias of the triode valve with the 'set zero' control. The voltmeter has a full scale deflection corresponding to a Q of 250. The deflection is linear for Q values greater than 80 and only obviously not linear at Q values less than 30. Q values may be read to ± 0.5 .

4.6 - The Additional Variable Standard Capacitor.

The total capacitance range of this capacitor is closely 50 picofarads with a linear capacitance change with angle of shaft rotation. It is compact and built of silver-plated metal with ceramic insulating bushes. The shaft carrying the moving vanes rotates in two ball bearings.

The capacitor (diagram (5)) is mounted in a brass screening box which is designed to be fixed permanently to the face plate of the Q meter by one locating pin and a fixing screw. The mounting is so arranged that the case of the capacitor is just clear of the 'capacitance test' terminals when the unit is in position. Two plug connectors of minimum length and which fit the test terminals connect the capacitance in parallel with the internal capacitance. Polystyrene is used as the insulator between the live plug



CONSTRUCTIONAL DETAILS OF THE ADDITIONAL
VARIABLE STANDARD CAPACITOR.

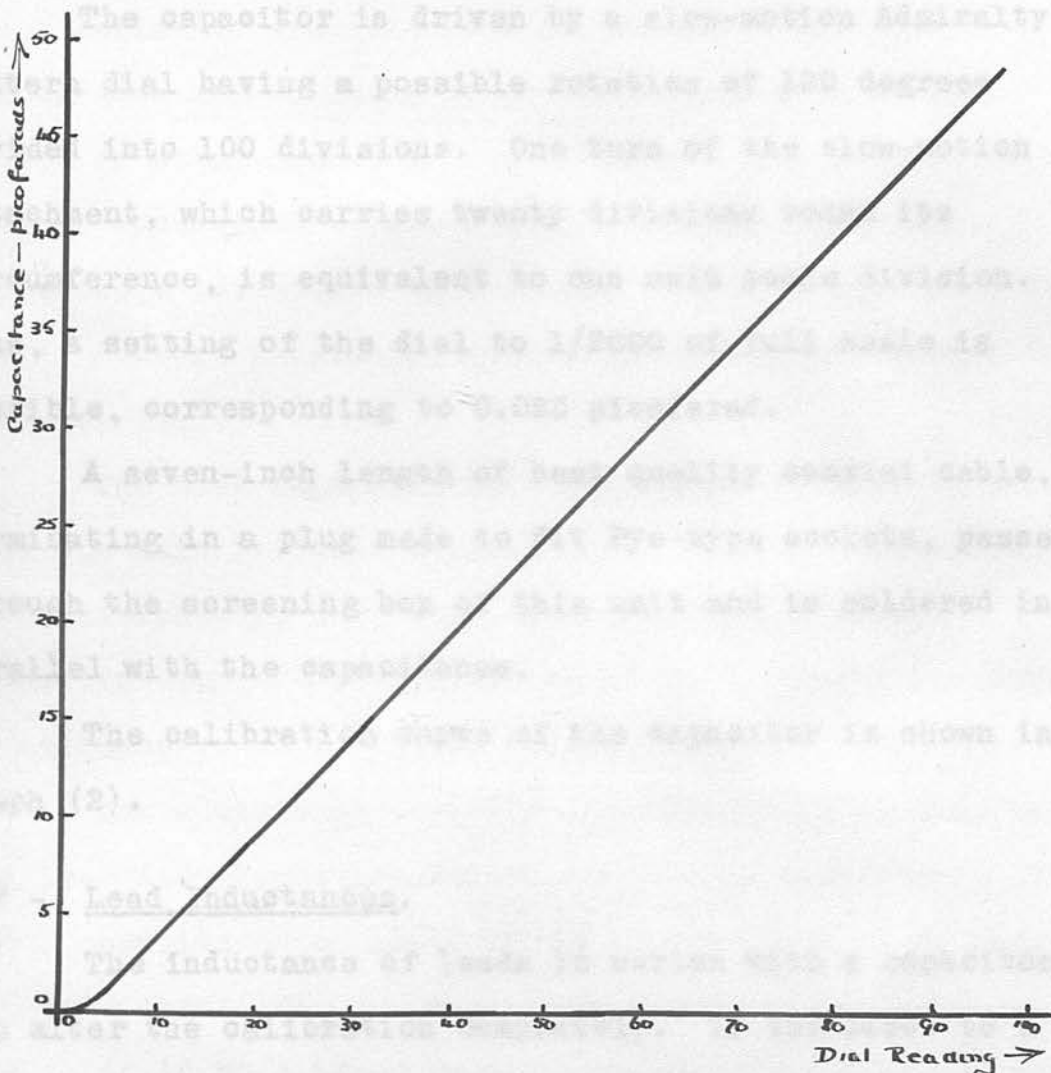
Diagram 5.

CALIBRATION DATA OF ADDITIONAL VARIABLE CAPACITOR

Graph 2.

Graph 2.

and the capacitor case to ensure that the stray capacitance introduced is of high quality.



Total Shunt Capacitance at Dial Reading 90 = 71 p.f.

CALIBRATION GRAPH OF ADDITIONAL VARIABLE CAPACITOR.

Graph 2.

This shows that the effect of lead inductance is to increase the effective capacitance.

In the present case lead inductance set an upper

and the capacitor case to ensure that the stray capacitance introduced is of high quality.

The capacitor is driven by a slow-motion Admiralty pattern dial having a possible rotation of 180 degrees divided into 100 divisions. One turn of the slow-motion attachment, which carries twenty divisions round its circumference, is equivalent to one main scale division. Thus, a setting of the dial to 1/2000 of full scale is possible, corresponding to 0.025 picofarad.

A seven-inch length of best quality coaxial cable, terminating in a plug made to fit Pye-type sockets, passes through the screening box of this unit and is soldered in parallel with the capacitance.

The calibration curve of the capacitor is shown in graph (2).

4.7 - Lead Inductances.

The inductance of leads in series with a capacitor can alter the calibration completely. If the leads to a capacitance, C , have an inductance, L , then the effective input impedance of the capacitance is

$$\begin{aligned}
 Z &= j\omega L + \frac{1}{j\omega C} \\
 &= \frac{1}{j\omega C} [1 - \omega^2 LC] \\
 &= \frac{1}{j\omega C'} \quad \text{where } C' = C / (1 - \omega^2 LC).
 \end{aligned}$$

This shows that the effect of lead inductance is to increase the effective capacitance.

In the present case lead inductances set an upper

frequency limit to the range of measurement. Diagram (6) shows the lead inductances of the 'test' circuit of the Q meter estimated from the lead dimensions (39). These inductances are of leads which are in the form of flat strips of metal almost $\frac{1}{8}$ inch broad and $1/50$ inch thick and have an inductance of about 0.01 microhenry per inch. Appreciable inductance also exists in the 'capacitance test' and 'inductor' terminals, amounting to 0.01 microhenry for each terminal.

The most important lead inductance is that in series with the main variable capacitance. It is of approximately 0.015 microhenry, and, when in series with a total capacitance of 400 picofarads at 25 Mc/s, causes the effective capacitance to be about 15% greater than the true capacitance.

The additional variable capacitance is also affected. Its lead inductance amounts to about 0.05 microhenry. The total capacitance is about 80 picofarads, and at 25 Mc/s the error is about 10%.

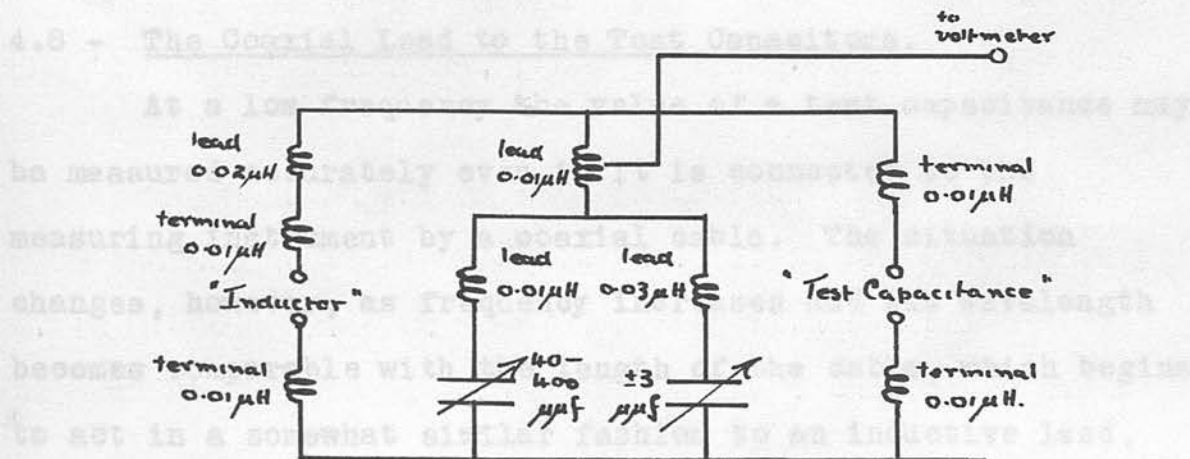
At 10 Mc/s these factors are each about 2% and are acceptable.

The inductance of the leads has a second effect. At 25 Mc/s the total tuning inductance required to resonate with 400 picofarads is 0.5 microhenry. Already there is about half of this value in the leads, and the remaining inductance required is given by a semi-circular bridge of copper wire between the terminals. This is practically the minimum size

Diagram 6.

of inductor which can be used and so 25 Mc/s is the upper limit attainable.

These two effects set an upper limit to the frequency of measurement. Results taken at a frequency of 10 Mc/s are regarded as correct; those at 25 Mc/s are recorded only for completeness.



Lead Inductances in the Test Circuit

of the Q Meter.

Since, in this case, the capacitance and inductance per unit length were not known the cable length

Diagram 6.

was kept to a minimum - just sufficient to allow ease of connection to the test capacitors. An experimental check showed that the values of test capacitance likely to be encountered could be measured accurately in spite of being measured through the coaxial cable.

4.9 - The Test Capacitors.

Diagram (7) shows the constructional details of the test capacitor units. A unit consists of four coaxial

of inductor which can be used and so 25 Mc/s is the upper limit attainable.

These two effects set an upper limit to the frequency of measurement. Results taken at a frequency of 10 Mc/s are regarded as correct; those at 25 Mc/s are recorded only for completeness.

4.8 - The Coaxial Lead to the Test Capacitors.

At a low frequency the value of a test capacitance may be measured accurately even if it is connected to the measuring instrument by a coaxial cable. The situation changes, however, as frequency increases and the wavelength becomes comparable with the length of the cable, which begins to act in a somewhat similar fashion to an inductive lead, i.e. the capacitance measured is greater than the true capacitance.

Since, in this present case, the capacitance and inductance per unit length were not known the cable length was kept to a minimum - just sufficient to allow ease of connection to the test capacitors. An experimental check showed that the values of test capacitance likely to be encountered could be measured accurately in spite of being measured through the coaxial cable.

4.9 - The Test Capacitors.

Diagram (7) shows the constructional details of the test capacitor units. A unit consists of four coaxial

Diagram 7.



TEST CAPACITOR UNITS.

Diagram 7.

capacitors each plugging into two short leads connected beneath a Pye socket, the four sockets being set at the corners of a square in a circular brass plate. This brass plate forms the lid of a dessicator so that, in use, the capacitors are suspended in an enclosure at constant humidity.

The capacitors are of the coaxial type and are all of the same dimensions, viz: -

total length	-	2 cm.
internal radius	-	0.590 cm.
external radius	-	0.830 cm.

The total capacitance of each, not including strays, is 3.28 picofarads.

These dimensions are chosen to satisfy three experimental conditions, viz. that (a) the total loss introduced into the test circuit should not lower the values to less than 60 near an absorption maximum so that the error in ϵ_2 is always less than 3% (equation 4.5), (b) the exposed surface area of the material in the capacitor should be relatively large compared with the total volume of material to give rapid drying, and (c) the total volume of material should not be too great. The quantities chosen are an exposed area of one sq.cm., a depth of two cm. and a weight of material of about two gms.

The coaxial form is used, as such a capacitor can be made accurately, and the true capacitance filled by the material may be calculated and need not be measured. This

is important as it is small and not readily measured.

The dielectric used to form the bases of the capacitors is chosen because of its rigidity and low loss properties. It is of unknown manufacture. The spacers in the Pye sockets are made of this same material to keep the losses of the test capacitors to a minimum, for these losses form a background to the $\epsilon_2(\omega)$ curves.

4.10 - The Constant Humidity Enclosures.

These are 6" dessicators with the lids replaced by the brass plate holding the capacitors. The acid to maintain the constant humidity is contained in a dish of 5 cm. dia. kept in the bottom of the dessicator. Thirty c.cs. of acid fills the dish.

Four small weighing tubes are kept in a rack on the tray of the dessicator. The tubes are one inch in length and weigh about 3 gms. each. A $\frac{1}{2}$ gm. of mineral fills about $\frac{1}{4}$ of the tube length. Three similar tubes, made from pyrex, are kept for the determination of the internal water content of halloysite. These tubes weigh just over 4 gms.

4.11 - The External Oscillator.

There is a vacant place on the coil turret of the Q meter, and, when the selection switch is in this position, no connection exists between the oscillator and the 'set power' unit. An external oscillator of lower frequency range may now be connected in its place at the

points marked AA on diagram (4). The input impedance at AA is nearly one ohm, and the current required to set up the standard voltage is 0.5 amp.

The oscillator used is a resistance-capacity oscillator made by Jackson, Ohio, U.S.A. It has a transformer output with an output impedance of 10 ohms. A second transformer of 9:1 impedance ratio is used to match this output impedance to the one ohm load.

In the Q meter the points AA are within the screening box of the oscillator. For convenience, in the present work, a short length of best quality coaxial cable is soldered to these terminals and is brought to a Pye-type socket on the front panel of the instrument. Experiment shows that the permanent connection of this cable and socket does not affect the normal operation of the instrument. A Pye plug connects the low frequency oscillator, with its matching transformer, to the socket and the 'set power' circuit. The current is adjusted using the output control on the oscillator.

The oscillator is designed to cover frequencies in the audio range and has an upper frequency limit of 20 Kc/s. It is frequency controlled by a 'Wien bridge' feedback network. The power output is lamp stabilised.

The dial of the oscillator is calibrated directly in frequency and the oscillator is always used at the frequencies 2.5, 5, 10 and 20 Kc/s according to the frequency dial. The actual frequencies of oscillation

the time required for a complete set of readings. It is seen that R_n and R must be almost equal if any appreciable increase in Q value is to be obtained, and this makes the stability of R_n and so of the active circuit of utmost importance.

Recently a useful circuit has been derived using the properties of the cathode follower. Diagram (8a) shows the essentials of the circuit. The voltage developed across the cathode resistance, and so that developed in the input circuit, is in phase with the input voltage, while the power developed at the input is much greater than the power consumed. Because of the very high negative feedback developed across the cathode resistance the circuit has exceptional stability.

A cathode follower must always give less than unity voltage gain between the valve grid and the cathode load, and so, to provide a higher voltage across the cathode load than across the input to the circuit, a transformer is required to step up the input voltage before it is applied to the grid of the valve. The actual transformer shown in diagram (8a) may be absorbed into the other components of the circuit as shown in the succession of diagrams (8a, b and c).

Power is fed back through the resistance R_p . This resistance is variable and controls the power fed back.

Details of two practical circuits are in the literature (17), (26), both reducing essentially to circuit (8d). Harris analyses the stability of the general circuit

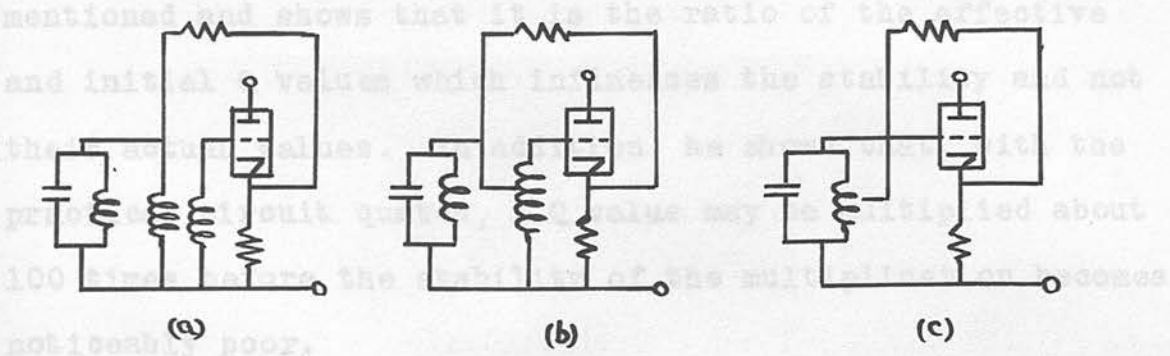
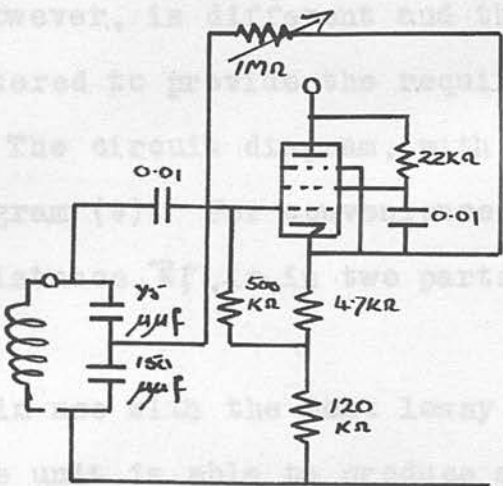


Diagram 8.

The negative resistance apparatus is based directly upon the circuit given by Harris. The valve, however, is different and the component values have been altered to give the required range of negative resistance. The circuit diagram and component values, is given in diagram 9. In operation the variable resistor is divided into two parts - a coarse and a fine control.



The circuit of the negative resistance unit.

Diagram 9.

When in use the variable resistor is divided into two parts - a coarse and a fine control. At 2.5 Mc/s, the unit produces an effective Q value of 300 with just a few turns of the control. At lower frequencies to be made. The estimated multiplication factor is about 100, and a variation of Q value from 200 to 2000 in one minute is usual. About 15 seconds are required for a reading. At the other frequencies, the multiplication factor used is much smaller because of the higher initial Q values, instability is not noticeable.

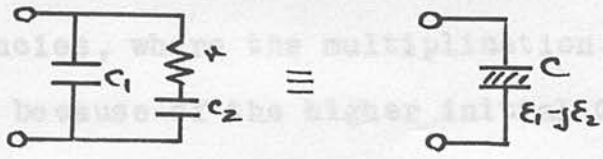


Diagram 10.

The unit is used for lower frequencies where only inductors of low initial Q values can be produced. The unit will function at frequencies up to at least 1 Mc/s, but

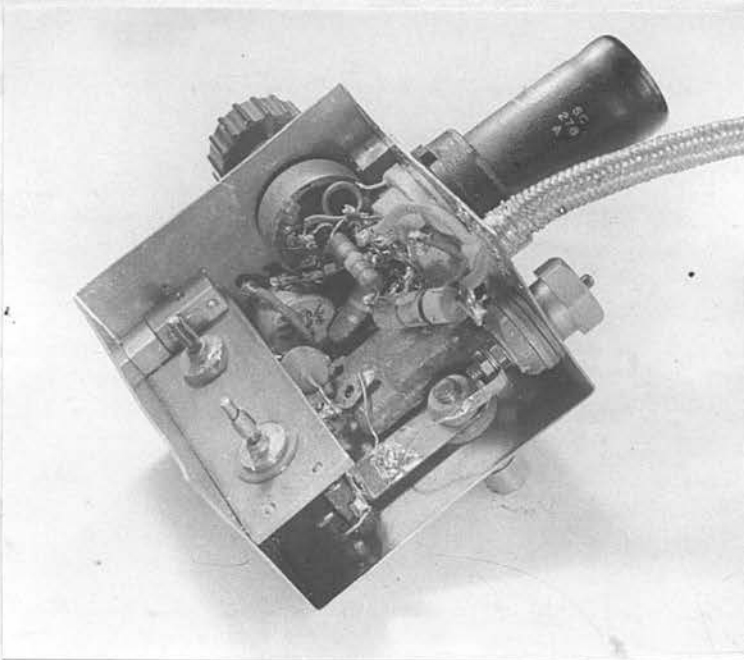
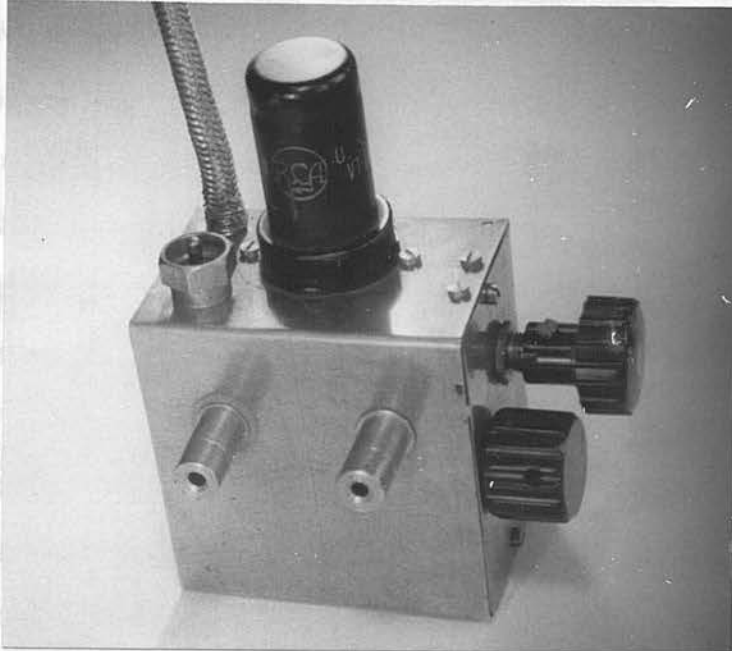
mentioned and shows that it is the ratio of the effective and initial Q values which influences the stability and not their actual values. In addition, he shows that, with the practical circuit quoted, a Q value may be multiplied about 100 times before the stability of the multiplication becomes noticeably poor.

The negative resistance unit used in the present apparatus is based directly upon the circuit given by Harris. The valve, however, is different and the component values have been altered to provide the required range of negative resistance. The circuit diagram, with component values, is given in diagram (9). For convenience in operation the variable resistance, R_f , is in two parts - a coarse and a fine control.

When in use with the most lossy inductor, i.e. at 2.5 Kc/s, the unit is able to produce an effective Q value of 200 with just sufficient stability to allow readings to be made. The estimated multiplication factor is about 100, and a variation of Q value from 200 to 200 ± 20 in one minute is usual. About 15 seconds are required for a reading. At the other frequencies, where the multiplication factor used is much smaller because of the higher initial Q values, instability is not noticeable.

The unit is used at the four lower frequencies where only inductors of low initial Q values can be produced. The unit will function at frequencies up to at least 1 Mc/s, but

Diagram 11.



THE NEGATIVE RESISTANCE UNIT.

Diagram 11.

its use offers no advantage in the present work.

Diagram (11) shows the constructional details of the unit which is designed to fit over the 'inductor' terminals of the Q meter. Electrical connection is made between the unit and the inductor terminals by two plugs which also serve to support the unit in position. The tuning inductor is plugged into either a pair of terminals, similar to the 'inductor' terminals, or into a Pye socket. Internal copper strips, across which the electrical circuit is connected, join these terminals with the plugs so that inductor and unit are in parallel across the 'inductor' terminals.

The power to operate the unit is obtained from the power supply of the Q meter.

4.13 - The Inductors.

For each frequency at which measurements are made, an inductor is required to resonate with a total capacitance of about 400 picofarads. The inductor must have as high a Q value as possible but not exceeding 250.

Complete details of the inductors used are given in table (1). All are specially made to suit the present application except the three for the frequencies 250 and 500 Kc/s and 1 Mc/s. These were supplied with the Q meter.

At the two lowest frequencies attainable, the inductances required can only be produced using laminated iron cores. Q values of only 5 and 2 are obtained owing to

the high magnetic losses in the cores which are not intended for use at these frequencies. The lower limit of frequency, 2.5 Kc/s, is set by the largest inductance which can be produced. An inductance for 1 Kc/s of 62.5 henrys is out of the question owing to its magnitude and probable losses.

4.14 - Calibration of the Loss Measurements.

To check upon errors whose magnitudes are unknown, a calibration is required of the apparatus as an instrument measuring $\mathcal{E}_2(\omega)$.

A likely source of error is the harmonic content of the output of the oscillators, particularly the low frequency oscillator. Harmonic currents flowing through the 'set power' circuit cause an additional deflection of the ammeter, with the result that the current of fundamental frequency is too low even though the power input is set correctly according to the ammeter. Thus the input voltage to the tuned circuit and so the Q value recorded are too low. This affects the \mathcal{E}_2 values calculated, for, if the true Q values are n times greater than the measured values, amending equation (4.5)

$$\text{true } \mathcal{E}_2 = \frac{C}{C_0} \left(\frac{1}{nQ_1} - \frac{1}{nQ_0} \right) = \frac{1}{n} \text{ measured } \mathcal{E}_2$$

Precisely the same form of error arises if the ammeter is incorrectly calibrated, but in the latter case the correction factor is the same at all frequencies, while in the former case it varies from frequency to frequency with

the harmonic content. Debye equations (3.3 and 3.4).

(Note. To provide an overall calibration, an $\epsilon_2(\omega)$ is required which is known at all frequencies. It is not possible to make measurements on an actual dielectric as no material with a standard ϵ_2 is known, but it is possible to make measurements on a resistance-capacitance circuit which shows properties like those of a dielectric.

Consider the circuit shown in diagram (10) consisting of a pure capacitance C_1 in parallel with a series resistance r and capacitance C_2 . If a steady voltage is suddenly applied to the circuit, the steady state is reached exponentially with a time constant $\tau = C_2 r$, as the second capacitance charges through the resistance. Such an exponential approach to equilibrium leads to a relaxation absorption.

This circuit is equivalent to a capacitance C filled with a lossy dielectric $\epsilon_1 - j\epsilon_2$. Equating the admittances of these equivalent circuits

$$j\omega\epsilon_1 C + \omega\epsilon_2 C = j\omega C_1 + \frac{1}{r + 1/j\omega C_2}$$

$$\text{or} \quad = j\omega \left[C_1 + \frac{C_2}{1 + \omega^2 C_2^2 r^2} \right] + \frac{\omega^2 C_2^2 r}{1 + \omega^2 C_2^2 r^2}$$

Equating real and imaginary parts and using $\tau = C_2 r$

$$\epsilon_1 = \frac{C_1}{C} + \frac{C_2}{C} \frac{1}{1 + \omega^2 \tau^2} \quad \epsilon_2 = \frac{C_2}{C} \frac{\omega \tau}{1 + \omega^2 \tau^2}$$

If $C_1 = \epsilon_\infty C$ and $C_2 = (\epsilon_s - \epsilon_\infty) C$, values, the series

$$\text{then} \quad \epsilon_1 = \epsilon_\infty + \frac{\epsilon_s - \epsilon_\infty}{1 + \omega^2 \tau^2} \quad \epsilon_2 = \frac{(\epsilon_s - \epsilon_\infty) \omega \tau}{1 + \omega^2 \tau^2}$$

which These are the Debye equations (3.3 and 3.4).

(Note, however, $\epsilon_s = \frac{C_2 + C_1}{C} = 1$, $\epsilon_\infty = \frac{C_1}{C_0} < 1$, $\epsilon_s - \epsilon_\infty = \frac{C_2}{C} < 1$).

Knowing this result it is possible to arrange a Debye absorption at any frequency for calibration purposes. A particular case is chosen in which the shunt capacitance C_1 is made zero, and so

$$C = C_2 \quad \epsilon_2(\omega) = \frac{\omega\tau}{1 + \omega^2\tau^2} \quad (4.7)$$

for which $\epsilon_2(\omega)_{\max} = \frac{1}{2}$ at $\omega\tau = 1$ or $\omega = \frac{1}{C_2\tau}$

The value of C_2 is determined by consideration of the total loss which is introduced into the test circuit when the calibration circuit is connected, as the same order of change in Q value is required in this case as when the test capacitance is connected. Thus, the calibration capacitance must be about 8 picofarads. Once C_2 is chosen the frequency at which the maximum loss occurs is set by the resistance r .

During calibration the coaxial cable from the Q meter is plugged into a Pye socket behind which the calibration circuit is soldered. Two precautions are taken to ensure that the shunt capacitance C_1 is zero - (a) the lead from the socket to the resistor is kept to a minimum length, and (b) connection is made by a soldered joint which is broken for each reading of Q.

In order to calculate the true $\epsilon_2(\omega)$ values, the series capacitance C_2 of the calibration circuit must be known. Its value is estimated from the effective shunt capacity

which the circuit introduces at a frequency which is so low that $\epsilon_2(\omega)$ is practically zero. The capacitance determined in this way is the effective capacitance in the circuit. Repeated estimation of its value shows that it may be determined to $\pm 3\%$.

4.15 - The Calibration of the Normal Range of the Q Meter.

The accuracy of measurement in the normal range of the Q meter is checked by taking ϵ_2 measurements using the calibration circuit as load. Altogether four absorption curves cover the frequency range 50 Kc/s to 25 Mc/s. These are shown in graph (3).

The experimental points plotted do not lie exactly upon curves given by equation (4.7) but fit those given by

$$\epsilon_2(\omega) = (1+k) \frac{\omega\tau}{1+\omega^2\tau^2} \quad (4.8)$$

The same value of k applies to all curves taken, and, therefore, it may be assumed that the ammeter of the set power unit is off calibration. Since the value of k is 0.1 the ammeter is reading 10% high.

It is possible to check that the ammeter is in error by comparing the Q value of an inductor (a) as given by the direct reading of the Q meter, and (b) as calculated by the incremental capacitance method. It is mentioned in section (4.3) that, for the second method, the injection voltage need not be known. Hence the results obtained do not depend

upon the ammeter calibration. The following table contains typical results obtained by the two methods using inductors of a range of Q values: -

Incremental Capacitance Method.	Direct Method.	Ratio.
Qc	Qd	Qc/Qd.
210	194	1.08
168	159	1.06
105	100	1.05
87.3	80	1.09
68.4	61	1.12
50	45	1.11
32.5	30	<u>1.095</u>
	Average	1.09 0.02

Qd, which depends directly upon the ammeter calibration, is found to be low by 9% thus confirming the value of k obtained earlier.

4.16 - The Calibration of the Extended Range.

A different approach has to be made in the frequency range 2.5 to 20 Kc/s where harmonic content, as well as an error in ammeter calibration, affects the correction factor which, therefore, must vary from frequency to frequency.

The calibration circuit is arranged to show a maximum value of $\xi_2(\omega)$ at a frequency between 2.5 Kc/s and

100 Kc/s and experimental values of ξ_2 are obtained. Altogether five curves, shown in graph (4), cover the whole range of frequency. They all have several points extending into the normal range of the Q meter, i.e. above 50 Kc/s, and a curve is fitted to these points using equation (4.8) with $k = 0.1$. This curve gives the true value of $\xi_2(\omega)$ at each of the low frequencies assuming the higher frequency measurements to be correct. The correction factors by which the experimental value must be multiplied to give the true value can then be calculated. The factors for each frequency calculated from each of the five curves are given in the table below. An average value and an average deviation from the mean is given for each frequency.

Frequency. Kc/s	Curve Numbers.					Average.	Average Deviation.
	1	2	3	4	5		
2.5	0.61	0.62		0.57	0.60	0.60	0.015
5.0	0.89	0.92	0.93	0.79	0.77	0.86	0.06
10.0	0.80	0.85	0.87	0.75	0.79	0.81	0.03
20.0	0.94	1.00	0.94	0.86	0.89	0.92	0.04

Calibration Curves

Normal Q-meter Range

Graph 3

$E_p(\omega)$

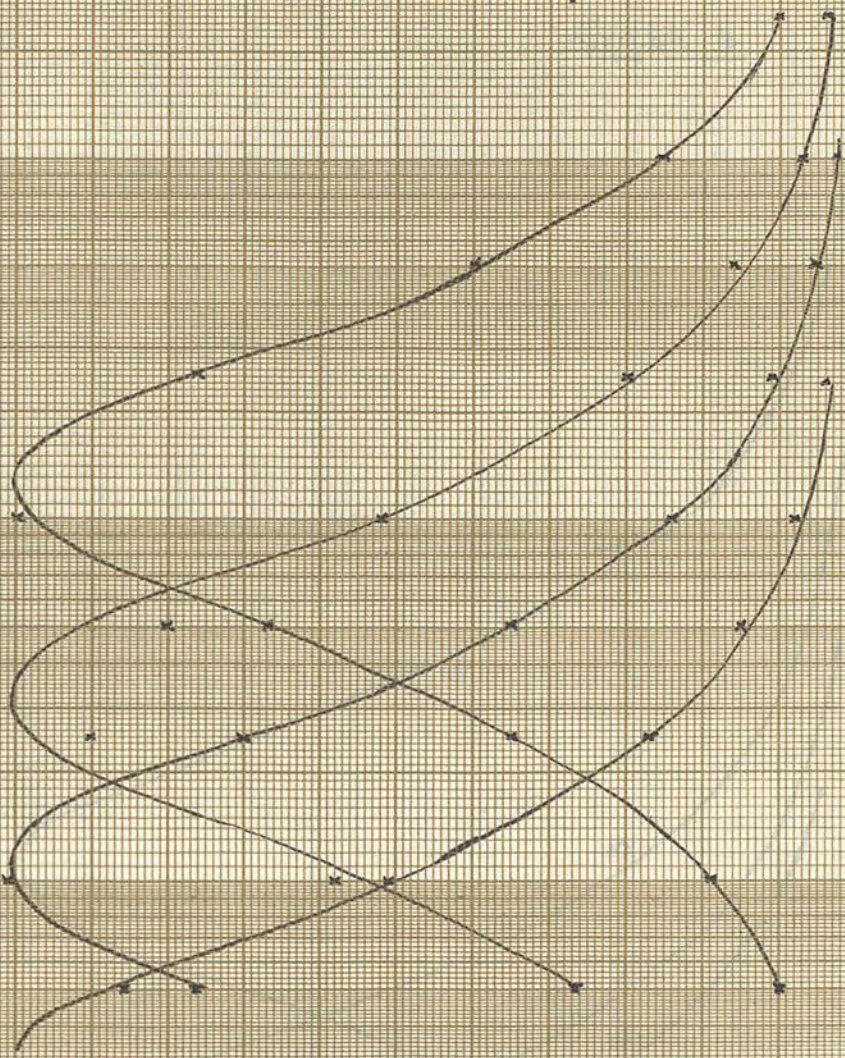
Frequency
C.P.S.

10^4

10^5

10^4

10^3



Calibration Curves

Extended Range

Graph 4

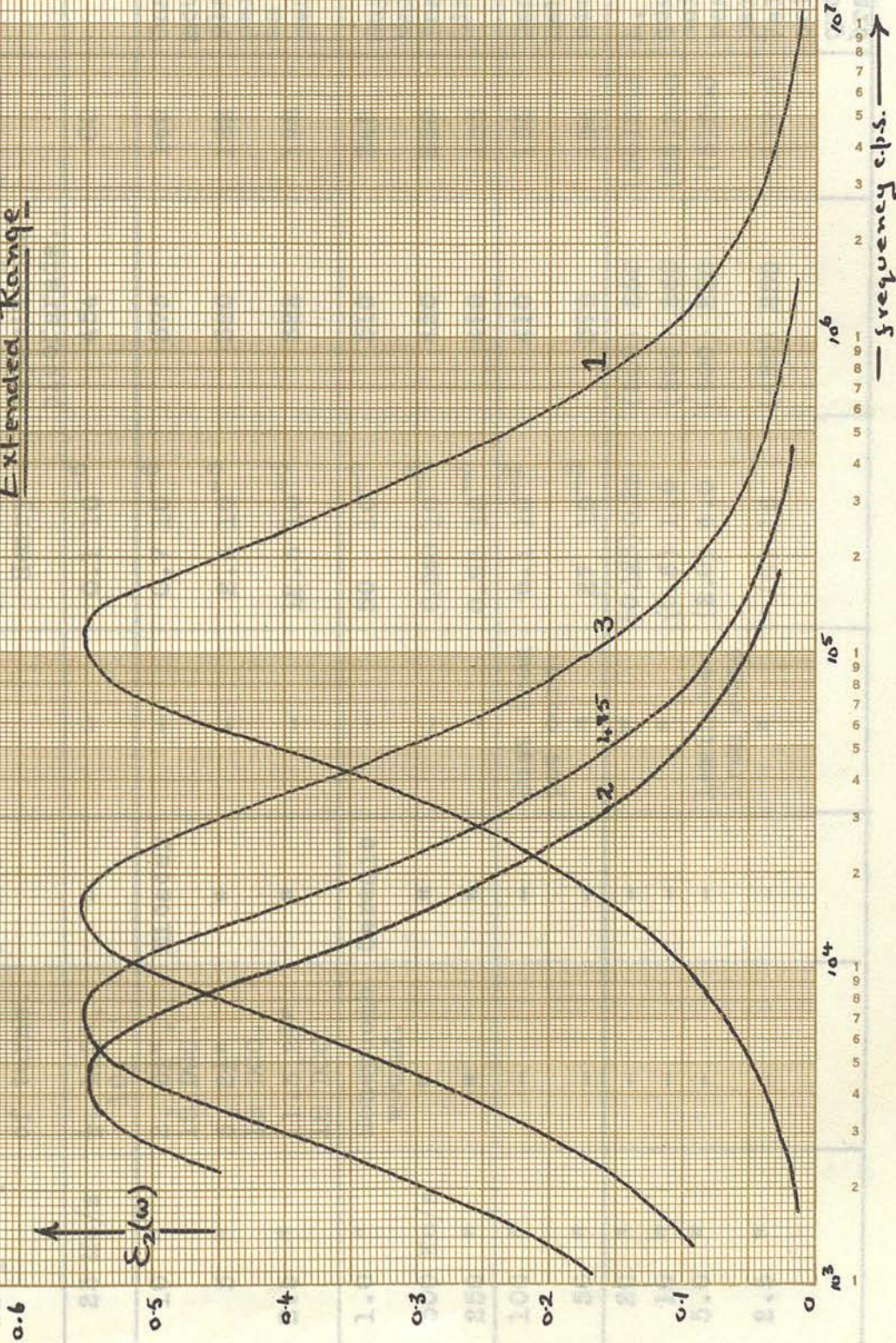


TABLE 1.

Frequency	No., dia., & S.W.G. of turns.	Former	Core	Approx. Inductance. Henry.	Approx. tuning capacitance picofarads.	Q value	Remarks
25 Mc/s	$\frac{1}{2}$, 1.5", 10.	-	-	0.1×10^{-6}	454	80	-
10 "	2, $2\frac{1}{4}$ ", 18 DCC.	Micadex	-	0.7×10^{-6}	375	140	Unscreened, mounted with plane of coil perpendicular to Q meter panel.
5 "	5, $2\frac{1}{4}$ ", 18 DCC.	"	-	2.6×10^{-6}	380	182	
2.5 "	11.5, $2\frac{1}{4}$ ", 18 DCC.	"	-	12.5×10^{-6}	322	198	
1.0 "	Honeycomb wound.	Ceramic	-	50×10^{-6}	510	245	Supplied by Marconi Instruments Limited.
500 Kc/s	"	"	-	0.240×10^{-3}	420	250	
250 "	"	"	-	0.95×10^{-3}	420	155	
100 "	-	-	Dust iron pot core.	6.1×10^{-3}	410	155	Connects to Q meter by coaxial lead.
50 "	-	-	"	27×10^{-3}	375	104	
20 "	-	-	"	(0.125) 0.25	(500) 250	(56) 200	L, C, and Q quoted for
10 "	-	-	"	(0.5) 1.0	(500) 260	(26) 200	coil with neg. res. unit in parallel.
5.0 "	-	-	laminated iron core.	(2.0) 4.0	(500) 250	(5) 200	Values for coil alone quoted in brackets.
2.5 "	-	-	"	(8) 16	(480) 250	(2) 200	

CHAPTER 5.

THE EXPERIMENTAL METHOD.

5.3 - An account of the method is given in section (2.11) and this chapter supplements the information given there.

5.1 - The Preparation of the Minerals.

The minerals were required in finely powdered form for the experiments. The Kaolinite, Talc and Gibbsite were received as fine powders, but the Halloysite was in rock form and had to be prepared.

5.2 - The Preparation of Halloysite.

The rock to be powdered was chosen for its apparent freedom from veins of coloured impurity. Before being crushed, each piece was scraped well to remove a shallow surface deposit, which was obviously of a different texture to that of the halloysite. Impurities hidden in the body of the rock were removed when they came to light during crushing. The powder was made to pass a 100 mesh sieve.

In this way a stock of 200 grams of powdered halloysite was accumulated, and, from it, all halloysite used was drawn. A sample, examined by Dr. J. Goodyear using X-ray powder pattern techniques, was found to contain some 3% impurity which was almost wholly Gibbsite. This impurity probably came from a part of the surface deposit

which had not been completely scraped away as the deposit was identified as Gibbsite (section (6.10)).

5.3 - The Preparation of the Intermediate States of Hydration.

Samples of halloysite with hydration states between full hydration and complete dehydration are produced from stock powder by drying above known concentrations of sulphuric acid.

The dehydration is carried out in vacuum, the powder and acid being sealed together in a preserving jar closed with a metal lid and rubber sealing ring. Sulphuric acid of the desired concentration is placed in the jar to about one inch depth, and then ten grams of powder, in a test tube, are put in. The metal lid is sealed in place by evacuating the jar.

The jar is stored for at least three weeks, usually a month, to allow the interlayer water content to reach an equilibrium state. The time required for dehydration is determined experimentally (section (7.1)).

5.4 - The Preparation of Metahalloysite.

Samples of Metahalloysite are prepared, as required, by heat-treating halloysite. The halloysite is placed in a porcelain crucible and heated in an electric furnace to a temperature between 300 and 360 °C, determined by a mercury

in glass thermometer. The heating is continued for at least three hours after which the sample is allowed to cool naturally.

5.5 - The Preparation of Capacitor Samples.

The test capacitor is loosely filled with the mineral until it is overflowing, and then the charge is compacted, at first gently, and then firmly, by tapping the capacitor on the bench, an excess of powder being kept piled on top. When no further shaking down occurs with tapping, the excess powder is cleared carefully from the top leaving the charge exactly level with the brim of the capacitor.

This method ensures a reasonably uniform state of packing of the charge. Further, because of the initial compacting, the charge does not shake down with normal handling during the period of measurements. The packing used gives a background loss which does not seriously interfere with the absorption losses (section 7.2 and 7.3).

When charged, the test capacitor is plugged into a socket in a test capacitor unit in a constant humidity enclosure. The enclosure is kept sealed for a minimum period of four days to allow the surface water content to reach equilibrium.

5.6 - The Maintenance of Constant Humidity.

The constant humidity in an enclosure is maintained

using a solution of sulphuric acid. A solution of given concentration has a standard vapour pressure lower than that for water at the same temperature and so will maintain a steady known relative humidity in an enclosure. The vapour pressures of solutions of sulphuric acid at 20 ° C are given in Landolt Tabellen 5, Auflage II, p.1395, 1923, and, from these, and the saturation vapour pressure of water at 20 ° C, the relative humidity maintained by a given acid concentration may be calculated. A graph of relative humidity against acid concentration is given in graph (5).

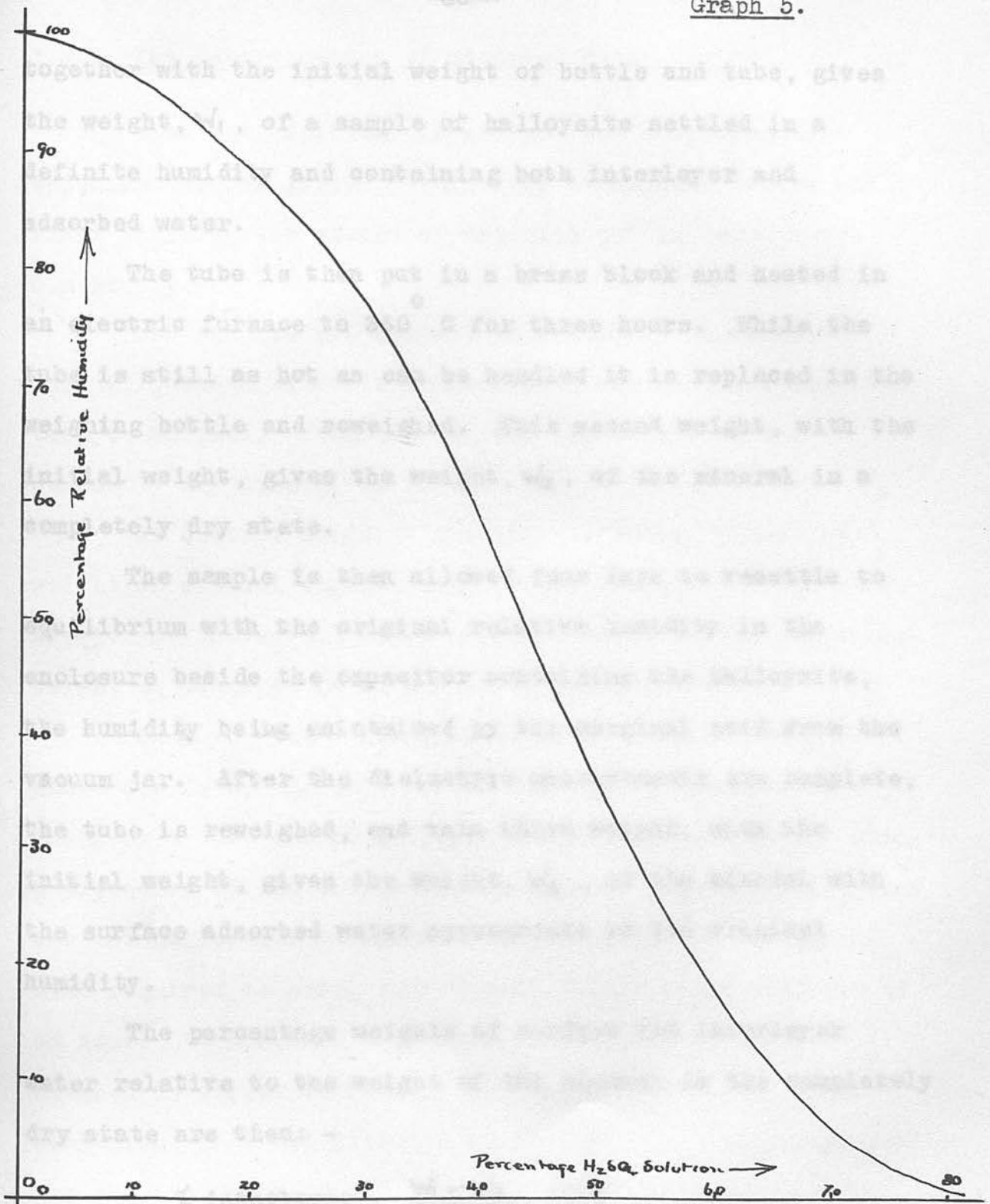
The two extreme humidities, 0% and 100% are obtained using Phosphorus Pentoxide and distilled water.

In the present work the exact relative humidities need not be known, for the state of hydration of the minerals is specified by the percentage weights of water absorbed and adsorbed by the mineral.

5.7 - Determination of the Interlayer Water Content of Halloysite.

The determination is based upon considerations detailed in section (6.6).

Immediately the seal is broken on the vacuum jar containing the halloysite in its intermediate dehydration state, a sample of about 0.5 gm. is transferred to a small pyrex tube. The tube with sample is weighed in a weighing bottle fitted with a ground stopper. This first weight,



Percentage relative humidities over solutions of H₂SO₄ at 20°C.

together with the initial weight of bottle and tube, gives the weight, W_1 , of a sample of halloysite settled in a definite humidity and containing both interlayer and adsorbed water.

The tube is then put in a brass block and heated in an electric furnace to 360°C for three hours. While the tube is still as hot as can be handled it is replaced in the weighing bottle and reweighed. This second weight, with the initial weight, gives the weight, W_2 , of the mineral in a completely dry state.

The sample is then allowed four days to resettle to equilibrium with the original relative humidity in the enclosure beside the capacitor containing the halloysite, the humidity being maintained by the original acid from the vacuum jar. After the dielectric measurements are complete, the tube is reweighed, and this third weight, with the initial weight, gives the weight, W_3 , of the mineral with the surface adsorbed water appropriate to the original humidity.

The percentage weights of surface and interlayer water relative to the weight of the mineral in the completely dry state are then: -

$$\% \text{ interlayer} = \frac{W_1 - W_3}{W_2} \cdot 100\%$$

$$\% \text{ adsorbed} = \frac{W_3 - W_2}{W_2} \cdot 100\%$$

(p. 94)

5.8 - The Determination of adsorbed Water Content.

When the capacitor is charged the corresponding weighing tube is filled. This tube is weighed before and after filling, the amount of material put in being about 0.5 gm.

The samples are allowed to settle at 0% relative humidity, the dielectric measurements are made and then the tube is weighed. From this weight the weight of the perfectly dry mineral is found.

At another humidity the same procedure gives the weight of mineral together with adsorbed water. From this weight and the weight at 0% relative humidity the percentage weight of adsorbed water may be calculated.

When more than one tube is to be weighed the enclosure is opened only for as long as is required to transfer a tube to the weighing bottle. Unfortunately such a procedure allows the weight of surface water on halloysite and metahalloysite to change by as much as 10% during the time required to weigh four tubes - about three quarters of an hour. To minimise this error the tubes are always weighed in strict rotation - the halloysite first, then kaolinite, talc and gibbsite in that order. All weighings are made to 0.1 m.gm.

5.9 - The Dielectric Measurements.

It is usual to start readings at the upper frequency

limit, i.e. at 25 Mc/s, and then to work downwards. This is done as the background loss, due to conductivity (section 7.2), becomes increasingly great as frequency decreases and often sets a higher limit to the readings than 2.5 Kc/s. Normally, readings are discontinued once a Q value less than 40 is obtained with the test capacitor in circuit.

Equation (4.5) shows that the greater the value of the tuning capacitance C the greater the value of ϵ_r which can be determined for given upper and lower Q values. For this reason C is chosen to have a value of about 400 picofarads, which is almost the maximum available with the standard used. An inductance is then chosen to resonate at the frequency of measurement with this capacitance.

At each frequency of measurement the oscillator frequency is set by the calibrated dial, and its power output is arranged to give the standard deflection on the 'set power' ammeter. The inductor appropriate to the frequency is plugged in place and the zero of the valve-voltmeter, i.e. the dial reading Q value, is set using the zero control. This is done with the main capacitance either at maximum or minimum but well away from the resonance value.

The dial of the additional variable capacitor is checked to be set to the standard dial mark - the reading 90 - at almost maximum capacitance, and the circuit is tuned to resonance which is indicated by a maximum deflection on

on the Q dial. A note is made of the total capacitance recorded on the dial of the tuning capacitance and of the Q value read from the meter.

The test capacitor is then brought into circuit by plugging the Pye-type plug into the appropriate socket in the lid of the constant humidity enclosure. The circuit is again brought to resonance using the additional variable capacitor. The new dial reading and the new Q factor of the circuit are noted.

The same performance is repeated at the next lower frequency and so on. The frequencies chosen run 10, 5, 2.5 and 1 through each decade, measurements at these frequencies being sufficient to record the absorption curves faithfully.

All the experimental results are recorded in one table together with the steps in the calculation of $\epsilon_2(\omega)$ from them using equation (4.5). This equation requires the total tuning capacitance at resonance which, in this case, is the capacitance read from the main capacitor dial plus the total shunt capacitance introduced by the additional variable capacitor when set at the dial mark, 90. The quantity C_0 is known from the capacitor dimensions. If desired, $\epsilon_1(\omega)$ may also be calculated from the results using equation (4.6).

A set of results is worked out immediately it is

taken so that readings obviously in error may be checked.

Once that is done the constant humidity enclosure is opened and weighings are made to complete the series of measurements for the sample in that humidity.

The acid is then replaced by a new concentration and again four days are allowed for the surface water content to reach equilibrium when a further set of results is taken.

With all the minerals except halloysite the same sample is used throughout the whole humidity range of a series of measurements, but with halloysite a fresh sample is used in each relative humidity. This is done to reduce the time required to complete a series of measurements since the interlayer water content takes three weeks to settle at each humidity. The material is previously prepared in the required relative humidity and a test capacitor is filled with it in the usual way. Four days are allowed for the surface adsorbed water content, which changes during the time required to fill the capacitor, to reach equilibrium again, the acid above which the sample was prepared being used to maintain the humidity in the enclosure.

Finally, all the dielectric loss curves of a series of measurements are recorded on one sheet of graph paper. Graph (11) is typical of this.

CHAPTER 6.

THE MINERALOGY OF HALLOYSITE AND RELATED MINERALS.

6.1 - Halloysite: Nomenclature.

An exact definition must be given of the terms halloysite, partially dehydrated halloysite and metahalloysite used throughout this work as there is confusion of terminology in the literature. It is necessary to distinguish two distinct cases. The first concerns the internal water content of the mineral: the second concerns the adsorbed water content.

In the first case, the fully internally hydrated mineral is named halloysite. Partially dehydrated halloysite refers to those states of halloysite retaining only some of the original internal water content, while metahalloysite is that form of halloysite produced when all the internal water content is driven off by heat treatment.

This terminology agrees with that proposed recently by MacEwan (33) who recommends that halloysite be used as a general term; that 'dehydrated halloysite' be used to indicate the intermediate states; and that metahalloysite be used to represent the dehydrated variety.

The terms halloysite and metahalloysite are used generally throughout the European literature with closely the meanings given above. Confusion arises when American

literature is considered. The terms, at present in general use, suggested by Alexander, et al. (1), are 'Endellite' for halloysite, and 'Halloysite' for metahalloysite. American papers published before 1938 use the European terms, while those published since 1938 may also use the terms proposed by Hendricks (27), viz. 'Hydrated Halloysite' for halloysite and 'Halloysite' for metahalloysite.

Considering the second case, the externally adsorbed water content depends upon the morphology of the crystal. This is a hollow tube in the fully internally hydrated mineral and may still be so in the states of the material produced by gentle dehydration above a drying agent. It is a split and partly unrolled tube when dehydration is produced by heat treatment. Thus, when a surface adsorbed water is being considered, halloysite refers to material, like the fully hydrated mineral, having a hollow cylindrical morphology, while metahalloysite refers to material with the morphology produced by heat treatment, i.e. a split and partly unrolled hollow cylinder. This distinction does not appear in the literature.

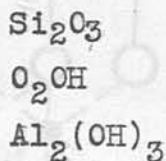
6.2 - The Structure of Halloysite.

Only the commonly accepted structure of halloysite will be discussed, viz. that proposed by Hendricks (27). The two alternative structures proposed by Mehmel (1935)

Diagram 12.

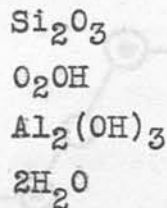
and Edelman and Favejee (1940) are criticised by Alexander et al. (1) on the grounds that (a) they are not fully in accord with X-ray data and (b) they do not account for the easy dehydration of the mineral.

Hendricks proposes a structure of alternate water and kaolin-type layers. The basic kaolin layer has the chemical formula $(Al_2O_3 \cdot 2SiO_2 \cdot 2H_2O)$ and has its atoms arranged in planes in a way which can be represented by the structural formula -



The chemical formula of halloysite is

$(Al_2O_3 \cdot 2SiO_2 \cdot 4H_2O)$ which may be written structurally as



i.e. a kaolin unit with an attached water layer.

The actual atomic arrangement of a unit cell of halloysite is shown in diagram (12 a,b). The mineral consists of these cells in layers extending indefinitely in directions (a) and (b) and stacked in direction (c).

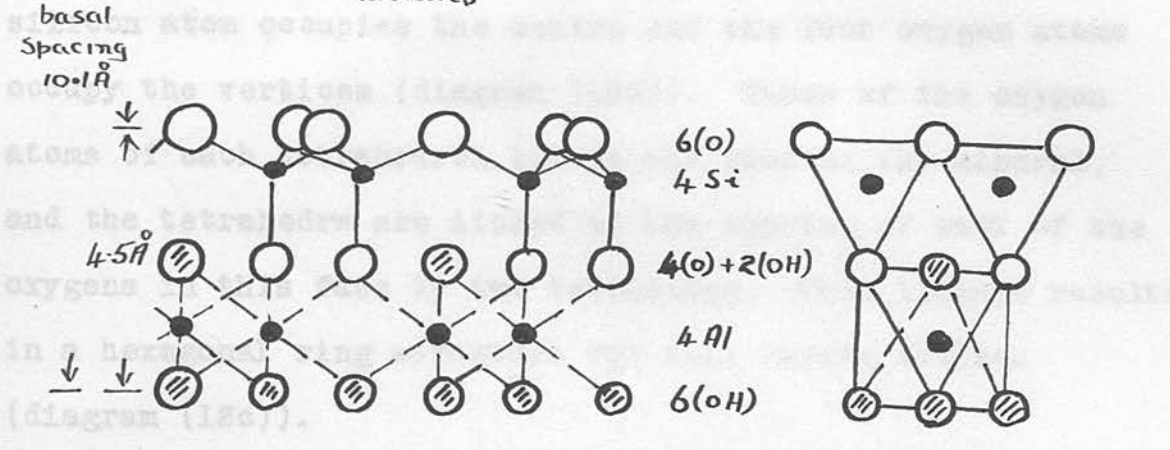
6.3 - The Layer of Oriented Water Molecules.

Following upon the structure just mentioned, Hendricks and Jefferson (28) propose a structure to apply generally to

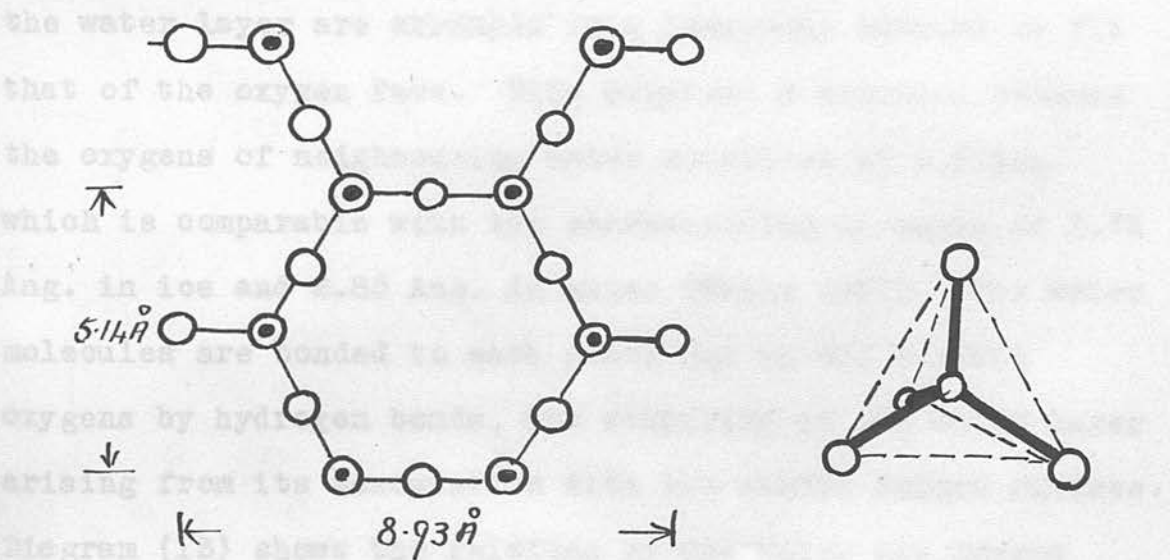
Diagram 12.

the water layers occurring in siliceous clay minerals. This structure is similar to that of ice but the water molecules are oriented in a definite direction. The water molecules are oriented in a definite direction.

one, the basal layer has one more water molecule than the layer of siliceous-oxygen tetrahedra. The water molecules are oriented in a definite direction.



(a) Side view. (b) End View.



(c) Arrangement of the oxygen surface. (d) A Silicon-oxygen tetrahedron.

THE ATOMIC ARRANGEMENTS IN HALLOYSITE.

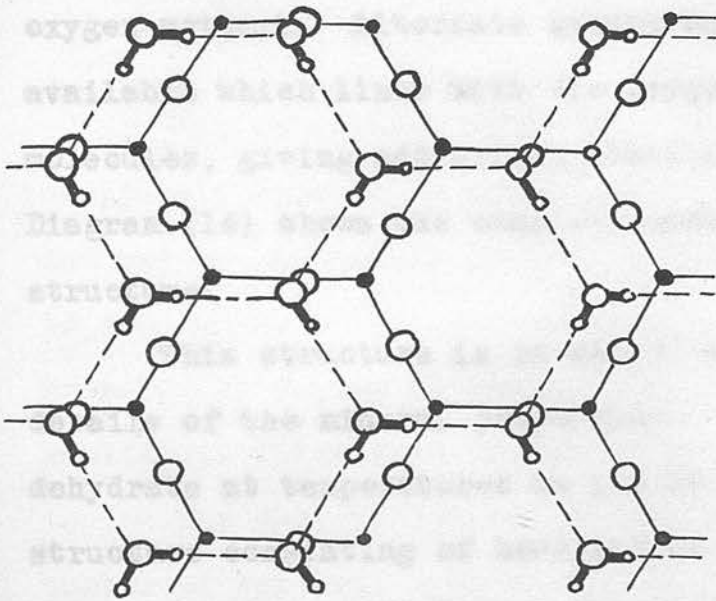
Diagram 12.

the water layers occurring in silicate clay minerals. This structure is based upon the knowledge that in the hydrated forms of the silicate layer minerals, of which halloysite is one, the mineral layer has one face in which lie the bases of silicon-oxygen tetrahedra. In each tetrahedron, the silicon atom occupies the centre and the four oxygen atoms occupy the vertices (diagram (12d)). Three of the oxygen atoms of each tetrahedron lie in the face of the mineral, and the tetrahedra are linked by the sharing of each of the oxygens in this face by two tetrahedra. This linkage results in a hexagonal ring structure for this oxygen surface (diagram (12c)).

Hendricks and Jefferson propose that the molecules of the water layer are arranged in a hexagonal network to fit that of the oxygen face. This requires a distance between the oxygens of neighbouring water molecules of 3.0 Ang. which is comparable with the corresponding distance of 2.76 Ang. in ice and 2.85 Ang. in water (Wells (40)). The water molecules are bonded to each other and to the surface oxygens by hydrogen bonds, the stability of the water layer arising from its association with the stable oxygen surface. Diagram (13) shows the relation of the water and oxygen layers. The dotted lines indicate hydrogen bonds.

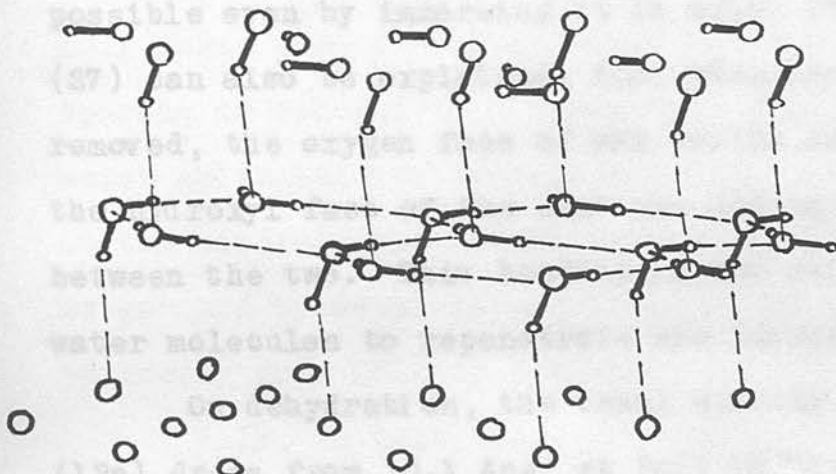
In halloysite, the water layer lies between an oxygen and a hydroxyl surface. The hydroxyl groups are arranged in a hexagonal network of nearly the same dimensions as the

Diagrams 13 & 14.



Water layer
fitting upon
oxygen surface.

Diagram 13.



Hydroxyl-group
surface.

Interlayer water.

Oxygen surface.

Diagram 14.

Hendricks' model for interlayer water.

oxygen network. Alternate groups have a hydrogen bond available which links with the oxygens of alternate water molecules, giving additional stability to the water layer. Diagram (14) shows the complete model of the water layer structure.

This structure is in accord with the experimental details of the mineral properties. The mineral is known to dehydrate at temperatures as low as 50° C (27) to a structure consisting of kaolin-type layers randomly oriented in the a,b plane. This can only be explained by a simple dehydration process, such as the removal of a water layer, and not by a complex process involving the breakdown of the structure as required by other proposals.

The fact that rehydration of metahalloysite is not possible even by immersing it in water for three months (27) can also be explained, for, when the water layer is removed, the oxygen face of one kaolin layer approaches the hydroxyl face of the next and hydrogen bonding arises between the two. This bonding is too strong to allow water molecules to repenetrate the layers.

On dehydration, the basal spacing shown in diagram (12a) drops from 10.1 Ang. at full hydration to 7.2 Ang. at complete dehydration which is consistent with the removal of a monomolecular layer of water for the effective spacing of 10.1 Ang., and the other by a basal spacing of diameter of a water molecule is almost 3 Ang.

6.4 - The Dehydration of Halloysite.

The interlayer water of halloysite is almost completely removed by heating overnight to 50° C (1, 27) and may be completely removed by heating for a few hours to 400° C (11). Intermediate water contents may be prepared by drying in atmospheres of lower relative humidity. These intermediate states are quite stable.

The dehydration of halloysite has been studied by a number of workers, e.g. Alexander et al. (1), and has been examined in considerable detail in relation to humidity, temperature and pressure by Brindley and Goodyear (9), and Brindley, Robinson and Goodyear (11), employing both X-ray and weighing techniques.

The basal spacing in the fully hydrated mineral is 10.1 Ang. When the water layer is completely removed this spacing is reduced to 7.2 Ang. If, during dehydration, water molecules are removed uniformly from all the layers in the mineral, the effective, average spacing of the oxygen and hydroxyl layers is to be expected to decrease uniformly from 10.1 to 7.2 Ang.

This, in fact, does not occur. In the naturally occurring mineral there are initially two phases present. That of major importance is characterised by a basal spacing of 10.1 Ang., and the other by a basal spacing of 7.9 Ang. As dehydration proceeds the material is

transformed steadily from the first phase into the second, the first phase disappearing completely upon dehydration in 5% relative humidity. This transformation is shown by the changing relative intensities of the first order basal X-ray reflections. During dehydration there is also a uniform variation of the peak positions of the reflections. That of the first phase changes to 9.5 Ang. for the remnants of the phase, and that of the generated phase to 7.4 Ang. in a 0% relative humidity.

Thus it appears that the water molecules can be removed more readily from one part of the mineral than another, hence the growth of the second phase at the expense of the first, but, in addition, water molecules are removed simultaneously from both phases.

The same writers show that, put in other terms, continuous dehydration takes place between the fully hydrated state of 1 water to 1 kaolin layer and the state having 2 water to 3 kaolin layers, and again between the states having 1 water to 3 kaolin layers and 1 water to 4 kaolin layers. In the intermediate states water is lost very rapidly. Further, in the driest atmosphere 1 water layer remains to every 4 kaolin layers.

Relative humidity alone cannot fully dehydrate the mineral. Basal spacings between 7.4 Ang. and 7.2 Ang. can only be produced by heat treatment at temperatures rising to 400^o C (11).

6.5 - Surface Adsorbed Water on Silicate Clay Minerals.

Hendricks and Jefferson note that one outer surface of each silicate clay mineral crystal has an oxygen face in which the oxygen atoms are in the hexagonal net arrangement of diagram (12c). Hence, adsorbed water molecules are expected to form a first layer which is hexagonally arranged to fit the oxygen surface upon which it is adsorbed, i.e. to take up a structure identical with that proposed for the interlayer water in halloysite.

A second layer of adsorbed molecules fits upon the first layer and binds to it by hydrogen bonds which join alternate water molecules in the second layer to corresponding oxygen atoms in the first layer. This arrangement is shown in diagram (15). Third and subsequent layers may be added in the same way, the final thickness of the adsorbed film being such that the vapour pressure of the outermost layer is equal to that of the surrounding atmosphere. The layers are not expected to have an extensive regular transverse structure but are expected to be organised in groups.

6.6 - The Determination of the Water Contents of Halloysite.

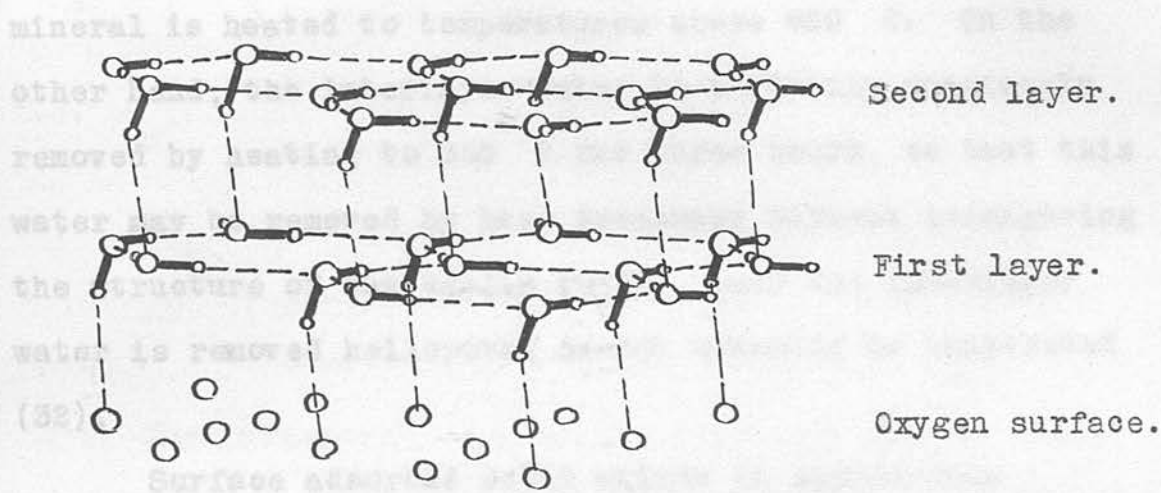
On the basis of the proposed model for halloysite there are three types of water associated with the mineral.

1. Constituent water of the kaolin layers,

Diagram 15.

- 1. Existing as hydroxyl groups.
- 2. Interlayer water.
- 3. Water adsorbed upon external surfaces.

Water of type (1) can only be removed by destroying the kaolin layers. The results of differential thermal analysis indicate that the structure breaks down when the mineral is heated to temperatures above 450 °C. On the other



HENDRICKS' MODEL FOR ADSORBED WATER.

quantities on samples... prove to be small... per gram of mineral... the whole of this water... reversible.

Once these points are reached... surface adsorbed water... the following weighting...

If the two columns... sample of partially... relative humidity of 100... material is removed...

heated to 350° existing as hydroxyl groups.

2. Interlayer water.
3. Water adsorbed upon external surfaces.

Water of type (1) can only be removed by destroying the kaolin layers. The results of differential thermal analysis indicate that the structure breaks down when the mineral is heated to temperatures above 650° C. On the other hand, the interlayer water is certainly completely removed by heating to 350° C for three hours, so that this water may be removed by heat treatment without endangering the structure of the kaolin layer. Once the interlayer water is removed halloysite cannot normally be rehydrated (32).

Surface adsorbed water exists in appreciable quantities on samples of halloysite as the crystallites prove to be small, giving a large effective surface area per gram of mineral. Normal dessication removes almost the whole of this water, the process being completely reversible.

Once these points are known the interlayer and the surface adsorbed water contents may be distinguished by the following weighing method: -

If the two contents are to be determined for a sample of partially dehydrated halloysite kept in a relative humidity of $R\%$, then about 0.5 gm. of the material is removed and weighed a first time. It is then

heated to 350^o C for three hours to remove all interlayer and adsorbed water and weighed a second time. Finally, it is allowed to reabsorb surface water in the R % relative humidity after which it is weighed a third time. If the weights recorded are respectively - W_1 , W_2 and W_3 then

W_1 - weight of metahalloysite plus weight of interlayer water plus weight of adsorbed water appropriate to R % relative humidity.

W_2 - weight of metahalloysite.

W_3 - weight of metahalloysite plus weight of adsorbed water appropriate to R % relative humidity.

The percentage weights of interlayer and adsorbed water relative to the weight of metahalloysite with which they are associated are -

$$\% \text{ interlayer} - \frac{W_1 - W_3}{W_2} \quad 100\%$$

$$\% \text{ adsorbed} - \frac{W_3 - W_2}{W_2} \quad 100\%$$

In this method the major assumption is made that the quantity of surface adsorbed water is the same in a given relative humidity whether the adsorbing surface is that of halloysite or metahalloysite. No experimental evidence exists yet to say that this is, or is not, so.

(p. 80 !)

6.7 - The Morphology of Halloysite.

In sections (6.2) and (6.4) only the c dimension of the kaolin unit cell is mentioned. That the a and b dimensions are also of considerable interest is shown by Bates, Hildebrand and Swineford (4).

Referring to diagram (12a), the kaolin layer has an upper face composed entirely of oxygen atoms. The b dimension of the unit cell measured along this face is 8.93 Ang. The other face is composed entirely of hydroxyl groups and, where such a face occurs free from the influence of neighbouring oxygen faces, as in Gibbsite $(Al_2(OH)_3)_n$, the unit cell spacing is only 8.62 Ang. Thus, a hypothetical isolated unit cell would be wedge-shaped.

In the mineral kaolinite, which is built up of layers of such unit cells extending indefinitely in the a and b directions and stacked in an orderly manner upon each other in the c direction, the oxygen face of one layer is less than 3 Ang. from the hydroxyl face of the next. The mineral occurs as large flat plates, and hence the bonding arising between the oxygen atoms and the hydroxyl groups must be so strong that the hydroxyl group spacing is stretched to equal that of the oxygen face.

However, in halloysite, water molecules intervene between the oxygen and hydroxyl faces of neighbouring kaolin-type layers. In effect the oxygen-hydroxyl bond is

weakened and the hydroxyl group spacing is not stretched appreciably. The kaolin type layers in halloysite are, therefore, composed of wedge-shaped unit cells and are curved and not plane. Calculating from the unit cell dimensions the layers curve into cylinders of 125 Ang. radius.

Layers cannot be built with less than this radius as this requires the hydroxyl groups to be compressed into a smaller spacing than is natural. Layers can, however, be built with a greater radius for this requires only a slight increase in hydroxyl group spacing. Thus a tube may be built up by the addition of other layers outside a first cylindrical layer of 125 Ang. radius. The thickness of the tube so built up will be limited by the strains set up in the outermost layers due to the stretching of the bonds between hydroxyl groups.

There is also a discrepancy in the unit cell dimensions in the a direction, and this gives rise to a similar curvature of the layers with a radius of curvature of 285 Ang.

Bates, Hildebrand and Swineford present the above explanation to account for the appearance of a hollow tube morphology for halloysite when studied with the electron microscope. The measured inner diameters of the tubes range from 200 to 1000 Ang. and are of the same order as those arising from the structure proposed. The measured thicknesses of the tubes range from 100 to 700 Ang., i.e.

from 14 to 99 layers.

Further, their micrographs show that the tubular structure is split and partially or completely unrolled. This they explain by supposing that, when halloysite is dehydrated, the oxygen and hydroxyl faces approach which results in an attempt by the oxygen face to stretch the hydroxyl face. Consequently, large internal strains are set up which can cause the tubes to split longitudinally and to unroll.

It is conceivable that some of the tubes are so strong that, given a sufficiently gentle dehydration, they do not split but retain a tubular structure with the neighbouring oxygen and hydroxyl layers held apart. It may be that the existence of such tubes accounts for the fact, discussed by MacEwan (32), that a fraction of a sample of halloysite 'gently dehydrated without heat (for example over P_2O_5)' may be regenerated as halloysite after treatment with ethylene glycol and later cold water.

6.8 - Other Points about Halloysite.

Halloysite is obtained naturally as a clay or a soft rock, normally white in colour - sometimes a little grey and occasionally faintly blue. This clay or rock is composed of aggregates of halloysite crystals which are known to be from 1 to 15 microns in length (4), and less than 0.2 micron in diameter. Because of their elongated

shape the particles cannot be oriented by sedimentation. Partial orientation under extreme pressures has been reported (11).

The surface area of metahalloysite is quoted by Daly and Hendricks (18) as 44.4 sq.m. per gm. measured by the Brunauer, Emmet and Teller (BET) method for a sample of particles of apparent diameters less than 2 microns prepared from Indiana halloysite by sedimentation.

In this connection, McDowall and Vose (34) show that particles of halloysite form a loose lattice structure in the suspension, and that this so impedes the settling that the particles do not separate into size groups on sedimentation. Hence the surface area quoted above probably applies equally to the finely powdered mineral and to the 2 micron fraction.

6.9 - The Related Minerals: Kaolinite, Talc and Gibbsite.

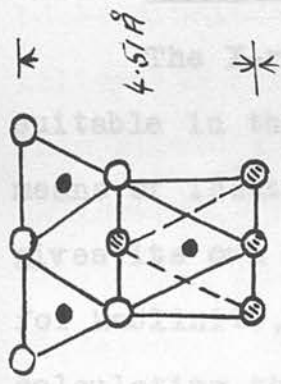
Kaolinite, $Al_2(OH)_4Si_2O_5$, is a silicate layer mineral (10b) with the structural formula

$$\begin{array}{r} Si_2O_3 \\ O_2OH \\ Al_2(OH)_3 \end{array}$$

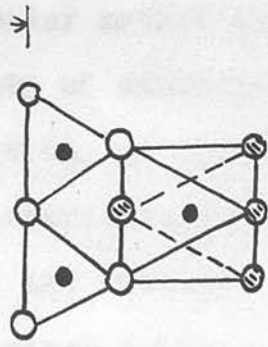
The atomic structure of the unit cell is exactly the same as that of metahalloysite, but the successive layers constituting the mineral are more closely spaced and stacked in a more orderly manner than in metahalloysite.

The structure is shown diagrammatically in diagram (16).

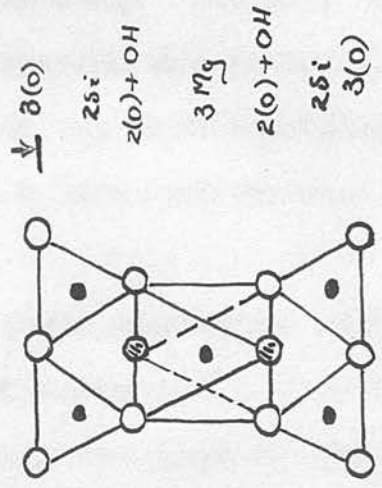
Diagram 16.



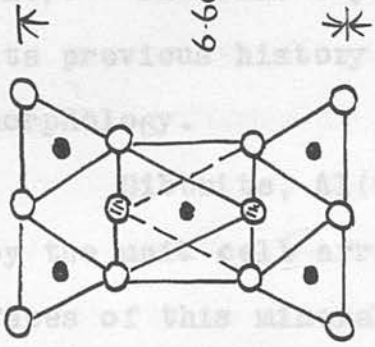
Kaolinite - $Al_2(OH)_4Si_2O_5$



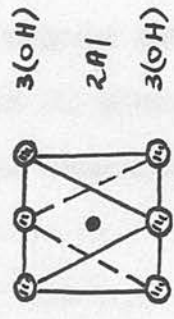
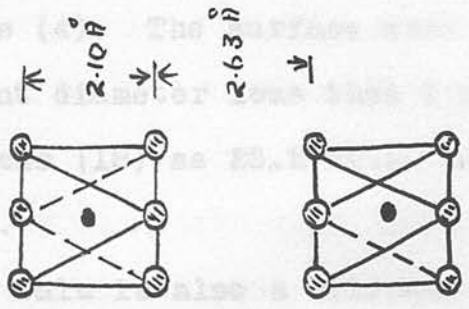
Talc - $Mg_3(OH)_2Si_4O_{10}$



Gibbsite - $Al_2(OH)_6$



UNIT CELL ARRANGEMENT OF MINERALS RELATED TO HALLOYSITE.



plates with a longer diameter than width than 100 to 200 microns (0.1 to 0.2 mm) and are apparently fibrous in appearance.

Hendrickson (1953) used the X-ray method to determine the unit cell dimensions of halloysite.

The unit cell of halloysite is composed of two silicate tetrahedra condensed with a brucite layer.

The arrangement of cells in the (100) plane is shown in Figure 16.

The crystal structure of halloysite is similar to that of kaolinite and talc.

The unit cell dimensions of halloysite are 6.60 Å, 5.65 Å, and 2.10 Å.

The unit cell dimensions of talc are 5.65 Å, 2.80 Å, and 2.10 Å.

The unit cell dimensions of kaolinite are 4.57 Å, 2.80 Å, and 2.10 Å.

The unit cell dimensions of gibbsite are 2.10 Å, 2.63 Å, and 2.10 Å.

The unit cell dimensions of halloysite are 6.60 Å, 5.65 Å, and 2.10 Å.

The unit cell dimensions of talc are 5.65 Å, 2.80 Å, and 2.10 Å.

The unit cell dimensions of kaolinite are 4.57 Å, 2.80 Å, and 2.10 Å.

The crystals of kaolinite are large pseudo-hexagonal plates with a longer diameter ranging from 0.25 to 3000 microns (4). The surface area of a sample of crystals of apparent diameter less than 2 microns is given by Daly and Hendricks (18) as 28.2 sq.m. per gram measured by the B.E.T. method.

Talc is also a silicate layer mineral and has a unit cell composed of two silicon oxygen tetrahedral sheets condensed with a brucite sheet, $Mg(OH)_2$. The unit cell and the arrangement of cells in the crystal are shown in diagram (16). The talc crystal may be of any size depending upon its previous history, but it has a flat, plate-like morphology.

Gibbsite, $Al(OH)_3$, has a layer structure represented by the unit cell arrangement in diagram (16). The hydroxyl faces of this mineral are precisely the same as those in kaolinite and halloysite.

6.10 - The X-Ray Examination of the Minerals.

The X-ray powder method of analysis is particularly suitable in the study of minerals and provides a powerful means of identification, as every crystalline substance gives its own characteristic powder pattern, e.g. those for kaolinite, talc and gibbsite (diagram (17)). By calculating the spacings between the lattice planes of the crystals and estimating relative intensities of the lines

recorded on a powder photograph, the individual materials constituting the powder can be identified.

The four minerals used in the present work were examined by Dr. J. Goodyear, employing the X-ray powder technique.

By this method it was shown that the kaolinite and talc were good specimens of the two minerals and did not contain any appreciable impurity.

The gibbsite gave the correct line spacings upon the powder photograph, but these lines appeared rather diffuse compared with those obtained with a natural gibbsite. Since the mineral used was supplied by a chemical suppliers as Aluminium Hydroxide, it may have been treated chemically.

Attention was paid mainly to the samples of halloysite. The relevant portions of the photographs obtained are reproduced in diagram (17). Photograph, a, was obtained from the prepared stock of halloysite. Photograph, g, was obtained from a surface impurity found on the halloysite which proved to be gibbsite. On the negative of the photograph for halloysite faint lines due to gibbsite were to be seen. This showed the presence of gibbsite impurity in the stock halloysite. The amount was estimated to be less than 3%.

The photographs of halloysite and metahalloysite differ only in the positions and character of the basal reflections, i.e. reflections from lattice planes parallel to the structural layers. The photographs a, b and c show

stages of dehydration. The line marked on the photographs is due to the first order basal reflections, and it is in a position in, a, corresponding to the 10.1 Ang. basal spacing of the fully hydrated halloysite. This line moves to the right as dehydration proceeds until in, c, the photograph for newly prepared metahalloysite, it is in a position corresponding to 7.2 Ang.

The remaining photograph, d, was taken using a sample of metahalloysite upon which a full series of dielectric measurements had been made. The sample was damp when photographed and had been in a 100% relative humidity for over three weeks. Comparison between this photograph and the preceding one shows that no rehydration has taken place.

CHAPTER 7.



(a) Halloysite, as supplied.



(b) Halloysite, heated to 100°C.



(c) Metahalloysite, freshly prepared.



(d) Metahalloysite, in 100% R.H. for three weeks.



(e) Kaolinite.



(f) Talc.



(g) Gibbsite.

X-RAY POWDER PATTERNS.

Diagram 17.

CHAPTER 7.

RESULTS.

7.1 - The Dehydration Rates.

(a) Interlayer water.

The dehydration rate of halloysite was studied in two different ways, the same conclusions being reached with both.

The dehydration of a sample was followed by weighing, the dehydrating sample being removed at successive time intervals from the constant relative humidity and weighed in a weighing bottle. Once the total weight of the sample became constant over several weighings the experiment was discontinued. The decrease in weight of the sample was calculated for each stage, and, from this and the final decrease in weight, the percentage approach to equilibrium was found. This was plotted against the time required to reach the stage. The curves of graph (6) are typical of the results obtained.

The form of the sample, i.e. its outward surface area, its thickness, the fineness of the powder and its degree of compactness, did not affect the dehydration rate, for the same experiment was performed on various forms of sample with always the same result. The samples used were -

1. - A sample contained in a capacitor, packed ready for dielectric measurements, having an exposed

area of 1 sq.cm. and a depth of 2 cm.

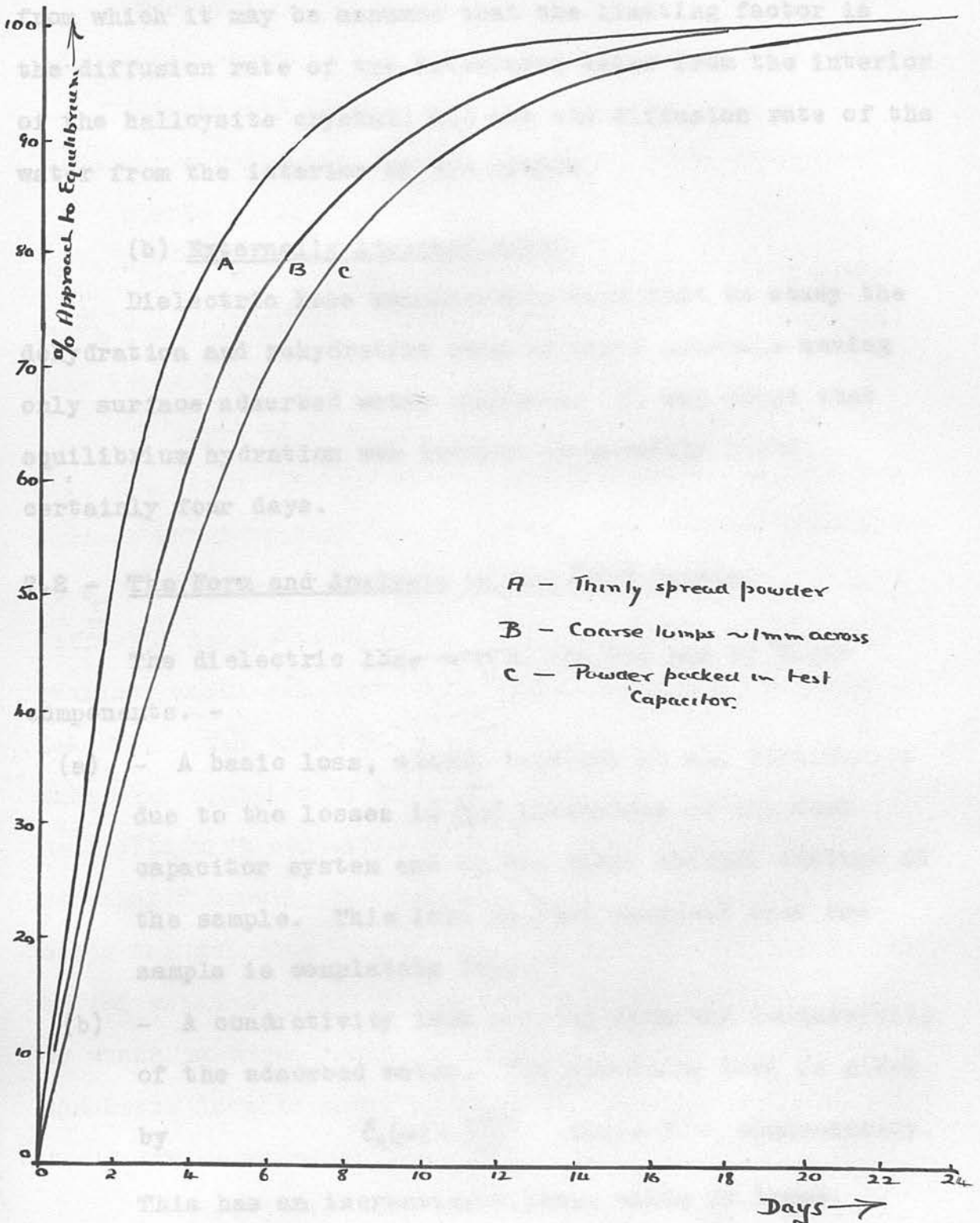
2. - A sample compacted to much the same extent as in (1) but spread over a watch glass and having a surface area of about 8 sq.cm. and a depth of about 3 mm.
3. - A sample in which the powder was pressed into a pellet, having a surface area of about 8 sq.cm. and a depth of about 2 mm. Its density was about 1.8 gm./cc. compared with 0.5 gm./cc. for (1).
4. - A number of lumps of halloysite broken from the natural rock to a size about 1 mm. across, density about 2.1 gm./cc.

The results, contained in (graph 6), were obtained for these various samples dehydrating in a 30% relative humidity, but curves closely resembling these apply at other humidities.

The dehydration was followed by dielectric loss measurements also. In this case a sample of natural halloysite was packed in a capacitor and placed in a constant humidity of 35%. The $\epsilon_2(\omega)$ curves of graph (13) were recorded at successive time intervals during the dehydration. This method had the advantage that the constant humidity enclosure was not opened at all during the period of test.

The results of both approaches show that the final state is reached in about 21 days with any form of sample,

Graph 6.



Dehydration Curves for three forms of Halloysite
dehydrating in 30% R.H.

from which it may be assumed that the limiting factor is the diffusion rate of the interlayer water from the interior of the halloysite crystal, and not the diffusion rate of the water from the interior of the sample.

(b) Externally Adsorbed Water.

Dielectric loss measurements were used to study the dehydration and rehydration rate of those minerals having only surface adsorbed water contents. It was found that equilibrium hydration was reached in possibly three, certainly four days.

7.2 - The Form and Analysis of the $\epsilon_2(\omega)$ Curves.

The dielectric loss curves are the sum of three components. -

(a) - A basic loss, almost constant at all frequencies, due to the losses in the insulators of the test capacitor system and in the basic mineral content of the sample. This loss is that measured when the sample is completely dry.

(b) - A conductivity loss arising from the conductivity of the adsorbed water. The resulting loss is given by

$$\epsilon_2(\omega) = \frac{4\pi\sigma}{\omega} \quad \text{where } \sigma = \text{conductivity.}$$

This has an increasingly large value at lower frequencies, but normally a negligible value at high

frequencies. The value of $\epsilon_2(\omega)$ depends upon the conductivity, the water content, and so upon the maintained humidity.

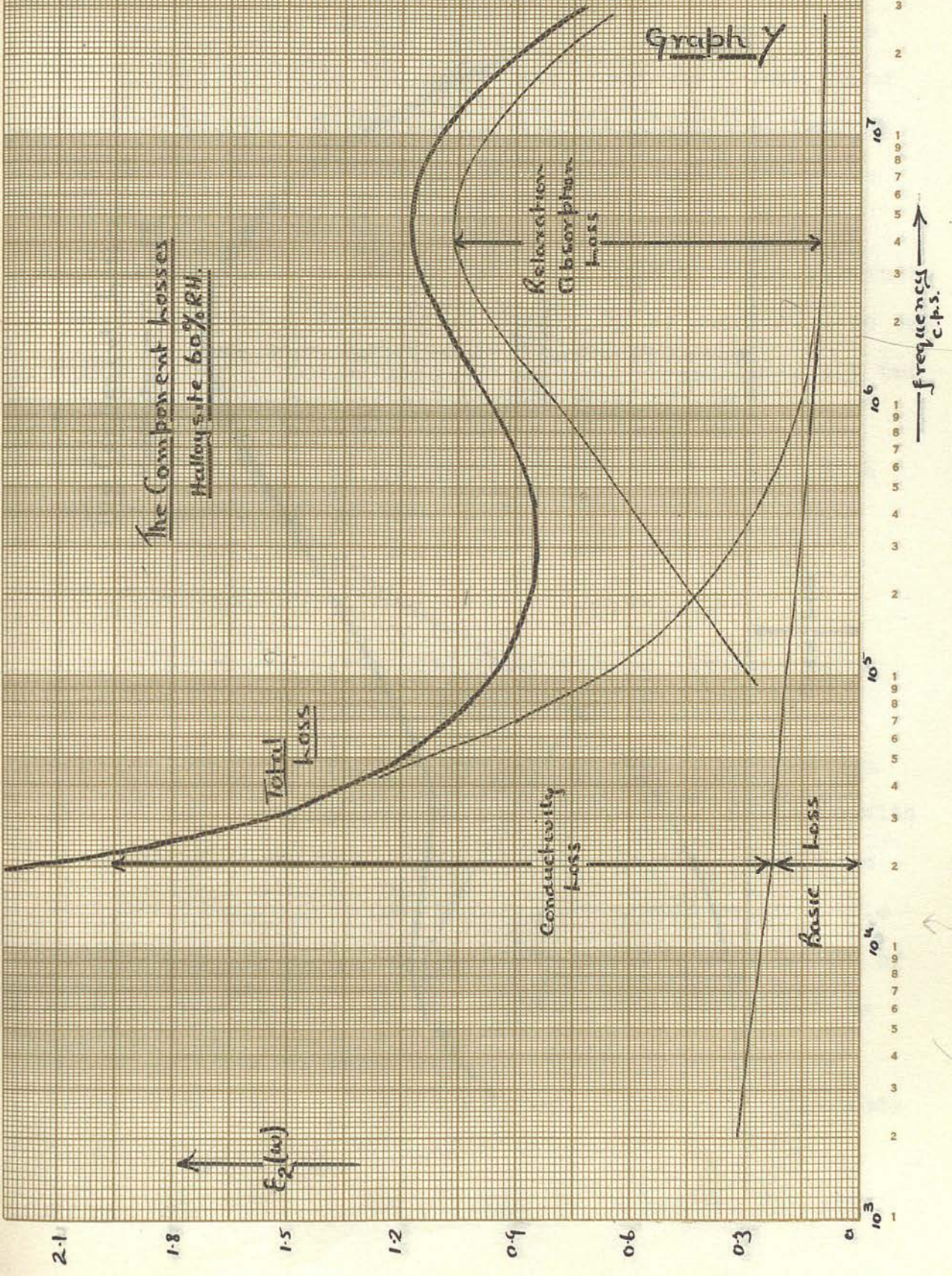
- (c) - A relaxation absorption loss of the generalised Debye type.

For illustration, graph (7) shows the experimental curve for halloysite in a 60% relative humidity analysed into three components.

A curve is analysed in the following way. First of all, the basic loss is found. Where a mineral has only a surface water content the basic loss is given by the curve in a 0% relative humidity, but for halloysite, where a different sample is used for each humidity and no sample is examined in 0% relative humidity, a different procedure is followed. The total weight of halloysite put in is noted when the capacitor is charged. The weights of water and metahalloysite contained in the capacitor can then be calculated knowing the percentage water content determined using the weighing sample data. The basic loss introduced by the metahalloysite may be calculated from the loss shown by actual metahalloysite samples in 0% relative humidity as the basic loss is directly proportional to the weight of the lossy material.

Once the basic loss is known, a curve is fitted to the low frequency values to account for the conductivity loss, i.e. the remainder of the loss at these frequencies.

The Component losses
Halfway site 60% RH.



Graph Y

frequency
c.p.s.

106

0.21

0.18

0.15

0.12

0.09

0.06

0.03

0

$\epsilon_2(\omega)$

The Component losses
Kaolinite in 30% RH

The lower
Absorption

The upper
Absorption

Basic loss

Graph 8

10^8

10^4

10^5

10^6

10^7

frequency \rightarrow

1
2
3
4
5
6
7
8
9
10
11
12
13
14
15
16
17
18
19
20
21
22
23
24
25
26
27
28
29
30
31
32
33
34
35
36
37
38
39
40
41
42
43
44
45
46
47
48
49
50
51
52
53
54
55
56
57
58
59
60
61
62
63
64
65
66
67
68
69
70
71
72
73
74
75
76
77
78
79
80
81
82
83
84
85
86
87
88
89
90
91
92
93
94
95
96
97
98
99
100

This curve is then extrapolated to the higher frequencies where, together with the basic loss, it forms a background to the relaxation absorption loss. The difference between the predicted background and the experimental curve gives the relaxation absorption curve.

A somewhat different situation arises in the kaolinite results where the experimental curve can be resolved into two separate relaxation absorption curves. In resolving the two it is assumed that they are Debye curves. A sample experimental curve of the kaolinite set is shown in graph (8) together with its components.

7.3 - Conductivity Loss.

The conductivity loss is of special interest as it forms a background which may mask the absorption loss. Experiment shows that the magnitude of the loss increases not only with the maintained relative humidity but also with the density of packing of the sample. As it is desirable that the relaxation absorption effects should be as little hidden as possible, it is necessary to use a loose state of packing, though the opposite is required if the sample is not to compact further during the period of a series of measurements. A reasonable compromise is found in the mode of packing described in section (5.5).

The effect of packing upon the background loss was

investigated mainly in a qualitative way, but illustrative results were obtained for the same sample of halloysite as a loose powder and as a firmly compacted pellet.

A die was prepared, in which powdered halloysite could be compressed into a parallel-sided pellet, one inch in diameter, one eighth inch thick and weighing about 4.5 gms. It was sufficiently firm to withstand normal usage, and its dielectric properties were measured with it gripped between the plates of a parallel plate capacitor in a humidity enclosure.

The curves obtained, graph (9), as the pellet dehydrated, showed only a very high conductivity loss at all stages of dehydration. It was presumed that pressing the material increased the cross-section and conductivity of bridges of water between the mineral particles to such an extent that the relaxation absorption loss was obscured by the conductivity loss.

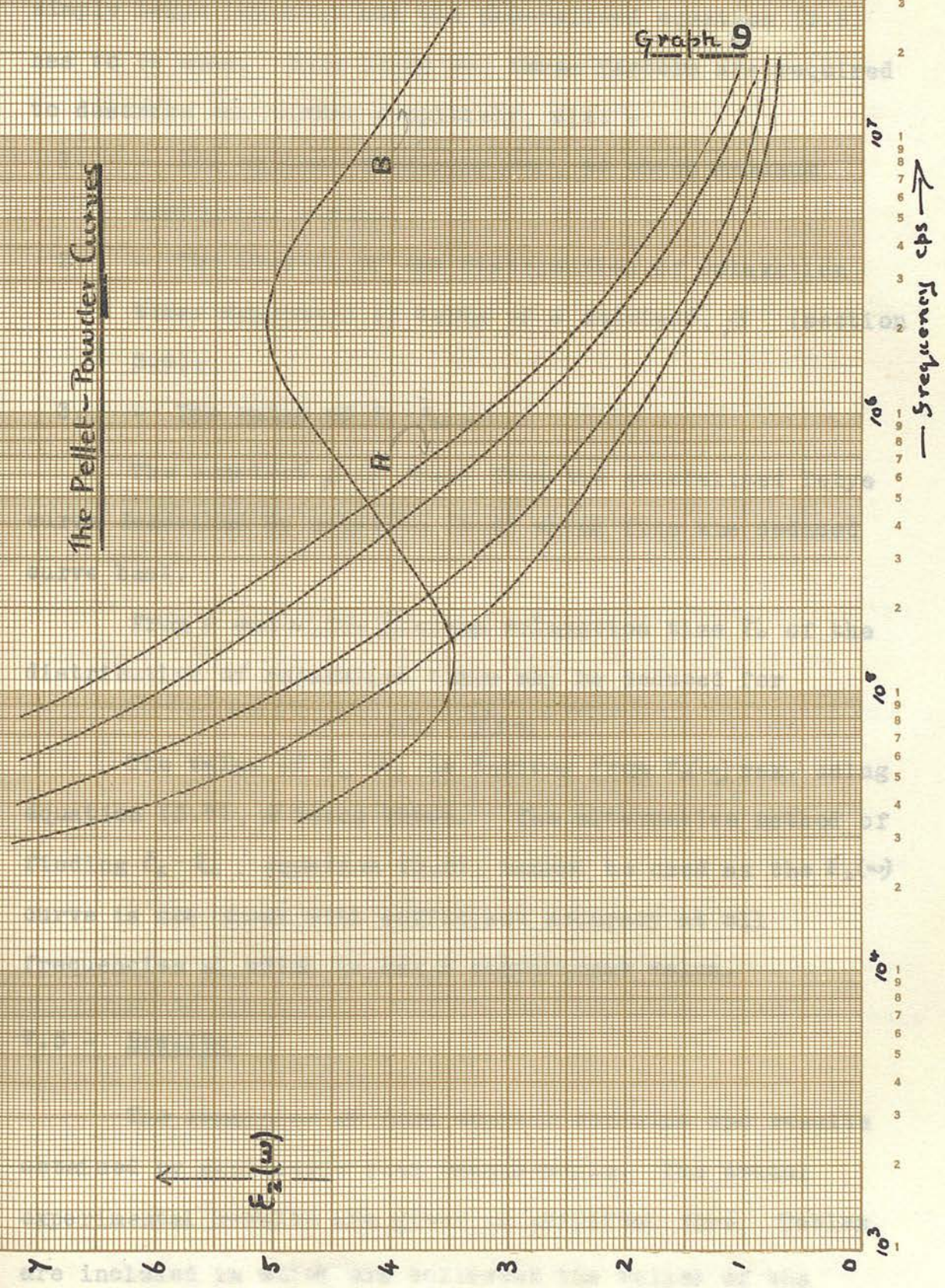
Pressing the halloysite into the pellet did not alter the nature of the material as a pellet giving a curve 'A' could be powdered and this powder would yield a curve 'B' identical with that for the original powder before compression.

7.4 - Deductions from the Relaxation Absorption Curves.

The Debye absorption curves deduced from the experimental results are too broad to be fitted by the

The Pellet - Powder Curves

Graph 9



simple Debye equation and the generalised equation (3.6) has to be used. This being so, three factors are required to describe the curves completely, viz: -

1. - The angular frequency, ω_m , at which maximum absorption occurs.
2. - The breadth of the distribution of relaxation times expressed in terms of a constant, β (section 3.6).
3. - The value of $\epsilon_s - \epsilon_\infty$.

The constant β is found from the generalised Debye curve described by equation (3.6) which fits the deduced curve best.

From β and ω_m the minimum relaxation time τ_0 of the distribution of relaxation times may be deduced for

$$\omega_m = 1/\beta\tau_0$$

The value of $\epsilon_s - \epsilon_\infty$ is derived from $\epsilon_2(\omega)$ max. using equation (3.7), β being known. The alternative method of finding $\epsilon_s - \epsilon_\infty$, equation (3.8), cannot be used as the $\epsilon_2(\omega)$ curve is not known with sufficient accuracy at all frequencies at which it has a significant value.

7.5 - Results.

The remainder of this chapter contains the results obtained by dielectric loss measurements. The actual experimental results are given in graphical form. Tables are included in which are collected the values of the

constants, such as β and τ_0 , referring to the relaxation absorption curves derived from the experimental curves.

The water contents at the various relative humidities are contained in other tables. Comments upon the results are contained under the heading of the mineral to which the results apply.

The accuracy of the results may best be assessed by noting firstly that individual readings of ϵ_2 at a given frequency for a given sample may be repeated to within 3%, and, secondly, that two like samples prepared separately yield $\epsilon_2(\omega)$ curves which are practically coincident at all frequencies. When non-identical samples are used the derived absorption curves lie at the same frequency for the same humidity. The absorption curves derived from the experimental curves are necessarily somewhat in doubt, but the quoted values of $\epsilon_2(\omega)_{max}$ are probably not in error by more than $\pm 5\%$. In the metahalloysite results the likely range of β is estimated for each humidity. The conclusions drawn from the results are based principally upon the frequency positions of the absorption maxima which are known to about one tenth of a decade compared with the total range of measurement of five decades.

7.6 - Metahalloysite.

The experimental curves are shown in graphs (10) and (11) together with some of the relaxation absorption curves

derived from them. Table 3 contains the constants derived from the curves. It is difficult to estimate the magnitude of the conductivity background in the two cases, 80 and 100% relative humidity. In the 80% relative humidity case there is not much doubt about the derived absorption curve as the high frequency values are not affected by the conductivity loss while the curve as a whole is symmetrical. In the 100% relative humidity case the conductivity background cannot be located precisely owing to the limited frequency range of measurement available. However, two limits can be set upon the background loss on the assumption that the resulting absorption loss curve must be symmetrical. This gives the probable limits within which the loss curve must lie and these are quoted in table (3).

At the lower humidities, the 30% relative humidity curve is resolved on the assumption that the conductivity background is of no importance. This is reasonable as the experimental curves show that the background becomes of lesser importance as humidity decreases. The frequency of maximum loss is judged for the results in 20% relative humidity on the assumption that the peak shape is the same for this and 30% relative humidity.

The deduced absorption curves are not perfectly symmetrical so that in finding the value of β the theoretical curve is chosen which best fits the deduced curve over a frequency range of five times on either side

of the maximum.

The values of β found for the various humidities are all about 10 with an uncertainty of ± 1 except for the 30% relative humidity where $\beta = 6 \pm 0.5$. Since the conductivity background cannot be allowed for in this latter case the β value may be much in error and can be ignored. Thus, it is assumed that $\beta = 10$ for all the metahalloysite curves. $\epsilon_s - \epsilon_0$ and τ_0 are then calculated on this assumption.

7.7 - Halloysite.

Two sets of data are included here. One set is obtained using samples settled at the various humidities (graph 12) and the other is obtained during the dehydration of halloysite above 35% relative humidity (graph 13). The derived constants are contained in tables (4) and (5).

In general the absorption curves are more readily obtained from the experimental curves for halloysite as the absorption occurs at higher frequencies for a given humidity when compared with metahalloysite. An approximate value for the frequency of maximum in 80% relative humidity is estimated from the trend of the experimental curve in the first set of data.

7.8 - Talc.

Deductions from the curves (graph 14) in this case are difficult because of the very low absorption losses

observed. Since the absorption occurs at the lower limit of the frequency range, no estimate can be made of the conductivity loss occurring, and consequently the values for β and $\epsilon_2(\omega)_{max}$ given in table (7) are estimated on the assumption that these losses are zero. This assumption is not wholly justifiable as the experimental curve for 100% relative humidity does show a slightly different shape which may be attributed to an appreciable conductivity background.

7.9 - Kaolinite.

With this mineral two absorption maxima may be derived from each experimental curve (graphs (15) and (16)). The data for each absorption curve are given separately in tables (8) and (9).

At 60% relative humidity and above, the absorption losses are obscured by the conductivity background. An estimate may just be made of the frequency of the upper $\epsilon_2(\omega)_{max}$ in the 60% relative humidity case. Little trouble arises in separating the two absorption curves for 50%, 40% and 30% relative humidity, although an estimate of the conductivity background has to be made in the first two cases to arrive at symmetrical curves. In the remaining three humidities the two absorption curves are very close together and may only be separated by assuming a simple Debye absorption for the fixed frequency

curve. Such a procedure gives some idea of the two frequencies of maximum and the maximum absorptions. It is not possible to separate the two absorption curves at 0% relative humidity.

7.10 - Surface Layer Thickness.

On the basis of the Hendricks and Jefferson model for the surface layer arrangement, the surface area covered by each adsorbed molecule may be calculated as the arrangement is such that there are two molecules of water per hexagonal oxygen ring of the adsorbing surface. The dimensions of the oxygen ring are given in diagram (12c), and, from them, the surface area covered by one water molecule is $11.19 \cdot 10^{-16}$ sq.cm. from which the weight of water required to cover one square meter of surface is 0.268 m.gms.

The surface areas of some of the minerals used are given by Dyal and Hendricks (18). They are for fractions having apparent diameters less than 2 microns and consequently may give an over estimate of the surface area of the actual samples used.

The values are: -

Metahalloysite	}	- 44.4 sq.m. per gm.
Halloysite		
Kaolinite		- 28.2 sq.m. per gm.


The materials used by Dyal and Hendricks were

Indiana halloysite and English china clay, i.e. from the same source as those used for the present experiments. It is assumed that the surface areas for halloysite and metahalloysite are the same.

The weights of water required to cover the total surface area of one gramme of each mineral with a monomolecular layer can best be expressed as the required percentage water content by weight. The percentage water contents to form a monolayer are: -

metahalloysite)	}	- 1.19%
halloysite)		
kaolinite		- 0.755%

The thicknesses of the adsorbed water films in terms of the number of molecular layers are calculated from this data and the measured weights of adsorbed water. The values are tabulated in tables (6) and (10).



Constants Derived from the Absorption Curves.

METAHALLOYSITE.

% Relative Humidity	Frequency of $\epsilon_2(\omega)_{max}$	β	$\epsilon_2(\omega)_{max}$	$\epsilon_s - \epsilon_0$	τ_0 sec.
0	-	-	-	-	-
10	-	-	-	-	-
20	~ 2 Kc/s.	-	-	-	$\sim 8.0 \ 10^{-6}$
30	11 "	6 ± 0.5	2.44	7.0	$1.4 \ 10^{-6}$
40	70 "	9.5 ± 1	2.26	7.45	$2.3 \ 10^{-7}$
50	400 "	10.5 ± 1	2.32	7.9	$4.0 \ 10^{-8}$
60	800 "	10.0 ± 1	2.40	8.05	$2.0 \ 10^{-8}$
80	5.8 Mc/s	9.0 ± 1	2.78	9.0	$2.7 \ 10^{-9}$
100	11)	10.0)	3.08)	10.3)	$1.45 \ 10^{-9}$)
))))	-10)
	18)	1.0)	2.78)	5.5)	$8.8 \ 10^{-10}$)

Table 3.

Table 3.

Constants Derived from the Absorption Curves.

HALLOYSITE.

<u>%</u> Relative Humidity	Frequency of $\epsilon_2(\omega)_{max}$	β	$\epsilon_2(\omega)_{max}$	$\epsilon_s - \epsilon_\infty$	τ_0 sec.
40	300 Kc/s.	12	1.49	5.3	4.4 10^{-8}
50	1.5 Mc/s.	10	1.46	4.9	1.0 10^{-8}
60	4.5 "	6	2.16	6.2	6.2 10^{-9}
80	~ 100 "	-	-	-	~ 3 10^{-10}

Table 4.

Table 4.

Constants derived from the Absorption Curves.

Halloysite - during dehydration in 35% Relative Humidity.

Table 5.

Time of dehydration. Days.	Frequency of $\epsilon_2(\omega)_{max}$	β	$\epsilon_2(\omega)_{max}$	$\epsilon_s - \epsilon_\infty$	$\tau_{sec.}$
0	6 Mc/s.	5	2.26	6.2	$2.7 \cdot 10^{-9}$
2	1.2 "	11	1.86	6.4	$1.3 \cdot 10^{-8}$
5	110 Kc/s	9	1.52	4.9	$1.4 \cdot 10^{-7}$
14	35 "	(10)	1.25	4.2	$4.5 \cdot 10^{-7}$
21) 28)	30 "	(10)	1.2	4.0	$5.3 \cdot 10^{-7}$

Table 6.

Interlayer and Adsorbed Water Data for
Halloysite and Metahalloysite.

% R.H.	HALLOYSITE				METAHALLOYSITE	
	Percentage interlayer water content.		Percentage adsorbed water.	No. of mono- molecular layers adsorbed.	Percentage adsorbed water.	No. of mono- molecular layers adsorbed.
	Referred to m.hall. content	Ref. to total wt.				
0	-	-	-	-	0	0
10	-	-	-	-	1.38	1.16
20	-	-	-	-	1.74	1.46
25	-	-	-	-	1.78	1.50
30	-	-	-	-	2.04	1.71
35	2.38	2.28	1.76	1.48	-	-
40	3.90	3.69	1.76	1.48	2.12	1.78
50	-	-	2.28	1.92	2.50	2.10
60	8.42	7.60	2.68	2.25	2.84	2.38
80	11.4	9.90	3.60	3.02	5.4	4.55
100	-	-	-	-	18.2	15.3

The surface areas of metahalloysite and halloysite - 44.4 sq.m. per gm.

The percentage weight of water required to cover the surface with a monomolecular layer is 1.19%.

Constants derived from the Absorption Curves.

Table 7.

TALC.

<u>%</u> Relative Humidity.	Frequency of $\epsilon_2(\omega)_{max}$	β	$\epsilon_2(\omega)_{max}$	$\epsilon_s - \epsilon$	τ_0 sec.
0	-	-	-	-	-
10	10 Kc/s.	(1)	0.061	0.122	$1.6 \cdot 10^{-6}$
40	10 "	(1)	0.152	0.30	$1.6 \cdot 10^{-6}$
60	10 "	2	0.58	1.25	$8 \cdot 10^{-7}$
80	5 "	9	2.19	7.1	$3.5 \cdot 10^{-6}$

Table 7.

Table 8.

Constants derived from the Absorption Curves.

The Lower Frequency Absorption with Kaolinite.

Relative Humidity.	Frequency of $\epsilon_2(\omega)_{max}$	β	$\epsilon_2(\omega)_{max}$	$\epsilon_s - \epsilon_\infty$	τ_0 sec.
0	~ 10 Kc/s.	-	-	-	-
10	6 "	(1)	0.069	0.138	2.8 10^{-5}
15	6 "	(1)	0.061	0.122	2.8 10^{-5}
20	6 "	(1)	0.076	0.152	2.8 10^{-5}
30	8 "	6	0.085	0.244	3.3 10^{-6}
40	10 "	5	0.107	0.295	3.2 10^{-6}
50	12 "	10	0.122	0.412	1.3 10^{-6}

Table 8.

Table 9. Constants derived from the Absorption Curves.

The higher frequency absorption with Kaolinite.

Relative Humidity.	Frequency of $\epsilon_2(\omega)_{max}$	β	$\epsilon_2(\omega)_{max}$	$\epsilon_s - \epsilon_0$	τ_0 sec.
0	10 Kc/s.	-	-	-	-
10	105 "	10	0.122	0.41	1.5 10^{-7}
15	150 "	8	0.125	0.39	1.1 10^{-7}
20	400 "	7	0.137	0.41	4.0 10^{-8}
30	1.5 Mc/s.	10	0.145	0.49	1.1 10^{-8}
40	2.0 "	10	0.147	0.49	8.0 10^{-9}
50	10.0 "	10	0.160	0.54	1.6 10^{-9}
60	50.0 "	-	-	-	-

Adsorbed Water Data for Kaolinite and Talc.

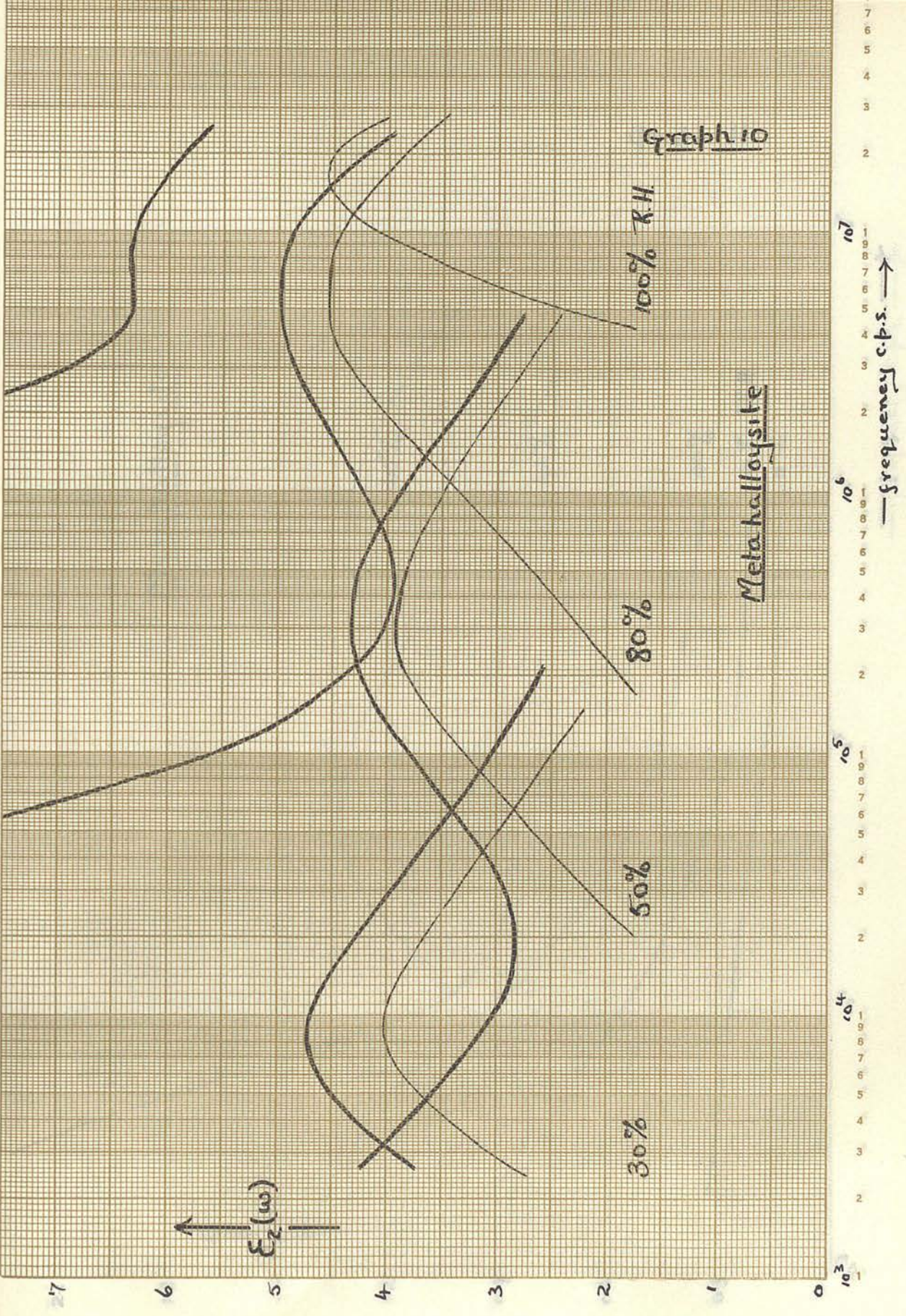
Table 10.

Relative Humidity %	KAOLINITE		TALC
	Percentage adsorbed water.	No. of monomolecular layers adsorbed	
0	-	-	-
10	0.914	1.2	0.16
20	1.14	1.49	-
30	1.22	1.58	-
40	1.24	1.62	0.94
50	1.48	1.94	-
60	1.60	2.09	1.14
80	3.8	5	1.4
100	7.7	10	4.9

The surface area of kaolinite is 28.2 sq.m. per gm.

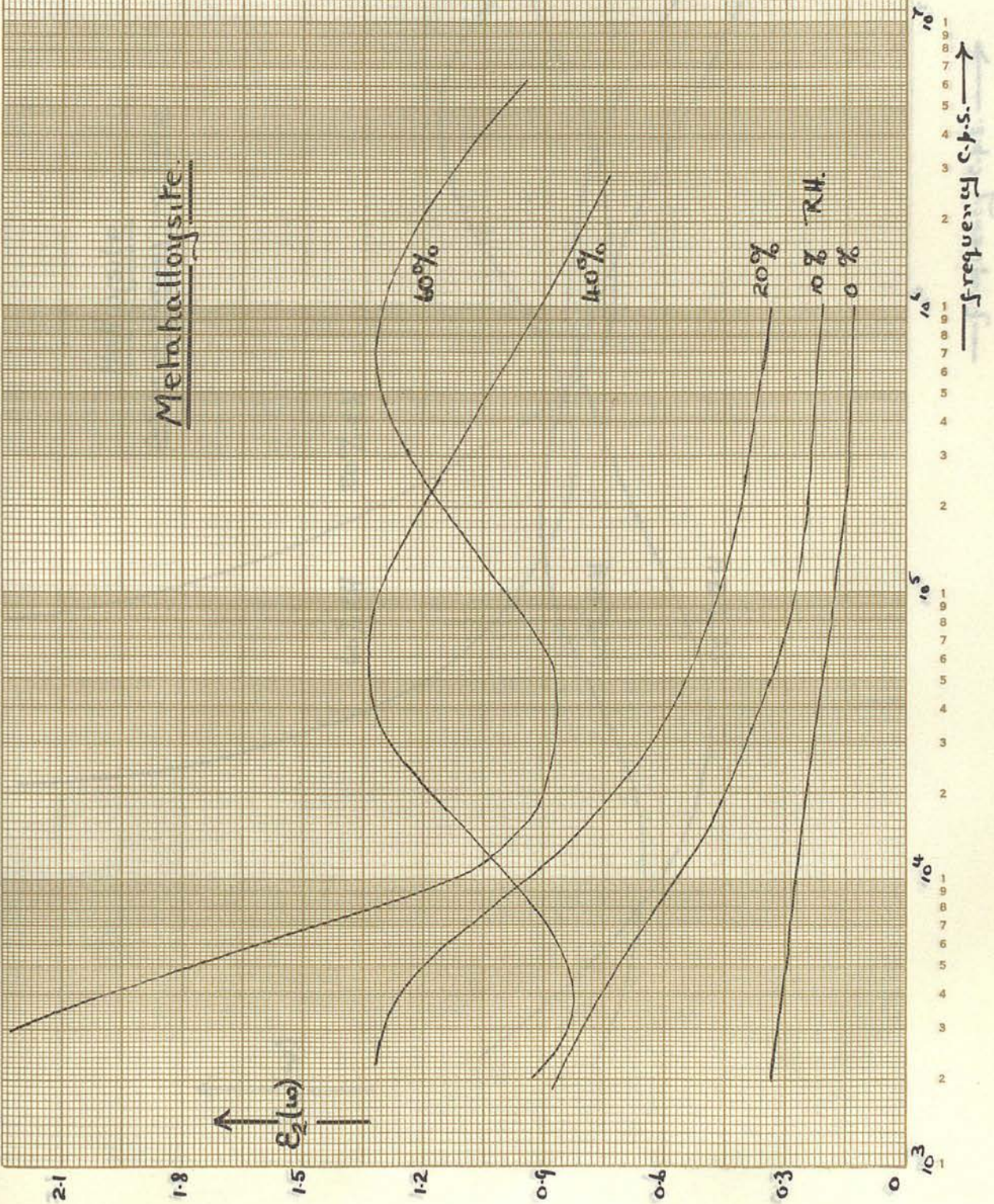
The percentage weight of water required to cover the surface with a monomolecular layer is 0.75%.

The surface area of talc is unknown.



Graph II

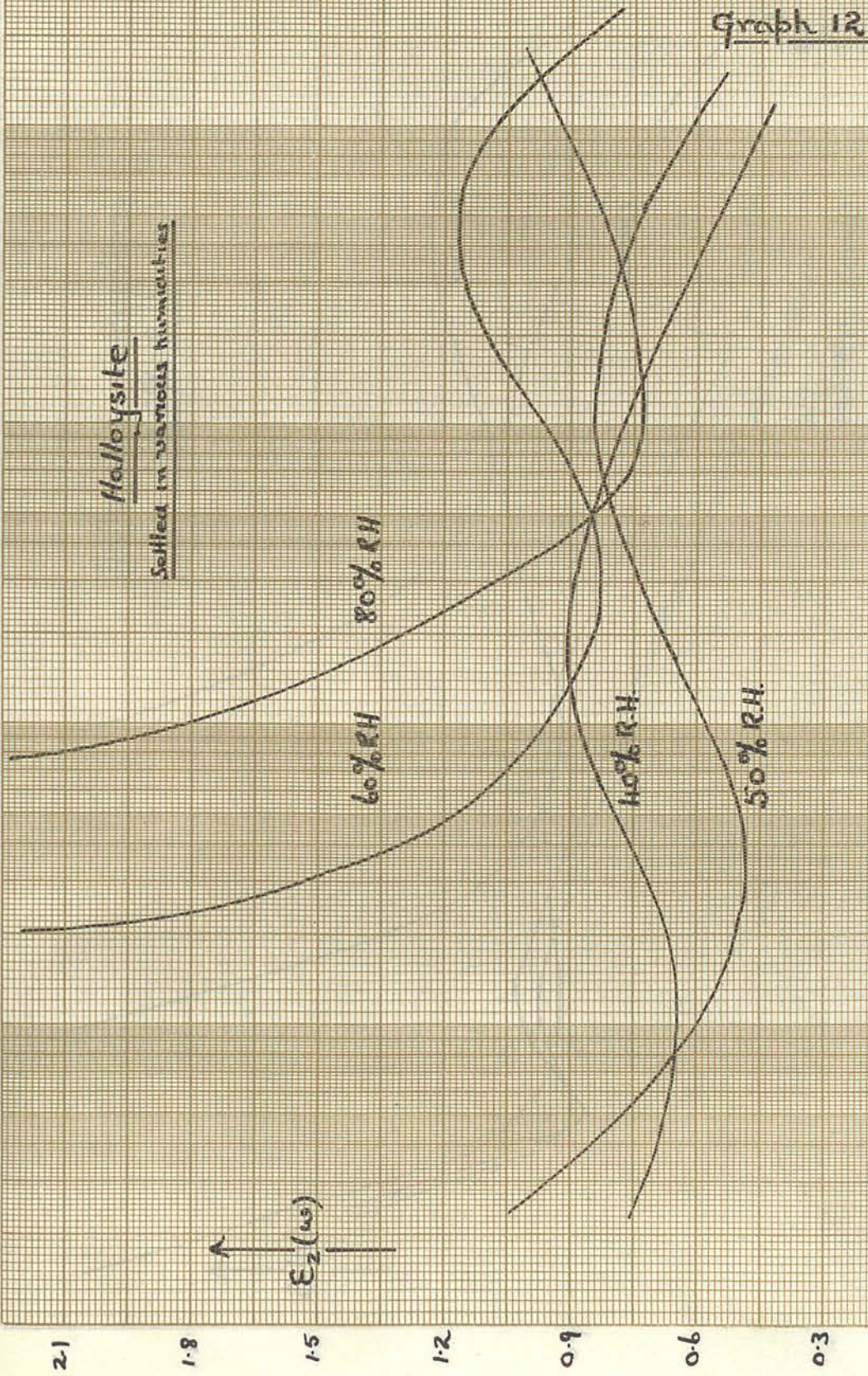
Metahalloysite



frequency C.P.S. →

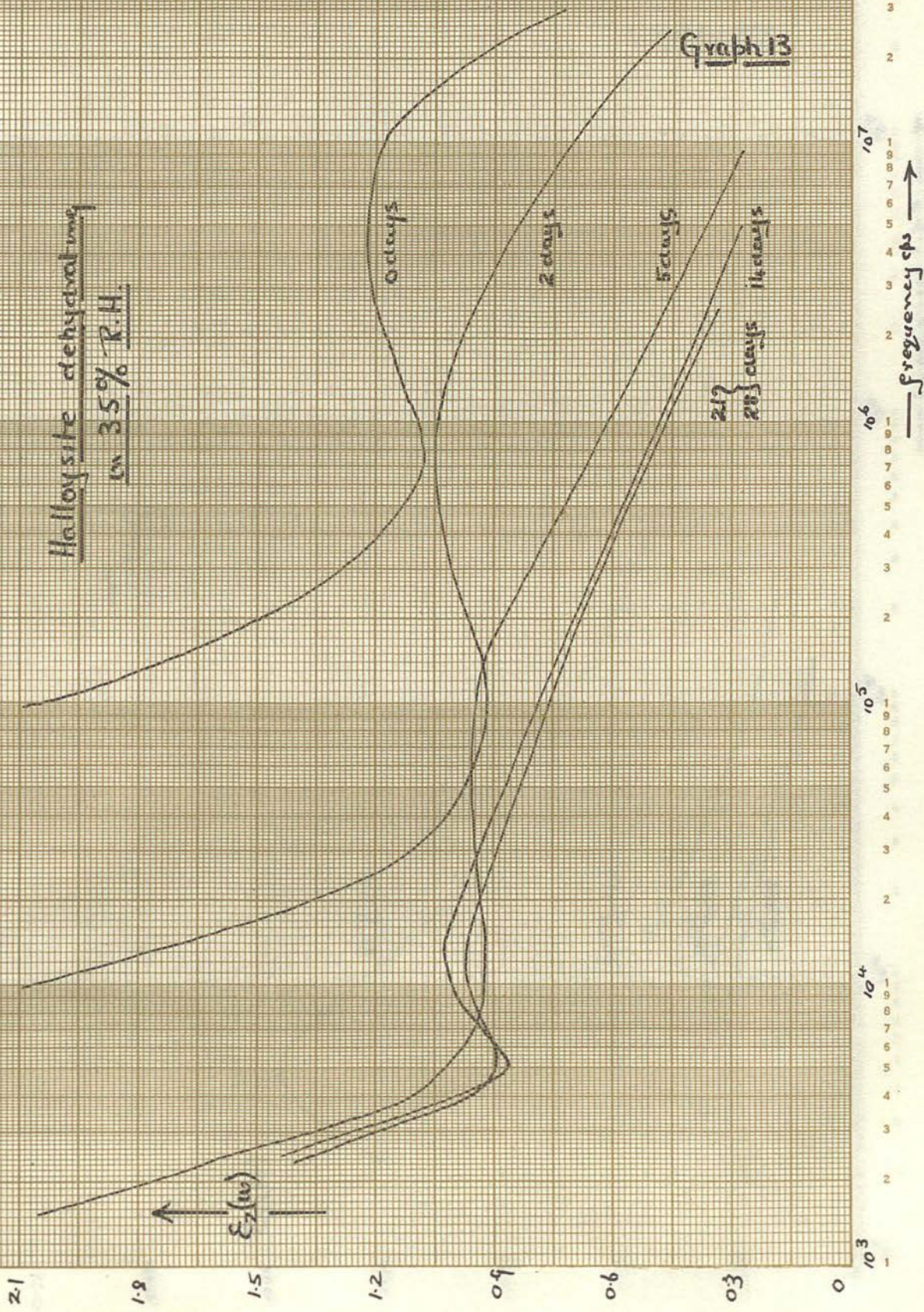
Malloysite

Soil in various humidities



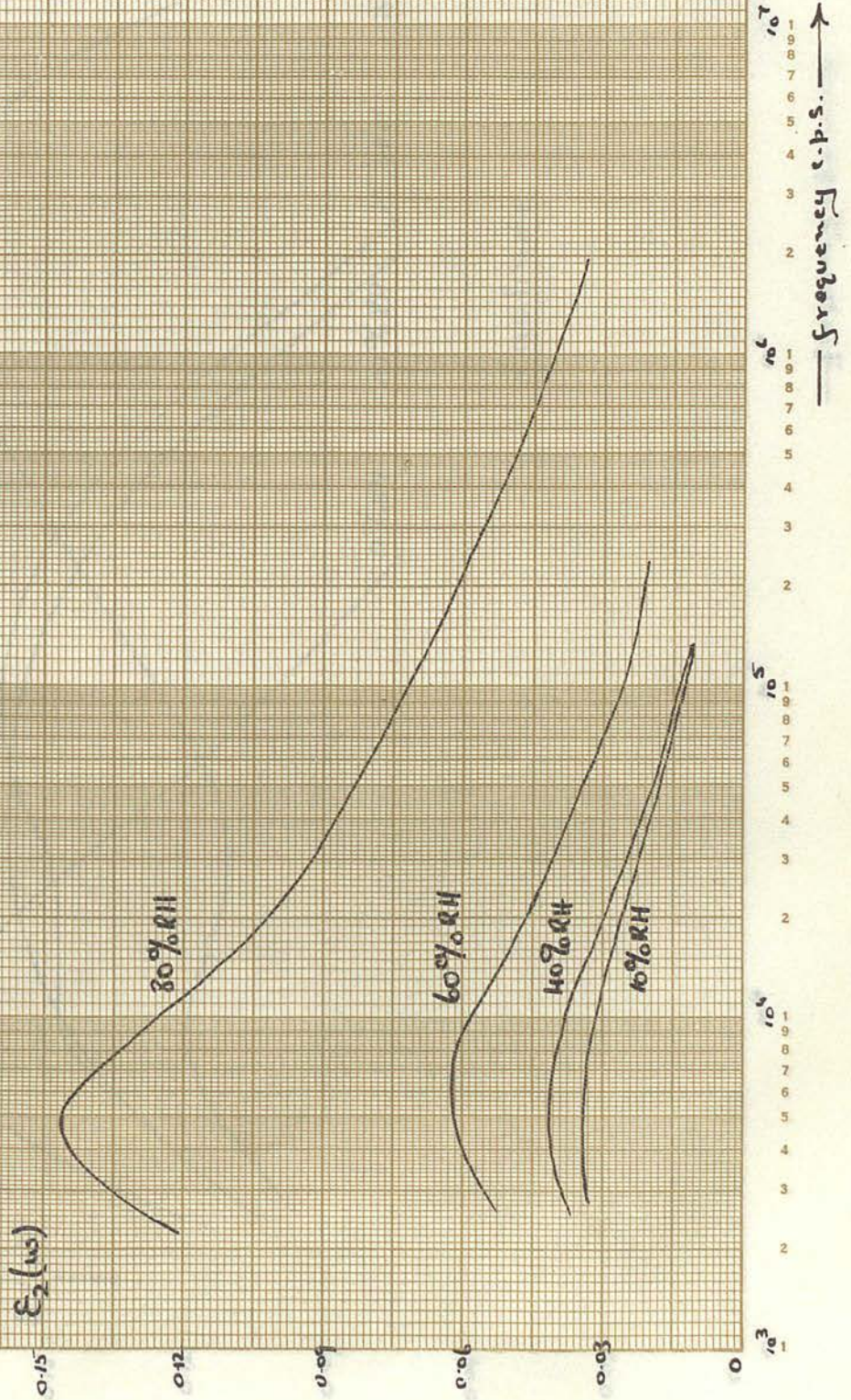
Halloysite dehydrating
in 35% R.H.

Graph 13

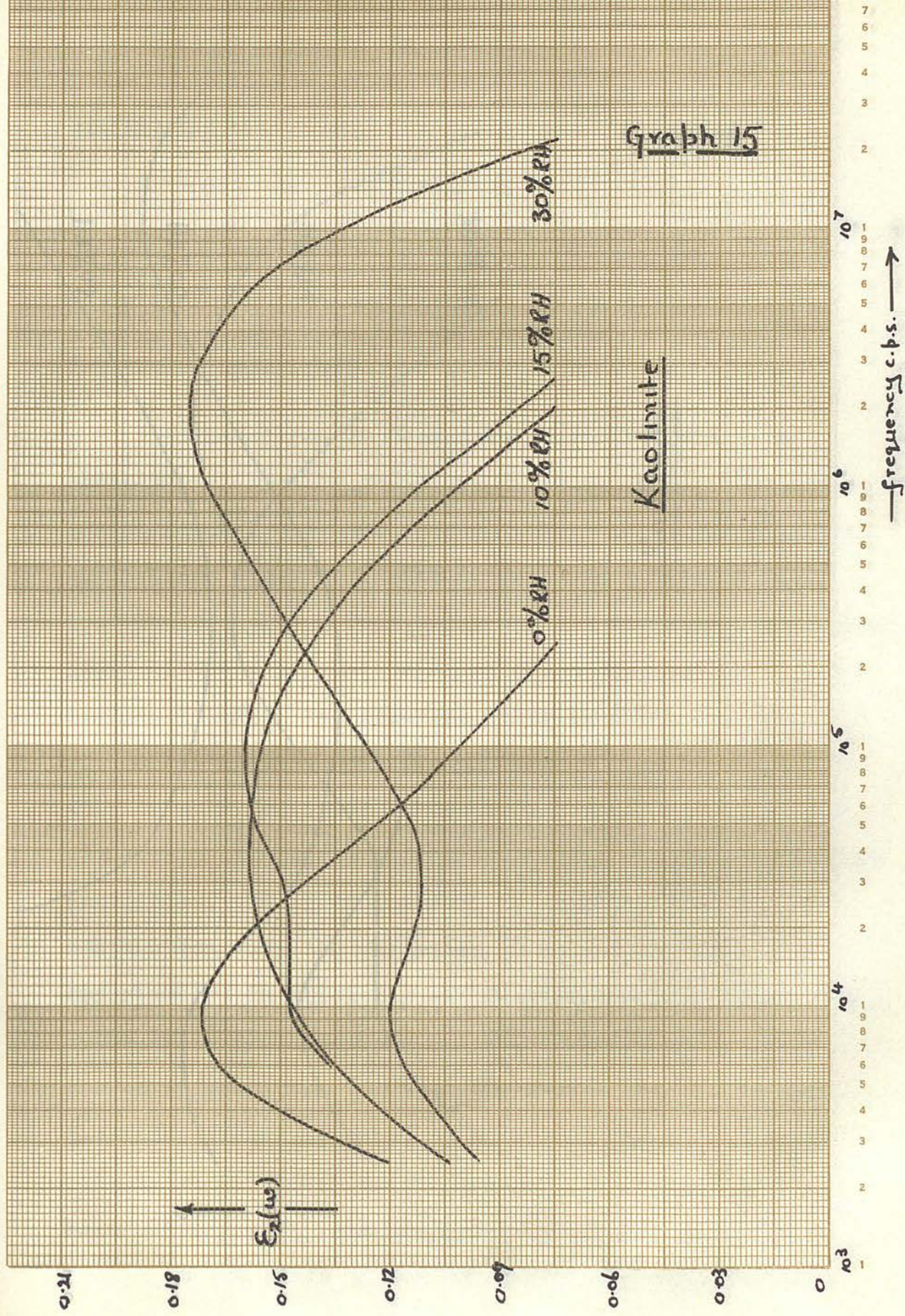


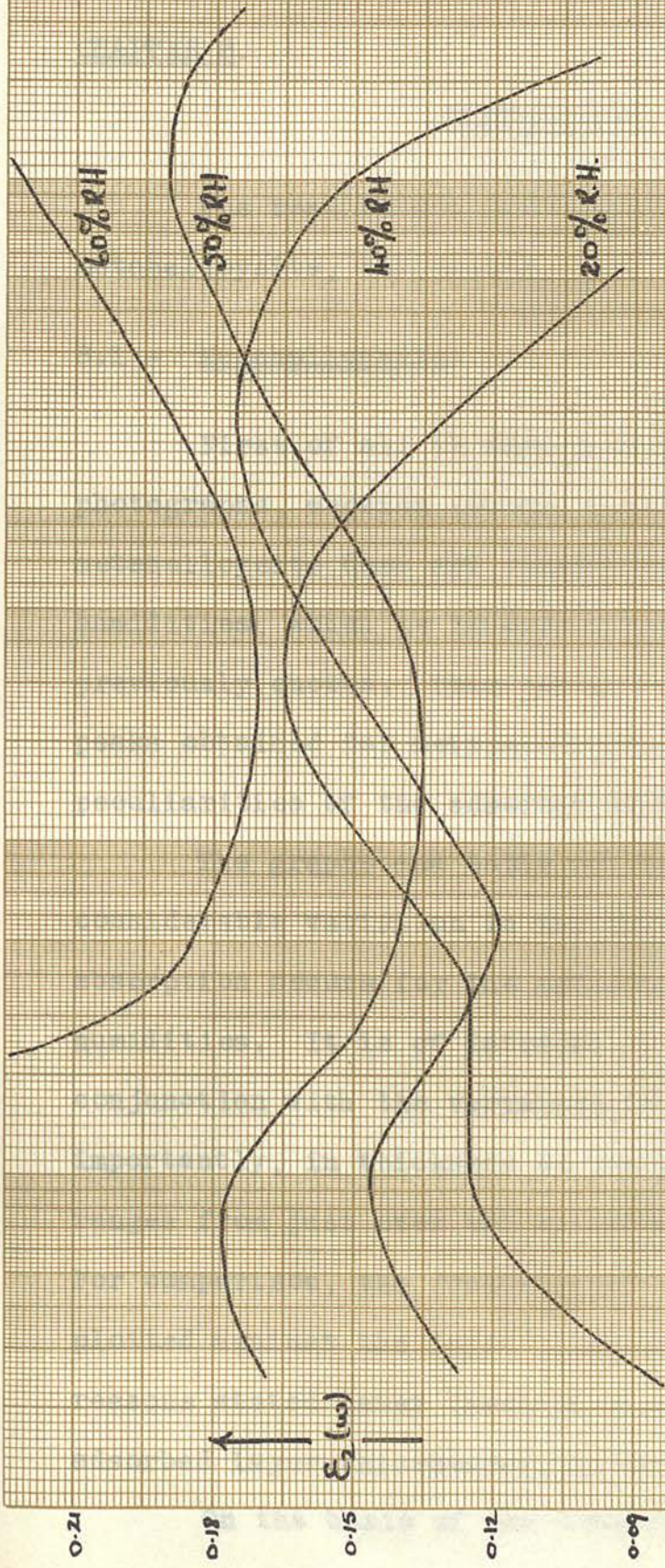
TALC

Graph 14



Frequency c.p.s. \rightarrow





Graph 16

Kaolinite

10^3 1 2 3 4 5 6 7 8 9
 10^4 1 2 3 4 5 6 7 8 9
 10^5 1 2 3 4 5 6 7 8 9
 10^6 1 2 3 4 5 6 7 8 9
 10^7 1 2 3 4 5 6 7 8 9
 — frequency cps. —→

CHAPTER 8.

CONCLUSIONS.

The results are considered in the order -
metahalloysite, halloysite, talc and kaolinite.

8.1 - Metahalloysite.

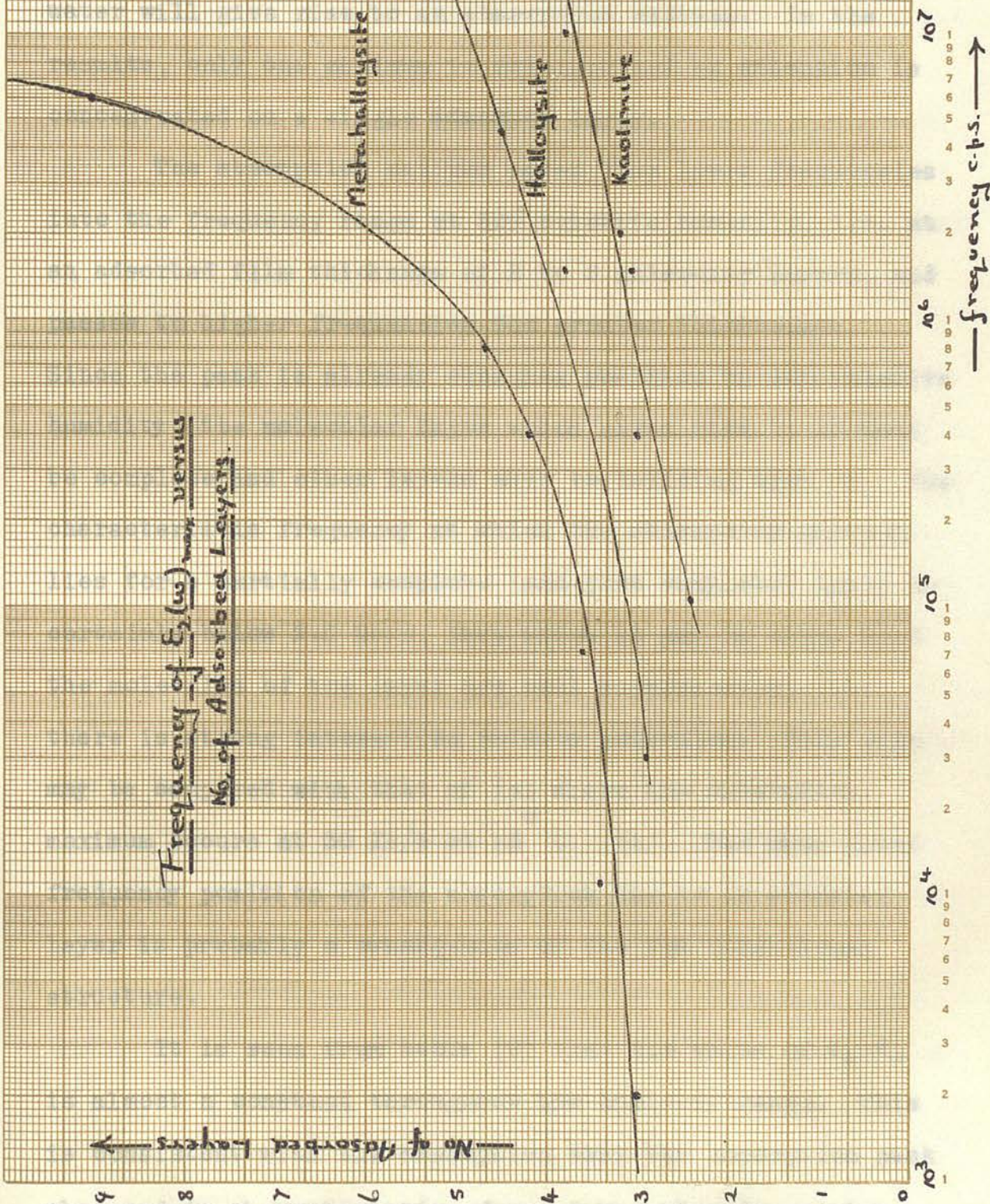
First of all it should be noted that the X-ray photographs, section (6.10), show conclusively that the metahalloysite does not rehydrate in the various relative humidities, which is in accord with the published data previously quoted. This being so, the dielectric absorption peaks obtained for metahalloysite can only be due to the peculiarities of the adsorbed water layer.

The graphs and table of results show that there is considerable variation in the frequency at which maximum absorption occurs for the material settled in the different humidities. It is of interest to consider this in conjunction with the variation in weight or, more importantly, in thickness of the adsorbed water film. This ranges from just over two to about thirty molecular layers. For comparison, the frequency of maximum absorption is plotted against the layer thickness in graph (17). For reasons stated later (section 8.5) it is taken that the adsorbed layer thicknesses are twice those tabulated.

On the basis of the considerations outlined in

Graph 17

Frequency of $E_2(\omega)_{max}$ versus
No. of Adsorbed Layers.



sections (2.5) and (2.6) certain conclusions may be drawn. There it is taken that each monomolecular layer of adsorbed water will give rise to an absorption maximum. In the results, only one maximum is obtained and so attention is concentrated on a single adsorbed layer.

The absorption maximum moves from lower frequencies into the frequency range at 30% relative humidity, i.e. at an adsorbed film thickness of 2 to 3 molecular layers, and passes to higher frequencies for greater thicknesses. Since the peak is already changing position by 30% relative humidity, the molecular layer which gives rise to it must be complete and other layers must be building upon it. The characteristic frequency at which the absorption maximum lies for a partially complete (and just complete) layer is certainly below 2.5 Kc/s, from which it may be taken that the molecules of the layer are well co-ordinated, i.e. there is strong interaction between molecules. This case may be compared with that of ice where the absorption maximum occurs at 30 Kc/s at -5° C. (31). The much lower frequency position of the absorption due to an adsorbed layer is probably a consequence of its two dimensional structure.

It is seen from table (3) that the value of $\epsilon_s - \epsilon_{\infty}$ is almost a constant throughout the humidity range. This is consistent with the assumption that the absorption peak observed is characteristic of one layer already complete,

for a constant value requires a constant number of adsorbing molecules.

The values of β quoted may only be taken as constant at $\beta = 10$. This large value indicates considerable irregularity in the environment of molecules in the layer, which may be interpreted as showing that the layer is composed of many small, well organised groups. The constant value indicates that these groups keep their same size throughout the humidity range.

The question is still open as to whether the peak observed is characteristic of the first or the second layer, both of which are complete at the outset. Several workers (15 and 36) point out that the first layer, owing to its rigid adhesion to the surface, has properties very different from those of the bulk liquid. Whether the properties of the layer dealt with here are sufficiently extreme for this to be a first layer cannot be judged from the present data which do not contain a second peak for comparison.

The position of the peak is sensitive to the variation in the number of adsorbed layers until over five are complete, and thereafter the effect of additional layers becomes less and less, the peak tending to a final position. Thus, the 'binding' of a layer is weakened by the addition of further external layers, the effect of each successive one being progressively less.

Within the range of humidities used there is no

evidence of peaks characterising either more tightly or less tightly bound layers. The fact that no second peak appears, from lower frequencies, in the frequency range does not assist in answering the question of whether the peak observed is characteristic of the first or the second layer, as presumably a tightly bound first layer, such as that supposed to exist on silica gel, would not be much affected by the addition of other layers. The non-appearance of a higher frequency absorption indicates that the next layer outside that observed must be very loosely bound, for the lowest frequency position of its absorption must lie above 25 Mc/s. Since this is only three decades in frequency below the region in which water in bulk shows its absorption maximum, the third, say, adsorbed layer on metahalloysite must be in the state of bulk water.

8.2 - Halloysite.

The results obtained with halloysite show the same type of variation of position of the absorption maximum as with metahalloysite. However, the interpretation might be different, for halloysite has the complication of an interlayer water content, so that the single peak observed might be due to either interlayer or adsorbed water, or peaks due to both might be superimposed at each humidity to give the composite curve. Fortunately the complication may be removed as the interlayers in halloysite cannot be

rehydrated while the surface adsorbed water content depends only upon the humidity. Thus, if the one absorption peak obtained experimentally is due wholly or partly to interlayer water, then the whole absorption peak or a portion of it will not shift when the material is placed in a higher relative humidity. Experiment, in fact, shows that a halloysite prepared in a lower relative humidity and then allowed to settle in a higher produces closely the curve appropriate to the higher humidity. The absorption maxima obtained are therefore due to the surface adsorbed water and not to the interlayer water.

From the results it is seen that a complete single layer of water on an external surface gives rise to an absorption maximum at a frequency below the lower limit of measurement. The absorption maximum for a complete interlayer is expected to be at a still lower frequency as the interlayers are acted on by two surfaces.

A curve linking the frequency of maximum absorption with the number of adsorbed layers is plotted in graph (17) and may be compared with the corresponding one for metahalloysite. The frequency of the absorption maximum for halloysite occurs at a much higher frequency for the same adsorbed layer thickness, which indicates a lesser co-ordination in the adsorbed layer.

It is interesting to compare the dehydration data obtained with those which have been published. First of

all, the dehydration time of three weeks is vastly in excess of the two days quoted by Brindley and Goodyear (9). They worked with Utah halloysite which may have a very different crystal length from the Indiana halloysite used here. This would explain the discrepancy.

Alexander et al. (1) and Brindley and Goodyear both quote dehydration data for samples of Utah halloysite. The results of the latter workers, which are in general agreement with those of the former, are for dehydration in relative humidities less than 25%, and are not comparable with the data quoted in table (6). However, comparison is possible with the results of Alexander et al. For this purpose, the data of table (6) have been recalculated to give the percentage weights of adsorbed and interlayer water which would be removed from a sample, initially settled in 80% relative humidity, when dehydrated in various lower relative humidities. The percentages, which are calculated relative to the total weight of sample in 80% relative humidity, may then be compared with those of Alexander et al. These latter results were calculated relative to the weight of the sample in 75% relative humidity. The comparison data are contained in table (11).

From the interlayer water results it is seen that the percentage weight of water removed in each humidity is greater for Indiana halloysite. This variety appears to be a more hydrated form of the mineral.

Comparison of the Water Contents of
Utah (1) and Indiana Halloysite.

% Relative Humidity	Percentage adsorbed water		Percentage interlayer water		Percentage total water	
	Utah	Ind.	Utah	Ind.	Utah	Ind.
27	3.4	-	1.9	-	5.3	-
35	-	1.6	-	7.8	-	9.5
40	2.7	1.6	0.3	6.5	3.0	8.1
60	1.0	0.8	0.0	2.6	1.0	3.4
75	0	-	0	-	0	-
80	-	0	-	0	-	0

Table 11.

The percentages of adsorbed water are also quoted. However, the adsorbed water contents quoted here and in table (6) may not be a true measure of the water content on a halloysite as they are for a sample the crystallites of which may have been modified morphologically by heat treatment. This is discussed later in section (8.6). The material of Alexander et al. was not heat treated.

If the adsorbed water content is in doubt, then so is the interlayer water content for the latter is calculated knowing the former (sections (5.7) and (6.6)). The total water contents may be a better means of comparison. Here again the Indiana halloysite shows the greater water content.

8.3 - Talc.

The pattern of results obtained in this case is very simple. An absorption maximum at 10 Kc/s is observed to build up as the relative humidity increases. From this it may be concluded that a layer of water molecules, probably the first, is being built up throughout the range of humidity. If this is so, there should be a linear relation between $\epsilon_s - \epsilon_\infty$ and the adsorbed water content, but the results quoted do not satisfy this, possibly because no allowance can be made for conductivity losses in deriving the values of $\epsilon_2(\omega)_{max}$.

The two main surfaces of talc are alike. They are plane and contain oxygen atoms only. Hence it may be concluded that the absorption maximum discovered at 10 Kc/s

is characteristic of a first layer of water molecules building up on an oxygen surface. Such a surface must be a poor adsorber since the first layer is still being completed in 80% relative humidity.

8.4 - Kaolinite.

Of the minerals examined, kaolinite produces the most complex curves of dielectric loss, two separate absorption maxima being apparent in the experimental results. One peak is practically stationary in frequency, its position ranging only from 6 to 12 Kc/s in the range 0 to 50% relative humidity. In addition, the peak builds up as humidity increases. A parallel may be drawn between this peak and that obtained with talc, for both peaks are stationary in frequency and the values of $\epsilon_2(\omega)_{\max}$ build up at comparable rates with increasing relative humidity.

The second peak moves rapidly to higher frequencies as the humidity increases and passes beyond the upper frequency limit of measurement for relative humidities over 50%. Its height increase^s slowly over the same range. This peak may be taken to resemble that obtained with the metahalloysite.

In dealing with talc, it was concluded that the stationary peak characterised a first adsorbed layer upon an oxygen surface. Since kaolinite has one of its two main surfaces a plane, oxygen surface exactly like that of talc,

the stationary peak in the kaolinite results may be interpreted as arising from the first adsorbed layer being built upon the oxygen surface.

The other main surface of a kaolinite crystal is a hydroxyl face, and the moving peak may be ascribed to a layer residing upon it. The results indicate that in a 0% relative humidity the layer still exists and gives rise to an absorption at about 10 Kc/s. This layer is very much affected by the addition of other layers as may be seen from the very rapid change in the absorption frequency with layer thickness, graph (17).

As with metahalloysite and halloysite, no evidence is found of any other absorption peak.

8.5 - Kaolinite, Metahalloysite and Halloysite.

8.6 - Surface shape effects.

The interpretation of a moving peak as being due to an adsorbed layer on a hydroxyl surface may be carried over to the results obtained with metahalloysite and halloysite, for these minerals, too, have one hydroxyl face.

Since the only peak observed with kaolinite is apparently due to the first layer upon the surface, the peaks observed with the other two minerals are probably also due to the first layer. The layers obtained on metahalloysite and halloysite are more regularly arranged than those on kaolinite, judging from the fact that in any humidity the frequency of the absorption maximum is greatest

for the kaolinite, although the thickness of the adsorbed film is less on kaolinite than on metahalloysite.

The other main face of metahalloysite and halloysite is an oxygen one, and it is to be expected that a fixed frequency peak arises due to the surface water on it. The fixed peak, however, probably occurs at the same frequency as that for a just complete hydroxyl adsorbed layer - as shown by the kaolinite results. With metahalloysite and halloysite this frequency is off the range of measurement.

The major part of the adsorbed water must reside upon the hydroxyl surface of these three minerals so that the adsorbing surface area is effectively halved. Consequently, the adsorbed film thicknesses are double those given in tables (6) and (10).

8.6 - Surface shape effects.

The absorption maxima for the first water layers upon metahalloysite, halloysite and kaolinite occur at different frequencies - even when all three minerals are settled in the same humidity. Since the three adsorbing surfaces are of the same type, the difference in the co-ordination in the adsorbed layers must arise from different surface shapes. The crystal of halloysite is known from electron-microscopy and other data, section (6.7), to be a hollow cylinder. That of metahalloysite is believed to be a crystal of halloysite which is split and

unrolled to an extent determined by the method of dehydration. Kaolinite is a plane-faced crystal.

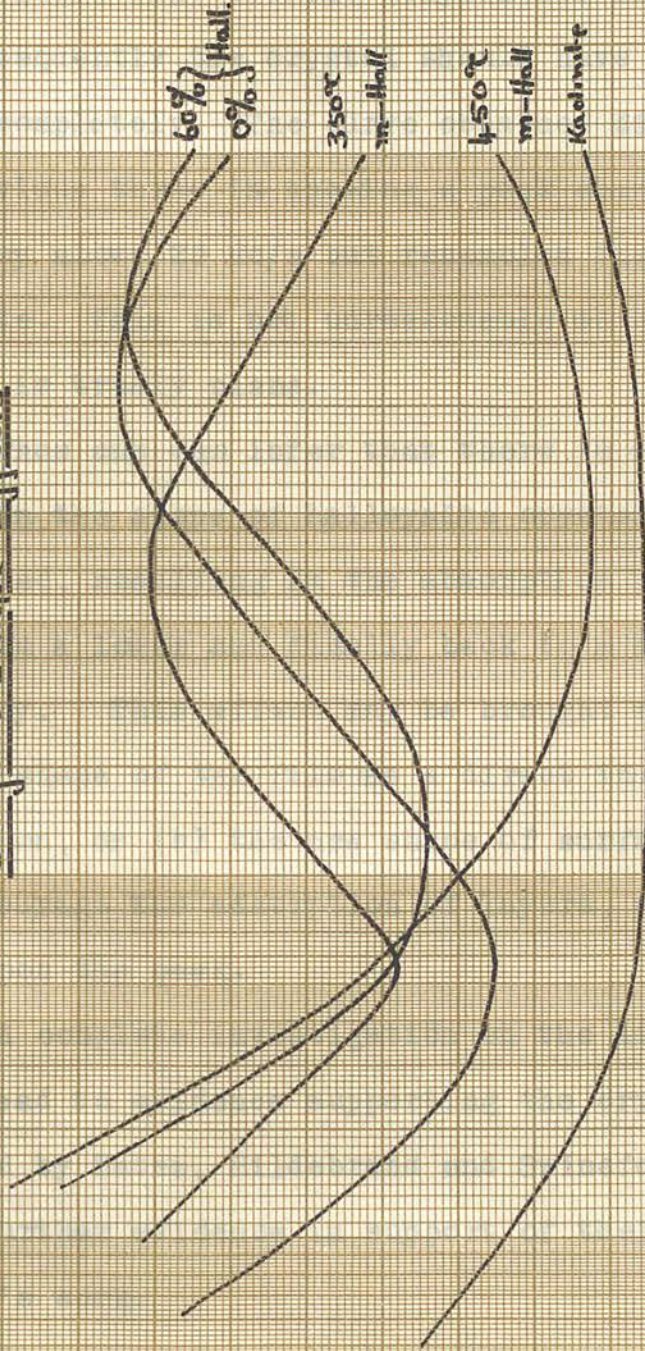
To examine the effect of surface shape upon the frequency of maximum absorption, five experimental curves were taken. These are plotted in graph 18. The vertical scales of the several curves have been altered to make easier the comparison of the frequency positions of maximum absorption. All curves are for materials settled in 60% relative humidity, the materials being - (1) a halloysite previously prepared in a 60% relative humidity, (2) a halloysite previously prepared in a 0% relative humidity, (3) a metahalloysite prepared in the usual way (section 5.4), (4) a metahalloysite prepared by heating halloysite to about 450^o C for three hours, and (5) a kaolinite.

From the curves for the first three materials it is seen that progressive dehydration of halloysite produces a crystal shape, the adsorbed film on which gives an absorption maximum at progressively lower frequencies. On the model dealt with in section (6.7) it is to be expected that progressive unrolling occurs with dehydration and that the movement of the absorption peak corresponds to the gradual flattening of the adsorbed film.

However, the curve for the fourth material is to be expected to be due to a completely flat adsorbed film, as the material was produced by dehydrating halloysite at such

Surface Shape Effects

$\epsilon_2(\omega)$



Graph 18

10⁷
1
9
8
7
6
5
4
3
2
10⁶
1
9
8
7
6
5
4
3
2
10⁵
1
9
8
7
6
5
4
3
2
10⁴
1
9
8
7
6
5
4
3
2
10³
1

— frequency c.p.s. —>

a temperature that violent dehydration should have occurred, and consequently the crystal should have split and unrolled almost completely. The curve obtained differs widely from the previous three in showing a peak absorption at some frequency above 25 Mc/s but resembles the curve for kaolinite. This is not unreasonable as the kaolinite surface is truly plane.

Thus one can infer that there is a progressive change in the shape of halloysite crystals as they are dehydrated, resulting in the absorption peak moving from a higher to a lower and finally back to a much higher frequency. This effect may be brought about in two ways - (a) the shape of the film has a direct influence on the absorption, or (b) the new shape of surface may encourage or discourage the adsorption of layers, which in turn react upon the peak.

A complete investigation on the lines mentioned here might lead to evidence supporting the crystal shapes proposed by Bates, Hildebrand and Swineford, and might yield further evidence in support of their explanation of MacEwan's work.

Particle size may also effect the absorption peak, particularly its breadth (section (2.6)). No attempt was made to separate ranges of particle size to examine this possibility.

8.7 - Concluding Remarks.

The work described in this thesis is in the main qualitative. No quantitative accuracy is possible because of the powder nature of the dielectrics. It is intended to be an exploratory survey of the phenomena encountered when the study of the bound water constituent of clay minerals is attempted by observing the Debye relaxation loss arising from the bound water itself. In this approach the difficulty of allowing for the losses arising from the conductivity of the water films is involved, but, despite this, the absorption maxima may be sufficiently well resolved for a qualitative survey.

This study, which to the author's knowledge is the first of its kind, shows that only a few layers of bound water exist upon the surface of a clay mineral such as halloysite and that probably the number of layers affected by the adsorbing surface does not exceed about three. At least one water layer, presumably the first on the adsorbing surface, is so strongly affected as to show greater long distance order than ice: this layer is retained at 0% relative humidity. In addition, the results are interpreted to show that a hydroxyl surface is a much more powerful adsorber of water than an oxygen surface.

The outcome suggests that the approach is sufficiently powerful to warrant additional development of

apparatus to encompass lower and higher frequencies, and to warrant application to other materials and adsorbed films, the approach being applicable to any dipolar adsorbed film.

2. Alexander, L.T. and Sorensen - J. Phys. Chem. 63, 1000 (1959)
3. Baughan and Razouk - Proc. Roy. Soc. A, 115, 100 (1927)
4. Bates, Hildebrand and Szwarc - J. Phys. Chem. 63, 1000 (1959)
5. Bikermann, - J. Phys. Chem. 63, 1000 (1959)
6. Bond, R.L., Griffiths, M., and ...
Disc. Faraday Soc., 1958, 1000
7. Bottcher, G.Y. - Theory of Dielectric Loss
Amsterdam, 1952.
8. Bowen and Bastow, Proc. Roy. Soc. A, 115, 100 (1927)
9. Brindley, G.W., and ...
Min. Mag., 25, 407 (1916)
- 10a. Brindley, G.W. and Robinson, ...
Trans. Faraday Soc., 43, 100 (1947)
- b. Brindley, G.W. and Robinson, ...
Min. Mag., 32, 342 (1917)
11. Brindley, G.W., ...
Min. Mag., 25, 407 (1916)
12. Robinson, F.J., ...
Robinson, F.J. - ...
13. Bulkeley - ...
14. Buswell, A.W. and ...
J. Am. Chem. Soc., 63, 1000 (1941)
15. Carpani, S. - ...
16. Collins, C.F. and ...
Trans. Faraday Soc., 43, 100 (1947)
17. Falvo, J.L. and ...

BIBLIOGRAPHY.

1. Alexander, L.T., Faust, G.T., Hendricks, S.B.,
Insley, H., and McMurdie, H.F. - Am.Min., 28, 1 (1943).
2. Alexander, L.T. and Shaw - J.Phys.Chem., 41, 955 (1937).
3. Bangham and Razouk - Proc.Roy.Soc.A., 166, 572 (1938).
4. Bates, Hildebrand and Swineford - Am.Min., 35, 463 (1950).
5. Bikermann, - J.Phys.Chem., 46, 724 (1942).
6. Bond, R.L., Griffith, M., and Maggs, F.A.P. -
Disc.Faraday Soc., No.3, pp.29 & 40 (1948).
7. Bottcher, C.F. - Theory of Electric Polarisation,
Amsterdam, 1952.
8. Bowden and Bastow, Proc.Roy.Soc.A., 151, 220 (1935).
9. Brindley, G.W., and Goodyear, J. -
Min.Mag., 28, 407 (1948).
- 10a. Brindley, G.W. and Robinson, K. -
Trans.Faraday Soc., 42B, 198 (1946).
- b. Brindley, G.W. and Robinson, K. -
Min.Mag., 27, 242 (1946).
11. Brindley, G.W., Robinson, K., and Goodyear, J. -
Min.Mag., 28, 423 (1948).
12. Buchanan, T.J., Haggis, G.H., Hasted, J.B. and
Robinson, B.G. - Proc.Roy.Soc.A., 213, 379 (1952).
13. Bulkley - Bur.Stand.J.Res., 6, 89 (1931).
14. Buswell, A.M. and Dudenbostel, B.F. -
J.Am.Chem.Soc., 65, 2554 (1941).
15. Carpeni, G. - Comptes Rendus, 233, pp.158,249 & 309.
16. Collie, C.H., Ritson, D.M. and Hasted, J.B. -
Trans.Faraday Soc., 42A, 129 (1946).
17. Dalke, J.L. and Powell, R.C. - Electronics 24,224(1951).

18. Dyal, R.S. and Hendricks, S.B. -
Soil Science, 69, 421 (1950).
19. Freymann, M. and Freymann, R. -
Comptes Rendus, 232, 401 (1951).
20. Freymann, M. and Freymann, R. -
Comptes Rendus, 232, 1096 (1951).
21. Frohlich, H. - Theory of Dielectrics, Oxford, 1949.
22. Girard, P and Abadie, P. -
Trans.Faraday Soc., 42A, 40 (1946).
23. Gortner, R.A. - Trans.Faraday Soc., 26, 678 (1930).
24. Haggis, G.H., Hasted, J.B. and Buchanan, T.J. -
J.Chem.Phys., 120, 1452 (1952).
25. Handbook of Physical Constants, Geol.Soc. of Am.Jan'42.
26. Harris, H.E. - Electronics, 24, 130 (1951).
27. Hendricks, S.B. - Am.Min., 23, 295 (1938).
28. Hendricks, S.B., and Jefferson, M.E. -
Am.Min., 23, 863 (1938).
29. Hill, A.V. - Proc.Roy.Soc.A., 127, 9 (1930).
30. Joly, M. - Disc.Faraday Soc., No. 3, p114 (1948).
31. Lamb, J. - Trans.Faraday Soc., 42A, 238 (1946).
32. MacEwan, D.M.C. - Trans.Faraday Soc., 44, 349 (1948).
33. MacEwan, D.M.C. - Min.Mag., 28, 36 (1947).
34. McDowell, I. and Vose, W. - Nature, 170, 368 (1952).
35. Marinesco, N. - Comptes Rendus, 187, 718 (1928).
36. Neuhausen, B.S. and Patrick, W.A. -
J.Am.Chem.Soc., 43, 1844 (1921).
37. Roland, M.T. and Bernard, R. -
Comptes Rendus, 232, 1098 (1951).
38. Smyth, C.P. and Hitchkok, C.S. -
J.Am.Chem.Soc., 54, 4631 (1932).

39. Terman - Radio Engineering Handbook.
40. Wells, A.F. - Structural Inorganic Chemistry,
Oxford, 1950.
41. Wilsdon, B.H., Bonnell, D.R.G. and Nottage, M.E. -
Trans.Faraday Soc., 31, 1304 (1935).
42. Wolkowa - Koll.Zeit, 67, 280 (1934).